UNIT-STEP MOTION OF A WIDE DELTA WING

Thesis by

Geoffrey Vernon Parkinson

In Partial Fulfillment of the Requirements

For the Degree of

Doctor of Philosophy

California Institute of Technology

Pasadena, California

1951

ACKNOWLEDGMENTS

This problem was suggested to me by Dr. H. J. Stewart, who supervised my research and contributed greatly to its progress. Dr. P. A. Lagerstrom supplied several valuable ideas in connection with the method of analysis of the problem, and Dr. C. R. de Prima helped me over some mathematical obstacles. The final draft of the paper was prepared by Mrs. Elizabeth Fox.

To all the above, my sincere thanks.

ABSTRACT

The effect on a wide delta wing in supersonic flight of the sudden imposition of a small velocity perturbation normal to the plane of the wing is considered. The resulting pressure field on the wing is found in closed form in terms of elementary functions. The corresponding solution for the infinite swept wing with supersonic edges is obtained as a by-product, and for this the terms of the transient pressure coefficient are shown to have geometric significance. The force and moment coefficients are obtained by means of a method of descent, which simplifies the calculations and shows the nature of the dependence of these coefficients on the wing planform. Because of the short duration and moderate strength of the transient effects of the unit-step motion, it is considered to be of little practical importance. However, because of the simplicity of the solutions for the motion, it is also considered to be of possible theoretical value as a basis for Duhamel integration to obtain solutions for more general time-dependent motions of the wide delta wing.

TABLE OF CONTENTS

LIST OF FIGURES

LIST OF FIGURES (Contd)

I. INTRODUCTION

In recent years considerable attention has been given to the aerodynamic problems associated with the flight of airplanes and missiles at supersonic speed. Because of the difficulty of solution of the complete hydrodynamical equations, even under the assumption of non-viscous irrotational flow, further assumptions, which remove in some way the non-linearity of the equations, have generally been needed to make solution of these problems possible.

For problems involving the flight of wings at supersonic speed a fruitful procedure has been to assume that the wings are very thin and move essentially in one plane. Under these assumptions the disturbances produced in the gas by the motion of the wing are small in comparison with suitable reference quantities. In particular, the disturbance velocities are small compared to the velocity of the wing. As a result, the hydrodynamical equations governing the disturbances are linearized, and the problems become tractable. It should be kept in mind, however, that solutions to these linearized equations may not correspond closely with reality, particularly for non-steady motions. Nevertheless, when its results are applied with discretion, linearized supersonic wing theory is a useful and important branch of aerodynamics.

Further simplification of the equations results if the motion of the wing is not time-dependent. Accordingly, problems in which

this was true, were considered first, and as early as 1925 Ackeret (Reference 1) treated the problem of steady, supersonic flow past thin, two-dimensional airfoils. Since then, most of the problems of interest concerning the steady supersonic motion of thin wings have been solved, and more recently problems in which the motion is time-dependent have been given much attention. Possio's solution in 1937 (Reference 2) for an oscillating two-dimensional airfoil moving at supersonic speed was probably the first of this type.

Among finite wings which have been considered, the delta wing, whose planform is an isosceles triangle with the base as trailing edge, is the most common, being both simple mathematically and of practical interest. A delta wing is classified as wide or narrow depending on its speed of flight. If its supersonic speed is low enough for the wing to lie within the cone of disturbance from the vertex, the wing is a narrow delta. At some higher supersonic speed this cone of disturbance will be narrow enough for the wing to extend beyond it, and the wing is then classified as a wide delta. Among authors treating the wide delta wing are Puckett (1946) (Reference 3) for steady motion and Froehlich (1950) (Reference 4) for oscillatory motion. The narrow delta wing has been treated by such authors as Stewart (1946) (Reference 5) for steady motion and Hipsh (1951) (Reference 6) for oscillatory motion. It might be thought that the solutions obtained for the oscillatory

supersonic motion of delta wings would lead to solutions for more general time-dependent motions through the application of the Fourier integral. However, the solutions for oscillatory motion have been of such complexity that this procedure does not appear very promising.

An alternative procedure is to obtain the effect of a unit-step motion of the wing, and then seek solutions for other time-dependent motions through the application of some superposition integral. Several authors (References 7-12) have applied this unit-step technique to two-dimensional wings. Miles (1948) (Reference 7), for example, has treated the problem of a two-dimensional wing which experiences a unit increase in downwash instantaneously over its surface.

In the present paper a similar problem is considered for the wide delta wing*. More specifically, the problem is that of finding the pressure distribution over a wide delta wing of zero thickness which, moving initially in its own plane at supersonic speed, instantaneously acquires a small downward velocity which thereafter remains constant. That is, the wing experiences an instantaneous change in angle of attack without, however, rotating. This restriction is important, for if the wing experienced an

---

*Other recent papers on the same problem by Strang (1950) (Reference 14) and Miles (1950) (Reference 15) are discussed in Part V.

instantaneous rotation there would result an induced downwash distribution in addition to the desired step-function distribution. The induced distribution would be of linear variation chordwise and a Dirac delta function in time.

Thus the unit-step motion considered in this paper does not represent a very probable motion of the wing, but is important because of the possible use of the solution in a superposition integral giving solutions for more general time-dependent motions. Before the specific problem is considered, some small-disturbance wing theory will be reviewed in order to clarify the concepts and formulae needed in the analysis of the problem.

II. SMALL-DISTURBANCE WING THEORY

a. Linearization of the Hydrodynamical Equations. The isentropic flow of a non-viscous gas is specified by the following equations:

Continuity $$\frac{\partial d}{\partial \bar{t}} + \nabla \cdot d\vec{q} = 0 \tag{1}$$

Momentum $$d\frac{\partial \vec{q}}{\partial \bar{t}} + d\vec{q}\cdot\nabla\vec{q} + \nabla p = 0 \tag{2}$$

State $$\frac{p}{p_\infty} - \left(\frac{d}{d_\infty}\right)^K = 0 \tag{3}$$

where p, d, $\vec{q}$ are respectively the static pressure, density, and vector velocity in an $(\bar{x},\bar{y},\bar{z},\bar{t})$ coordinate system. $(\ )_\infty$ indicates values at infinity and K is the ratio of the specific heats at constant pressure and constant volume of the gas. From Equation (3), $p = p(d)$ so that

$$\nabla p = \left(\frac{dp}{dd}\right)\nabla d = a_l^2 \nabla d \tag{4}$$

where a_l is the local velocity of sound. It is convenient to express the density in the form

$$d = d_\infty(1+s) \tag{5}$$

If now $\vec{q}$ is taken as the disturbance velocity produced in the gas, which is undisturbed at infinity, by the motion of a thin wing moving essentially in its own plane with velocity $\vec{Q}$, then it may

reasonably be assumed that

$$\left|\frac{\vec{q}}{\vec{Q}}\right| << 1$$

In the same way:

$$|s| << 1$$

Moreover, the derivatives of $\vec{q}$ and s may be assumed small compared to suitable reference quantities associated with the wing and its motion. As a result squares and products of these small quantities may be assumed negligibly small compared to the quantities themselves, and terms containing them may be dropped from the equations. Also, a_l^2 may be replaced by a^2, the value at infinity. With the incorporation of Equations (4) and (5), and the above assumptions, Equations (1) and (2) become:

Continuity $$\frac{\partial s}{\partial t} + \nabla \cdot \vec{q} = 0 \qquad (6)$$

Momentum $$\frac{\partial \vec{q}}{\partial t} + a^2 \nabla s = 0 \qquad (7)$$

Finally, the motion of the gas may be assumed irrotational, so that $\nabla \times \vec{q} = 0$. It is then possible to define a velocity potential φ by the relation $\vec{q} = \nabla\varphi$. Substituting for $\vec{q}$ in Equation (7) gives:

$$\nabla\left\{\frac{\partial \varphi}{\partial t} + a^2 s\right\} = 0 \qquad (8)$$

the order of differentiation being immaterial. Integration of Equation (8) yields the equation

$$\frac{\partial \varphi}{\partial t} + a^2 s = 0 \qquad (9)$$

The integration gives zero on the right side of the equation because of the conditions at infinity. Finally, the linearized differential equation governing the flow is obtained by substituting for s from Equation (9) in Equation (6):

$$\nabla^2\varphi - \frac{1}{a^2}\frac{\partial^2\varphi}{\partial \bar{t}^2} = 0 \tag{10}$$

This is of course the wave equation and it, together with the boundary and initial conditions of the problem, determines the flow field in the $(\bar{x},\bar{y},\bar{z},\bar{t})$ system, which is fixed with respect to the fluid at infinity. In particular the pressure, which may be expressed by a pressure coefficient C_p defined by

$$C_p = \frac{p - p_\infty}{\frac{d_\infty}{2} U^2} \tag{11}$$

where U is the magnitude of the main velocity of the wing, is given in terms of φ. Using the linearized pressure relation

$$p - p_\infty = a^2 s\, d_\infty$$

and substituting for $a^2 s$ from Equation (9):

$$C_p = -\frac{2}{U^2}\frac{\partial\varphi}{\partial \bar{t}} \tag{12}$$

It is also important to be able to determine the flow in a coordinate system fixed with respect to the main motion of the wing. This can be achieved by a Galilean transformation. Suppose the wing

to be moving mainly in the negative $\bar{x}$-direction with constant velocity of magnitude U. Then the new coordinate system (x,y,z,t) is defined by the relations

$$\left.\begin{aligned} x &= \bar{x} + U\bar{t} \\ y &= \bar{y} \\ z &= \bar{z} \\ t &= \bar{t} \end{aligned}\right\} \tag{13}$$

On the introduction of these new coordinates into Equation (10) it becomes

$$\nabla^2\varphi - \frac{U^2}{a^2}\frac{\partial^2\varphi}{\partial x^2} - 2\frac{U}{a^2}\frac{\partial^2\varphi}{\partial x\partial t} - \frac{1}{a^2}\frac{\partial^2\varphi}{\partial t^2} = 0 \tag{14}$$

Equation (14) and the boundary and initial conditions of the problem determine the flow in the (x,y,z,t) system. In this system, the pressure coefficient is given by

$$C_p = -\frac{2}{U^2}\left\{\frac{\partial\varphi}{\partial t} + U\frac{\partial\varphi}{\partial x}\right\} \tag{15}$$

Both coordinate systems will be used in this paper, some of the methods being more easily developed in the $(\bar{x},\bar{y},\bar{z},\bar{t})$ system, and more easily applied in the (x,y,z,t) system.

b. Linearization of the Boundary Condition on the Wing. The exact boundary condition on a body in motion through a fluid is that the flow must be tangent to the body at every point of its surface. This condition is expressed by the relation

$$\vec{n}\cdot\vec{q} = \vec{n}\cdot\vec{Q} \tag{16}$$

where $\vec{n}$ is the outward normal to the body surface at any point, and $\vec{q}$ and $\vec{Q}$ are respectively the velocities of the fluid and the body at that point. In general, all are functions of $\bar{x}$, $\bar{y}$, $\bar{z}$, and $\bar{t}$. For small-disturbance wing theory, Equation (16) can be simplified.

Consider a thin wing moving mainly in the negative $\bar{x}$-direction with velocity of magnitude U, but also executing small motions in and about the plane $\bar{z} = 0$, so that

$$\vec{Q} = (-U+u)\vec{i} + v\vec{j} + w\vec{k} \tag{17}$$

where $\vec{i}$, $\vec{j}$, $\vec{k}$ are unit vectors in the directions of positive $\bar{x}$, $\bar{y}$, $\bar{z}$ respectively, and u, v, w are numerically much smaller than U. The normal $\vec{n}$ may be decomposed according to the relation

$$\vec{n} = \cos\varepsilon\sin\alpha\,\vec{i} + \sin\varepsilon\,\vec{j} + \cos\varepsilon\cos\alpha\,\vec{k} \tag{18}$$

where ε and α are as given in Figure 1. It is customary to call α the local instantaneous angle of attack, positive as shown. For a thin wing as considered here $\sin\alpha$ and $\sin\varepsilon$ are numerically much less than 1. The fluid velocity $\vec{q}$ is as defined previously. Therefore, if products of small quantities are neglected, and $\tan\alpha$ is replaced by α, Equation (16) is reduced to

$$\frac{\partial\varphi}{\partial\bar{z}} = -\alpha U + w$$

at the surface of the wing. Moreover, since it is assumed that the surface of the wing is everywhere and at all times very close to the plane $\bar{z} = 0$, and derivatives of $\frac{\partial \varphi}{\partial \bar{z}}$ are small, it is permissible to evaluate $\frac{\partial \varphi}{\partial \bar{z}}$ on $\bar{z} = 0$ instead of on the wing. In general, quantities may differ on the upper and lower surfaces of the wing, so two equations result:

$$\frac{\partial \varphi}{\partial \bar{z}}(\bar{x}, \bar{y}, 0_+, \bar{t}) = W(\bar{x}, \bar{y}, \bar{h}_u, \bar{t}) - U\alpha(\bar{x}, \bar{y}, \bar{h}_u, \bar{t}) \tag{19a}$$

$$\frac{\partial \varphi}{\partial \bar{z}}(\bar{x}, \bar{y}, 0_-, \bar{t}) = W(\bar{x}, \bar{y}, \bar{h}_\ell, \bar{t}) - U\alpha(\bar{x}, \bar{y}, \bar{h}_\ell, \bar{t}) \tag{19b}$$

where $\bar{h}_u, \bar{h}_\ell$ are the $\bar{z}$-coordinates of points on the upper and lower surfaces, respectively. The same form of this boundary condition holds in the (x,y,z,t) system, since the relative motion of the fluid and the wing is the same in both systems.

c. The Fundamental Wing Formula. At any instant an edge of a wing is called a leading edge if air flows across it onto the wing, and is called a trailing edge if air flows across it off the wing. Leading and trailing edges of a wing in supersonic flight are called supersonic when the cones of disturbance (Mach cones) from all points on these edges lie completely behind them. The wide delta is such a wing.

It follows that conditions on the upper and lower surfaces of a wing with supersonic edges are independent of each other,

and may be considered separately. Moreover, no disturbances exist ahead of the wing, while those behind cannot affect conditions on the wing. It appears then that a formula giving φ for $\bar{z} > 0$ in terms of the upwash $\frac{\partial \varphi}{\partial \bar{z}}$ over the plane $\bar{z} = 0+$ would be very useful, since the upwash is specified by Equation (19a) over the part of the plane corresponding to the wing, and is zero in the only other part of the plane which need be considered if φ is wanted on the wing, as is usually true. Such a formula will now be obtained.

The intuitive idea behind the formula is that of representing the wing in motion by a superposition of spherical pulses. The spherical pulse is an idealization of the effect of a point disturbance which acts for a very short time. As is commonly true of fundamental solutions of linear differential equations, it has no physical existence but may be considered either as an approximation to reality or merely as a tool useful for superposition to obtain solutions which have physical meaning. The velocity potential φ_1 at $(\bar{x}, \bar{y}, \bar{z})$ at time $\bar{t}$ due to a spherical pulse of strength S emitted at $(\bar{\xi}, \bar{\eta}, \bar{\zeta})$ at time $\bar{\tau}$ is

$$\varphi_1(\bar{x}, \bar{y}, \bar{z}, \bar{t}) = \frac{S}{\bar{r}} \delta\left(\bar{t} - \bar{\tau} - \frac{\bar{r}}{a}\right) \tag{20}$$

where

$$\bar{r}^2 = (\bar{x} - \bar{\xi})^2 + (\bar{y} - \bar{\eta})^2 + (\bar{z} - \bar{\zeta})^2$$

and δ is the Dirac delta function, defined by

$$\delta(\bar{x}) = 0 \ , \ \bar{x} \neq 0$$

$$\int_{-\infty}^{\infty} \delta(\bar{x})\, d\bar{x} = 1$$

The delta function in an integral "picks out" the value of the integrand at one point, thus:

$$\int_{-\infty}^{\infty} \delta(\bar{x}-b)\, g(\bar{x})\, d\bar{x} = g(b)$$

The form of the fundamental solution given by Equation (20) follows from the assumed nature of the pulse and from the well-known solution of the wave equation in spherical polar coordinates for a diverging wave with radial symmetry:

$$\varphi(\bar{r},\bar{t}) = \frac{1}{\bar{r}} f(\bar{t}-\frac{\bar{r}}{a}) \qquad (21)$$

where

$$\bar{r}^2 = \bar{x}^2 + \bar{y}^2 + \bar{z}^2$$

and f is any twice-differentiable function. This last condition seems to rule out the delta function, but since unruly behaviour of a fundamental solution is not unusual, Equation (20) is used and it is shown later that this heuristic procedure leads to a correct result.

The spherical pulse, as defined above, has two important properties which in fact make it possible to represent the moving wing by such pulses. These properties, which are illustrated in

Figure 2, are:

1) Pulses from P_2 contribute no upwash at P_1, because the velocity is purely radial for a pulse. Therefore the upwash at P_1 is entirely due to the pulses from P_1.

2) The pulse from P_1 emitted at time $\bar{t}_1$, has no effect at P_1 at time $\bar{t}_2$, since by Huyghens' principle the wave leaves no after-effect. Therefore the upwash at P_1 at time $\bar{t}$ depends only on the pulse from P_1 at $\bar{t}$.

Moreover, the relation between the pulse strength S and the upwash is clearly linear, so that

$$S(\bar{x},\bar{y},\bar{t}) = G\frac{\partial \varphi}{\partial \bar{z}}(\bar{x},\bar{y},0,\bar{t})$$

where G is a constant to be determined.

Suppose now there is a continuous distribution of spherical pulses over the plane $\bar{z} = 0$, and the motion under consideration begins at time $\bar{t} = 0$. Then the total effect at a point $(\bar{x},\bar{y},\bar{z})$ at time $\bar{t}$ is obtained by integrating the fundamental solution over the entire plane $\bar{z} = 0$ and over the time history of the disturbances:

$$\varphi(\bar{x},\bar{y},\bar{z},\bar{t}) = \iint_{\substack{\text{plane}\\ \bar{z}=0}} \frac{1}{\bar{r}} \int_0^{\bar{t}} S(\bar{\xi},\bar{\eta},\bar{\tau})\,\delta(\bar{t}-\bar{\tau}-\tfrac{\bar{r}}{a})\,d\bar{\tau}\,dA \qquad (22)$$

where dA is the area element in $\bar{z} = 0$. By use of the properties of the delta function, Equation (22) is reduced to

$$\varphi(\bar{x},\bar{y},\bar{z},\bar{t}) = \iint_{\substack{\text{plane}\\ \bar{z}=0}} \frac{1}{\bar{r}} S(\bar{\xi},\bar{\eta},\bar{t}-\tfrac{\bar{r}}{a})\,dA \qquad (23)$$

Only the part of the plane $\bar{z} = 0$ for which $\bar{r} \leq a\bar{t}$ can contribute to this integral. It is convenient to introduce polar coordinates $\bar{\rho}, \bar{\theta}$ in the plane $\bar{z} = 0$, as shown in Figure 3. Now

$$\bar{\rho}^2 = \bar{r}^2 - \bar{z}^2 \tag{24}$$

and with respect to the integration in Equation (23) $\bar{z}$ is a constant, so that

$$\bar{\rho}\, d\bar{\rho} = \bar{r}\, d\bar{r}$$

on differentiating Equation (24). It follows that Equation (23) may be rewritten:

$$\varphi(\bar{x},\bar{y},\bar{z},\bar{t}) = \int_{\bar{z}}^{a\bar{t}} \int_{0}^{2\pi} S(\bar{\rho},\bar{\theta},\bar{t}-\tfrac{\bar{r}}{a})\, d\bar{\theta}\, d\bar{r} \tag{25}$$

where $\bar{\rho}$ is given by Equation (24). It is now possible to determine G by differentiating Equation (25). Thus

$$\frac{\partial \varphi}{\partial \bar{z}}(\bar{x},\bar{y},\bar{z},\bar{t}) = -\int_{0}^{2\pi} S(0,\bar{\theta},\bar{t}-\tfrac{\bar{z}}{a})\, d\bar{\theta} + \int_{\bar{z}}^{a\bar{t}} \int_{0}^{2\pi} \frac{\partial S}{\partial \bar{\rho}}(\bar{\rho},\bar{\theta},\bar{t}-\tfrac{\bar{r}}{a})\left(-\frac{\bar{z}}{\bar{\rho}}\right) d\bar{\theta}\, d\bar{r}$$

This can be written more simply in the form

$$\frac{\partial \varphi}{\partial \bar{z}}(\bar{x},\bar{y},\bar{z},\bar{t}) = -2\pi S(\bar{x},\bar{y},\bar{t}-\tfrac{\bar{z}}{a}) - \bar{z} \int_{\bar{z}}^{a\bar{t}} \int_{0}^{2\pi} \frac{1}{\bar{\rho}} \frac{\partial S}{\partial \bar{\rho}}(\bar{\rho},\bar{\theta},\bar{t}-\tfrac{\bar{r}}{a})\, d\bar{\theta}\, d\bar{r} \tag{26}$$

The integral on the right side of the equation is bounded as $\bar{z} \to 0+$, so that in the limit the desired result follows:

$$S(\bar{x},\bar{y},\bar{t}) = -\frac{1}{2\pi} \frac{\partial \varphi}{\partial \bar{z}}(\bar{x},\bar{y},0+,\bar{t}) \tag{27}$$

On the introduction of a new integration variable $\bar{\tau} = \bar{t} - \frac{\bar{r}}{a}$, and by use of Equation (27), Equation (25) is put in the final form

$$\varphi(\bar{x},\bar{y},\bar{z},\bar{t}) = -\frac{a}{2\pi}\int_0^{\bar{t}-\frac{\bar{z}}{a}}\int_0^{2\pi} \frac{\partial \varphi}{\partial \bar{z}}(\bar{\xi},\bar{\eta},0;\bar{\tau})\,d\bar{\theta}\,d\bar{\tau} \qquad (28)$$

where

$$\bar{\xi} = \bar{x} + \sqrt{a^2(\bar{t}-\bar{\tau})^2 - \bar{z}^2}\,\cos\bar{\theta} \quad , \quad \bar{\eta} = \bar{y} + \sqrt{a^2(\bar{t}-\bar{\tau})^2 - \bar{z}^2}\,\sin\bar{\theta}$$

This is the fundamental formula of small-disturbance wing theory. It is a classical solution of the wave equation and is given, although essentially in the form of Equation (23), by Rayleigh (Reference 13). It gives the specified upwash on $\bar{z} = 0$, and it satisfies the initial condition that no disturbances existed for $\bar{t} < 0$. Thus the heuristic approach by which Equation (28) was obtained is justified.

The physical interpretation of Equation (28) is simple. $\bar{\tau}$ is the time at which a disturbance must be propagated from $(\bar{\xi},\bar{\eta},0)$ in order to affect $(\bar{x},\bar{y},\bar{z})$ at the later time $\bar{t}$. $\bar{\tau}$ is therefore constant for concentric circles in the plane $\bar{z} = 0$ with center $(\bar{x},\bar{y},0)$ and radius $\bar{\rho} = \sqrt{a^2(\bar{t}-\bar{\tau})^2 - \bar{z}^2}$. The inner integration in Equation (28), including the factor $\frac{1}{2\pi}$, gives the average value of upwash over one of these circles, and the outer integration sums over all such circles which can contribute the effect of their disturbances at $(\bar{x},\bar{y},\bar{z})$ at time $\bar{t}$. The lower limit $\bar{\tau} = 0$ expresses the fact that no disturbances existed for $\bar{\tau} < 0$, and the upper limit $\bar{\tau} = \bar{t} - \frac{\bar{z}}{a}$ expresses the fact that no disturbances propagated from any point in the plane $\bar{z} = 0$

will have had time to reach $(\bar{x},\bar{y},\bar{z})$ by time $\bar{t}$ for $\bar{\tau} > \bar{t} - \frac{\bar{z}}{a}$.

So far Equation (28) is quite general. The application to a particular wing problem is made by suitably specifying the upwash function in the integrand. It will be recalled that in the $(\bar{x},\bar{y},\bar{z},\bar{t})$ system the wings considered move essentially in the negative $\bar{x}$-direction with velocity U. For some purposes it is inconvenient to have the wing moving through the region of integration of Equation (28), so that it is useful to obtain the corresponding fundamental formula in the (x,y,z,t) system. After a formal change of variables, Equation (28) becomes

$$\varphi(x,y,z,t) = -\frac{a}{2\pi}\int_0^{t-\frac{z}{a}}\int_0^{2\pi} \frac{\partial \varphi}{\partial z}(\xi,\eta,\theta,\tau)\,d\theta\,d\tau \qquad (29)$$

where

$$\xi = x - U(t-\tau) + \sqrt{a^2(t-\tau)^2 - z^2}\cos\theta \quad , \quad \eta = y + \sqrt{a^2(t-\tau)^2 - z^2}\sin\theta$$

The formula is useless, however, in the form of Equation (29) because the circles on which the inner integration is performed are no longer concentric. This is clear from Equation (29), and the regions of integration for the two systems are shown as the shaded areas in Figure 4 for the case when $M = \frac{U}{a}$ is greater than one, applicable to the problem of a wing in supersonic flight.

The logical integration variables in the (x,y,z,t) system are (ξ,η) as defined by Equation (29). To make the formal change

of variables from (θ,τ) to (ξ,η) it is necessary to obtain the Jacobian of the transformation, which is found to be

$$\frac{\partial(\theta,\tau)}{\partial(\xi,\eta)} = \frac{1}{\sqrt{a^2(x-\xi)^2-(U^2-a^2)\{(y-\eta)^2+z^2\}}} \tag{30}$$

Also, when τ is expressed in terms of ξ,η by eliminating θ from Equation (29) it is seen that in general two values of τ correspond to one point (ξ,η). The fundamental wing formula can therefore be written in the (x,y,z,t) system in the form

$$\varphi(x,y,z,t) = -\frac{1}{2\pi}\iint_R \frac{\frac{\partial\varphi}{\partial z}(\xi,\eta,0,t-t_1) + \frac{\partial\varphi}{\partial z}(\xi,\eta,0,t-t_2)}{\sqrt{(x-\xi)^2-(M^2-1)\{(y-\eta)^2+z^2\}}}\, d\xi d\eta \tag{31}$$

where

$$t_{1\atop 2} = \frac{1}{a(M^2-1)}\left\{M(x-\xi) \mp \sqrt{(x-\xi)^2-(M^2-1)\{(y-\eta)^2+z^2\}}\right\}$$

and, for $M>1$, R is the shaded region of Figure 4b. R is bounded partly by the hyperbola

$$(x-\xi)^2 = (M^2-1)\{(y-\eta)^2+z^2\} \tag{32}$$

which is the envelope of the circles of the inner integration of Equation (29). However, for a point (ξ,η) inside the circle with center $(x-Ut,y,0)$ $\tau_2=t-t_2$ is negative, so that $\frac{\partial\varphi}{\partial z}(\xi,\eta,0,t-t_2)=0$, and for a point (ξ,η) beyond this circle upstream both τ_1 and τ_2 are negative, so that the integrand vanishes. The effective region R is thus the interior of the circle of center $(x-Ut,y,0)$ and radius $\sqrt{a^2t^2-z^2}$, over which the integrand has $\frac{\partial\varphi}{\partial z}(\xi,\eta,0,t-t_2)=0$, and

the closed region bounded by this circle and the above hyperbola, over which both upwash functions act.

The equations of small-disturbance wing theory will now be applied to the specific problem of the unit-step motion of a wide delta wing.

III. PRESSURE DISTRIBUTION FOR THE WIDE DELTA WING

a. Statement of the Problem. Consider a flat delta wing of zero thickness and chord c. The sweepback angle of the leading edges is σ. It is convenient to locate the origin of an (x,y,z,t) system at the vertex of the wing, which points in the negative x-direction, as shown in Figure 5. The fact that the wing is a wide delta is expressed by the inequality

$$\beta > k$$

where

$$\beta = \sqrt{M^2-1} \qquad k = \tan\sigma$$

and M is the Mach number of the free stream, as defined previously.

For the unit-step motion of this wing considered in the (x,y,z,t) system, the wing is initially at rest in the plane z = 0. At time t = 0 it is given a constant velocity of magnitude w_0 in the negative z-direction, where $\frac{w_0}{U} << 1$. The problem is to determine the pressure distribution over the wing resulting from this motion. As was pointed out in PART II, only the top side of the wing need be considered. The pressure is obtained simply from the velocity perturbation potential φ, which will therefore be obtained first.

Now φ is given directly by Equation (31) for any point

(x,y,z) in the half space $z \geq 0$ at any positive time t, if the upwash $\frac{\partial \varphi}{\partial z}$ is known over the region of integration R in the plane $z = 0$. This is so here, where R includes only points on the wing or ahead of it. Ahead of the wing $\frac{\partial \varphi}{\partial z}$ is everywhere zero at all times, and on the wing $\frac{\partial \varphi}{\partial z}$ is specified by Equation (19a), in which here

$$\alpha(x,y,h_u,t) = 0 \qquad w(x,y,h_u,t) = -w_0\, 1(t)$$

where $1(t)$ is the unit-step function, defined by

$$1(t) = 0 \quad , \quad t < 0$$
$$= 1 \quad , \quad t \geq 0$$

Therefore $\frac{\partial \varphi}{\partial z}$ on the wing is given by

$$\frac{\partial \varphi}{\partial z}(x,y,0+,t) = -w_0\, 1(t) \tag{33}$$

and φ is given for points on the wing by the integral

$$\varphi(x,y,0+,t) = \frac{w_0}{2\pi} \int_{R_w} \int \frac{1(t-t_1) + 1(t-t_2)}{\sqrt{(x-\xi)^2 - \beta^2(y-\eta)^2}}\, d\xi\, d\eta \tag{34}$$

where R_w is the portion of the region R shown in Figure 6 which falls on the wing. R is subdivided into R_1 and R_2. It follows from Equation (31) and the nature of the unit-step function that in R_1 $1(t-t_1) = 1$ and $1(t-t_2) = 0$, while in R_2 $1(t-t_1) = 1(t-t_2) = 1$.

It can be seen from Equation (34) that at a particular time t, φ depends on the particular point of evaluation on the wing (x,y) only to the extent that this point affects the size and shape of R_w. Therefore, in determining φ over the wing the simplest procedure

is to divide the wing into zones in which R_w has the same general form, and consider the solution of Equation (34) for points in each zone separately. Since R_w depends only on the relation of the point of evaluation (x,y) to the leading edges of the wing, the zones are determined completely by the regions of influence of points on the leading edges. The region of influence of such a point is merely a region R as in Figure 6, but extending downstream rather than upstream from the point. The resulting zones of the wing are shown in Figure 7. Only points on the right half of the wing need be considered, from symmetry.

Before applying Equation (34), however, it is worthwhile to make some general observations about the problem as it now appears. First of all it can be shown that the perturbation flow field is conical in space-time with respect to the wing vertex. This follows from the known invariance of the governing equations under uniform dilatation, and the conical shape of the wing, which makes the boundary conditions conical in space-time.

Thus if the chord c of the wing in Figure 7 is made infinite, the figure applies to all positive times, since the zones merely expand uniformly with time. The perturbation velocity components and the pressure (but not the velocity potential) at points on the finite delta wing (since the trailing edge does not influence the flow field over the wing) are then functions of the ratios $\frac{x}{t}$, $\frac{y}{t}$ only,

and not of the coordinates themselves. Use of this property is made later in the examination of the pressure field, although conical methods are not used in obtaining the pressure.

Another pertinent observation about the problem is that in some zones the results are known either from fundamental principles or from previous applications of thin-wing theory, to which appropriate reference is made later.

For example, in zone I there is no effect of the wing edges since the disturbances arising at $t = 0$ along the leading edges have not had time to reach the points in zone I. The flow field in zone I is determined by purely local conditions, and locally the unit-step motion of the wing is equivalent to the sudden motion in the z-direction of a one-dimensional piston. The resulting pressure therefore has what is commonly called the piston value, which is determined by elementary considerations of simple one-dimensional progressive acoustic waves.

However, in what follows, application of the fundamental wing formula to the solution for each of the seven zones is indicated, although the solution is not carried out in detail where the results are known.

b. Pressure in Zones I, II, and III. It is convenient to group zones I, II, and III together because points in these zones have in common that they are not influenced by the left leading edge of the wing.

They are, so to speak, unaware of its existence.

Zone I. In zone I it is clear that R_w is the complete region R. Therefore it follows from Equation (34) that, for a given time t, φ is constant throughout zone I. Evaluation of φ from Equation (34) is straightforward, but since there is no leading-edge effect it is even simpler to evaluate φ from Equation (28) in the equivalent $(\bar{x},\bar{y},\bar{z},\bar{t})$ system, by which here

$$\varphi_I(\bar{x},\bar{y},0+,\bar{t}) = -\frac{a}{2\pi}\int_0^{\bar{t}}\int_0^{2\pi}\frac{\partial\varphi}{\partial\bar{z}}(\bar{\xi},\bar{\eta},0+,\bar{\tau})\,d\bar{\theta}\,d\bar{\tau} \tag{35}$$

where

$$\frac{\partial\varphi}{\partial\bar{z}}(\bar{\xi},\bar{\eta},0+,\bar{\tau}) = -W_0 I(\bar{\tau})$$

Therefore

$$\varphi_I(\bar{x},\bar{y},0+,\bar{t}) = W_0 a\int_0^{\bar{t}} I(\bar{\tau})\,d\bar{\tau} = W_0 a\bar{t}$$

or

$$\varphi_I(x,y,0+,t) = W_0 a t \tag{36}$$

The pressure coefficient C_p in zone I is then given by Equation (15):

$$C_{p_I}(x,y,0+,t) = -\frac{2}{U^2}W_0 a$$

so that the pressure is seen to be constant in zone I. The value is the piston value, obtainable by elementary considerations as mentioned above. If an effective angle of attack α_0 is defined by $\alpha_0 = \frac{W_0}{U}$, then

$$C_{p_I}(x, y, 0+, t) = -\frac{2\alpha_0}{M} \tag{37}$$

This may be called the initial pressure coefficient. It acts over the entire surface of the wing at time t = 0+, and over a shrinking zone I as t increases, until eventually all points of the wing are influenced by leading-edge disturbances, and zone I vanishes.

Zone II. Inspection of Figure 7 shows that R_w at a given time t is the same for points on lines parallel to the right leading edge in zone II. Therefore φ is constant on such lines, which are the lines

$$x - ky = \text{constant}$$

It is therefore convenient in evaluating φ at a point (x,y) in zone II to eliminate y by introducing a new origin of coordinates at the point (ky,y), the new coordinates being denoted by primes.

For the purposes of the integration in Equation (34), R_w in zone II appears in six different forms, the variations stemming from the different ways in which the leading edge can cut through R, as shown in Figure 8. Intuitively one would expect integration over any of these variations of R_w to lead to the same function for φ in zone II, and this in fact is true, although six superficially different forms of φ result from integration over the six variations. It appears

from Figure 8 that the differences arise from the relative positions of points 1, 2, 4, 5, 6, 7 on the circle bounding the original region R_1 of Figure 6. Points 1 and 2 are the intersection points of this circle with the leading edge. Points 4 and 6 are the points with tangents in the x'-direction, and points 5 and 7 are the tangent points of the lines from the point of evaluation (x',0) bounding the region R_2 of Figure 6. It will be shown later that a change in the relative positions of these points corresponds to a change in the branch of an inverse trigonometric function, and that these changes can be reconciled so that φ is actually given by one function throughout zone II. Only the first form, corresponding to R_w of Figure 8a, will be worked out in detail here, and it will be shown later that the other five reduce to the same form as the first.

In applying Equation (34), it is convenient to evaluate the integral over $(R-R_w)$ as indicated in Figure 8a, and subtract this from the integral over R, which is of course φ_I. Thus

$$\varphi_{II}(x',0,0;t) = W_0 at - \frac{W_0}{2\pi}\int_{\eta_1'}^{\eta_2'} d\eta' \int_{x'-Ut-\sqrt{a^2t^2-\eta'^2}}^{k\eta'} \frac{d\beta'}{\sqrt{(x'-\beta')^2-\beta^2\eta'^2}} \tag{38}$$

where

$$\eta_{1,2}' = \frac{1}{1+k^2}\left\{k(x'-Ut) \mp \sqrt{(1+k^2)a^2t^2-(x'-Ut)^2}\right\}$$

Therefore, after the inner integration is carried out

$$\varphi_{II}(x',0,0;t) = W_0 at - \frac{W_0}{2\pi}\int_{\eta_1'}^{\eta_2'} d\eta' \log\left\{\frac{(Ut+\sqrt{a^2t^2-\eta'^2})+\sqrt{(Ut+\sqrt{a^2t^2-\eta'^2})^2-\beta^2\eta'^2}}{(x'-k\eta')+\sqrt{(x'-k\eta')^2-\beta^2\eta'^2}}\right\} \tag{39}$$

$$= W_0 at - \frac{W_0}{2\pi}\int_{\eta_1'}^{\eta_2'} d\eta' \log\left\{\frac{(M+1)(at+\sqrt{a^2t^2-\eta'^2})}{(x'-k\eta')+\sqrt{(x'-k\eta')^2-\beta^2\eta'^2}}\right\}$$

After integration by parts, Equation (39) can be written in the form

$$\varphi_{II}(x',0,0^+;t) = W_0 at - \frac{W_0}{2\pi}\left[\eta' \log\left\{\frac{(M+1)(at+\sqrt{a^2t^2-\eta'^2})}{(x'-k\eta')+\sqrt{(x'-k\eta')^2-\beta^2\eta'^2}}\right\}\right]_{\eta_1'}^{\eta_2'} - \frac{W_0}{2\pi}\int_{\eta_1'}^{\eta_2'} \frac{\eta'^2 d\eta'}{\sqrt{a^2t^2-\eta'^2}\{at+\sqrt{a^2t^2-\eta'^2}\}}$$

$$+\frac{W_0}{2\pi}\int_{\eta_1'}^{\eta_2'} \frac{k\eta' d\eta'}{\sqrt{(x'-k\eta')^2-\beta^2\eta'^2}} + \frac{W_0}{2\pi}\int_{\eta_1'}^{\eta_2'} \frac{\beta^2\eta'^2 d\eta'}{\sqrt{(x'-k\eta')^2-\beta^2\eta'^2}\{(x'-k\eta')+\sqrt{(x'-k\eta')^2-\beta^2\eta'^2}\}}$$

$$= W_0 at - \frac{W_0}{2\pi}\left[\eta' \log\left\{\frac{(M+1)(at+\sqrt{a^2t^2-\eta'^2})}{(x'-k\eta')+\sqrt{(x'-k\eta')^2-\beta^2\eta'^2}}\right\}\right]_{\eta_1'}^{\eta_2'} - \frac{W_0}{2\pi}\int_{\eta_1'}^{\eta_2'} \frac{at\, d\eta'}{\sqrt{a^2t^2-\eta'^2}} + \frac{W_0}{2\pi}\int_{\eta_1'}^{\eta_2'} d\eta'$$

$$+\frac{W_0}{2\pi}\int_{\eta_1'}^{\eta_2'} \frac{k\eta' d\eta'}{\sqrt{(x'-k\eta')^2-\beta^2\eta'^2}} + \frac{W_0}{2\pi}\int_{\eta_1'}^{\eta_2'} \frac{(x'-k\eta')\, d\eta'}{\sqrt{(x'-k\eta')^2-\beta^2\eta'^2}} - \frac{W_0}{2\pi}\int_{\eta_1'}^{\eta_2'} d\eta' \qquad (40)$$

In Equation (40), the logarithmic term vanishes identically because the numerator and denominator of the logarithm are equal at both limits. Other terms cancel, and the two integrals remaining are evaluated directly without difficulty, the result being

$$\varphi_{II}(x',0,0^+;t) = W_0 at - \frac{W_0 at}{2\pi}\left[\sin^{-1}\left\{\frac{\eta'}{at}\right\}\right]_{\eta_1'}^{\eta_2'} + \frac{W_0 x'}{2\pi\sqrt{\beta^2-k^2}}\left[\sin^{-1}\left\{\frac{kx'+(\beta^2-k^2)\eta'}{\beta x'}\right\}\right]_{\eta_1'}^{\eta_2'} \qquad (41)$$

where all inverse functions are principal values.

With the values of η_2' and η_1' as given by Equation (38), Equation (41) is rather complicated algebraically. Fortunately it can be simplified considerably. From Figure 8a it can be seen that

$$\sin^{-1}\left\{\frac{\eta_2'}{at}\right\} - \sin^{-1}\left\{\frac{\eta_1'}{at}\right\} = \gamma = 2\cos^{-1}\left\{\frac{x'-Ut}{\sqrt{1+k^2}\,at}\right\} \qquad (42)$$

so that the first two terms of Equation (41) can be rewritten:

$$W_0 at - \frac{W_0 at}{2\pi}\left[\sin^{-1}\left\{\frac{\eta'}{at}\right\}\right]_{\eta_1'}^{\eta_2'} = \frac{W_0 at}{2\pi}\left[2\pi - 2\cos^{-1}\left\{\frac{x'-Ut}{\sqrt{1+k^2}\,at}\right\}\right] = \frac{W_0 at}{\pi}\cos^{-1}\left\{\frac{Ut-x'}{\sqrt{1+k^2}\,at}\right\} \qquad (43)$$

where

$$\frac{\pi}{2} + \sigma \leq \cos^{-1}\left\{\frac{Ut - x'}{\sqrt{1+k^2}\,at}\right\} \leq \pi \tag{43a}$$

The lower limit corresponds to coincidence of points 2 and 6, and the upper limit to coincidence of points 1 and 2 on the left side of the circle.

The last term of Equation (41) is simplified through the use of trigonometric identities. Thus

$$\left\{\frac{kx' + (\beta^2 - k^2)\eta_2'}{\beta x'}\right\} = \left\{\frac{k\{(1+k^2)x' + (\beta^2-k^2)(x'-Ut)\} + (\beta^2-k^2)\sqrt{(1+k^2)a^2t^2 - (x'-Ut)^2}}{\beta x'(1+k^2)}\right\}$$

$$= \left\{\frac{Mk}{\beta\sqrt{1+k^2}}\right\}\left\{\frac{Mx' - (\beta^2-k^2)at}{\sqrt{1+k^2}\,x'}\right\} + \left\{\frac{\sqrt{\beta^2-k^2}}{\beta\sqrt{1+k^2}}\right\}\left\{\frac{\sqrt{\beta^2-k^2}\sqrt{(1+k^2)a^2t^2 - (x'-Ut)^2}}{\sqrt{1+k^2}\,x'}\right\}$$

or, symbolically,

$$G = g_1 g_2 + \sqrt{1-g_1^2}\,\sqrt{1-g_2^2}$$

Therefore

$$\sin^{-1} G = \sin^{-1} g_1 + \cos^{-1} g_2$$

or

$$\sin^{-1}\left\{\frac{kx' + (\beta^2-k^2)\eta_2'}{\beta x'}\right\} = \sin^{-1}\left\{\frac{Mk}{\beta\sqrt{1+k^2}}\right\} + \cos^{-1}\left\{\frac{Mx' - (\beta^2-k^2)at}{\sqrt{1+k^2}\,x'}\right\} \tag{44}$$

Similarly

$$\sin^{-1}\left\{\frac{kx' + (\beta^2-k^2)\eta_1'}{\beta x'}\right\} = \sin^{-1}\left\{\frac{Mk}{\beta\sqrt{1+k^2}}\right\} - \cos^{-1}\left\{\frac{Mx' - (\beta^2-k^2)at}{\sqrt{1+k^2}\,x'}\right\} \tag{45}$$

All inverse functions in Equations (44) and (45) are principal values, and in particular

$$\sin^{-1}\left\{\frac{Mk}{\beta\sqrt{1+k^2}}\right\} \leq \sin^{-1}\left\{\frac{kx'+(\beta^2-k^2)\eta_2'}{\beta x'}\right\} \leq \sin^{-1}\left\{\frac{Mk+\beta^2}{\beta(M+k)}\right\} \tag{44a}$$

and

$$\sin^{-1}\left\{\frac{Mk+1-M^2\left(\frac{1-k^2}{1+k^2}\right)}{\beta(M+k)}\right\} \leq \sin^{-1}\left\{\frac{kx'+(\beta^2-k^2)\eta_1'}{\beta x'}\right\} \leq \sin^{-1}\left\{\frac{Mk}{\beta\sqrt{1+k^2}}\right\} \tag{45a}$$

The limit $\sin^{-1}\left\{\frac{Mk}{\beta\sqrt{1+k^2}}\right\}$ in Equations (44a) and 45a) corresponds to coincidence of points 1 and 2 on the left side of the circle, and the other limits to coincidence of points 6 and 2. It follows that

$$0 \leq \cos^{-1}\left\{\frac{Mx'-(\beta^2-k^2)at}{\sqrt{1+k^2}\,x'}\right\} \leq \cos^{-1}\left\{\frac{1+k^2+Mk}{(M+k)\sqrt{1+k^2}}\right\} < \frac{\pi}{2} \tag{46}$$

where

$$\cos^{-1}\left\{\frac{1+k^2+Mk}{(M+k)\sqrt{1+k^2}}\right\} = \sin^{-1}\left\{\frac{Mk+\beta^2}{\beta(M+k)}\right\} - \sin^{-1}\left\{\frac{Mk}{\beta\sqrt{1+k^2}}\right\} = \sin^{-1}\left\{\frac{Mk}{\beta\sqrt{1+k^2}}\right\} - \sin^{-1}\left\{\frac{Mk+1-M^2\left(\frac{1-k^2}{1+k^2}\right)}{\beta(M+k)}\right\}$$

Therefore, with the application of Equations (43), (44), and (45) to Equation (41), it becomes

$$\varphi_{II}(x',0,0+,t) = \frac{W_0 at}{\pi}\cos^{-1}\left\{\frac{Ut-x'}{\sqrt{1+k^2}\,at}\right\} + \frac{W_0 x'}{\pi\sqrt{\beta^2-k^2}}\cos^{-1}\left\{\frac{Mx'-(\beta^2-k^2)at}{\sqrt{1+k^2}\,x'}\right\} \tag{47}$$

where the inverse functions are principal values as specified by Equations (43a) and (46).

Equation (47) gives φ_{II} corresponding to the R_w of Figure 8a. It was obtained by simplifying Equation (41). When the equations for φ_{II} equivalent to Equation (41) are worked out for the other five variations of R_w, each can be expressed in two terms. In all cases the first term appears either in the form

$$\frac{W_0 at}{2\pi}\mathcal{F}_1 = \frac{W_0 at}{2\pi}\left[\pi + \sin^{-1}\left\{\frac{\eta_2'}{at}\right\} + \sin^{-1}\left\{\frac{\eta_1'}{at}\right\}\right]$$

or in the form

$$\frac{W_0 at}{2\pi}\mathcal{F}_2 = \frac{W_0 at}{2\pi}\left[\sin^{-1}\left\{\frac{\eta_2'}{at}\right\} - \sin^{-1}\left\{\frac{\eta_1'}{at}\right\}\right]$$

and the second term appears either in the form of Equation (41) or in one of the forms

$$\frac{W_0 x'}{2\pi\sqrt{\beta^2-k^2}}\mathcal{F}_3 = \frac{W_0 x'}{2\pi\sqrt{\beta^2-k^2}}\left[\pi - \sin^{-1}\left\{\frac{kx'+(\beta^2-k^2)\eta_2'}{\beta x'}\right\} - \sin^{-1}\left\{\frac{kx'+(\beta^2-k^2)\eta_1'}{\beta x'}\right\}\right]$$

or

$$\frac{W_0 x'}{2\pi\sqrt{\beta^2-k^2}}\mathcal{F}_4 = \frac{W_0 x'}{2\pi\sqrt{\beta^2-k^2}}\left[2\pi - \sin^{-1}\left\{\frac{kx'+(\beta^2-k^2)\eta_2'}{\beta x'}\right\} + \sin^{-1}\left\{\frac{kx'+(\beta^2-k^2)\eta_1'}{\beta x'}\right\}\right]$$

Again all inverse functions are principal values.

Now $\mathcal{F}_1$ corresponds to variations (b) and (d) of R_w in Figure 8. In these, points 6 and 2 have their order on the circle reversed from that of variation (a), and it can be seen from the figures that the geometric angle given in Figure 8a by $\sin^{-1}\left\{\frac{\eta_2'}{at}\right\}$ is given in Figures 8b and 8d by $\pi - \sin^{-1}\left\{\frac{\eta_2'}{at}\right\}$. Thus $\mathcal{F}_1$ represents the same geometric angle as the bracketed term in Equation (43), and it can be expressed in the form of Equation (43). The same is true of $\mathcal{F}_2$, which corresponds to variations (c), (e), and (f) of R_w. In these, points 4 and 1 also have their order reversed on the circle. Therefore

$$\mathcal{F}_1 = 2\pi - \gamma = 2\cos^{-1}\left\{\frac{Ut - x'}{\sqrt{1+k^2}\,at}\right\} \qquad (48)$$

where

$$j = 1,2 \qquad 0 \le \cos^{-1}\left\{\frac{Ut - x'}{\sqrt{1+k^2}\,at}\right\} \le \frac{\pi}{2} + \sigma \tag{48a}$$

so that $\frac{W_0 at}{2\pi}\mathcal{F}_1$ and $\frac{W_0 at}{2\pi}\mathcal{F}_2$ reduce to the first term of Equation (47). The lower limit in Equation (48a) corresponds to coincidence of points 1 and 2 on the right side of the circle, and the upper limit agrees with the lower limit of Equation (43a).

The second term of the equations for φ corresponding to variations (b) and (c) of R_w in Figure 8 appears in the form of Equation (41). The analysis leading to Equations (44) and (45) is used again without change, and the second term reduces to the second term of Equation (47). Here

$$\cos^{-1}\left\{\frac{1+k^2+Mk}{(M+k)\sqrt{1+k^2}}\right\} \le \cos^{-1}\left\{\frac{Mx' - (\beta^2-k^2)at}{\sqrt{1+k^2}\,x'}\right\} \le \frac{\pi}{2} - \sin^{-1}\left\{\frac{Mk}{\beta\sqrt{1+k^2}}\right\} \tag{49}$$

The lower limit in Equation (49) agrees with the upper limit in Equation (46), and the upper limit corresponds to coincidence of points 2 and 7.

$\mathcal{F}_3$ corresponds to variations (d) and (e) of R_w, in which points 2 and 7 have their order on the circle reversed from that of variations (a), (b), and (c). This reversal means a change in the branch of the angle previously represented by $\sin^{-1}\left\{\frac{kx' + (\beta^2-k^2)\eta_2'}{\beta x'}\right\}$. Similarly $\mathcal{F}_4$ corresponds to variation (f) of R_w, in which points 1 and 5 also have their order reversed, resulting in a change in the

branch of the angle previously represented by $-\sin^{-1}\left\{\frac{kx'+(\beta^2-k^2)\eta_1'}{\beta x'}\right\}$.

Thus to reduce $\frac{W_0 x'}{2\pi\sqrt{\beta^2-k^2}}\mathcal{F}_3$ and $\frac{W_0 x'}{2\pi\sqrt{\beta^2-k^2}}\mathcal{F}_4$ to the second term of Equation (47), it is necessary only to observe that in $\mathcal{F}_3$

$$\pi - \sin^{-1}\left\{\frac{kx'+(\beta^2-k^2)\eta_2'}{\beta x'}\right\}, \text{ where } -\sin^{-1}\left\{\frac{Mk}{\beta\sqrt{1+k^2}}\right\} \le \sin^{-1}\{\} \le \frac{\pi}{2}$$

can be replaced by

$$\sin^{-1}\left\{\frac{kx'+(\beta^2-k^2)\eta_2'}{\beta x'}\right\}, \text{ where } \frac{\pi}{2} \le \sin^{-1}\{\} \le \pi + \sin^{-1}\left\{\frac{Mk}{\beta\sqrt{1+k^2}}\right\}$$

Then the analysis leading to Equation (44) goes through as before, and the condition

$$\frac{\pi}{2} - \sin^{-1}\left\{\frac{Mk}{\beta\sqrt{1+k^2}}\right\} \le \cos^{-1}\left\{\frac{Mx'-(\beta^2-k^2)at}{\sqrt{1+k^2}\,x'}\right\} \le \pi \qquad (50)$$

results. The lower limit agrees with the upper limit of Equation (49), and the upper limit corresponds to coincidence of points 1 and 2 on the right side of the circle. Similar statements apply to the change in branch of the other angle, occurring in $\mathcal{F}_4$. It follows that Equation (47) is valid throughout zone II. Finally, the potential in zone II is written in terms of the original coordinates:

$$\varphi_{II}(x,y,0+,t) = \frac{W_0 at}{\pi}\cos^{-1}\left\{\frac{Mat-(x-ky)}{\sqrt{1+k^2}\,at}\right\} + \frac{W_0(x-ky)}{\pi\sqrt{\beta^2-k^2}}\cos^{-1}\left\{\frac{M(x-ky)-(\beta^2-k^2)at}{\sqrt{1+k^2}\,(x-ky)}\right\} \qquad (51)$$

where

$$0 \le \cos^{-1}\{\} \le \pi \qquad (51a)$$

The limits in Equation (51a) result from Equations (43a), (46), (48a), (49), and (50).

The pressure coefficient in zone II is obtained by applying Equation (15) to Equation (51). Terms arising from differentiation of the inverse functions cancel identically, and the result is

$$C_{p_{II}}(x,y,0+,t) = -\frac{2\alpha_0}{\pi}\left[\frac{1}{M}\cos^{-1}\left\{\frac{Mat-(x-ky)}{\sqrt{1+k^2}\,at}\right\} + \frac{1}{\sqrt{\beta^2-k^2}}\cos^{-1}\left\{\frac{M(x-ky)-(\beta^2-k^2)at}{\sqrt{1+k^2}(x-ky)}\right\}\right] \tag{52}$$

where

$$0 \leq \cos^{-1}\{\;\} \leq \pi$$

Zone III. Inspection of Figure 7 shows that R_w in zone III does not vary with time and is the same for points on lines parallel to the right leading edge. R_w is shown in Figure 9, and Equation (34) takes the form, using primed coordinates again,

$$\varphi_{III}(x',0,0+,t) = \frac{W_0}{\pi}\iint_{R_w}\frac{d\xi'd\eta'}{\sqrt{(x'-\xi')^2-\beta^2\eta'^2}} \tag{53}$$

This integral is easily evaluated, and Puckett (Reference 3) has given the results, which are

$$\varphi_{III}(x',0,0+,t) = \frac{W_0 x'}{\sqrt{\beta^2-k^2}} \tag{54}$$

and

$$C_{p_{III}}(x',0,0+,t) = -\frac{2\alpha_0}{\sqrt{\beta^2-k^2}} \tag{55}$$

In the original coordinates, then,

$$\varphi_{III}(x,y,0+,t) = \frac{W_0(x-ky)}{\sqrt{\beta^2-k^2}} \tag{56}$$

and

$$C_{p_{III}}(x,y,0+,t) = -\frac{2\alpha_0}{\sqrt{\beta^2-k^2}} \tag{57}$$

so that the pressure is constant in zone III. It can be seen from Figure 7 that zone III is initially a narrow strip along the right leading edge which expands with time until eventually it covers the entire right wing outside the Mach cone from the vertex. Thus the steady-state pressure, reached when the transient effect of the increment in downwash has disappeared, for points on the wing outside the Mach cone from the vertex is given by $C_{p_{III}}$.

The relation between zones I, II, and III can be seen by considering such a point (x,y) on the wing as time increases from zero. Initially the point lies in zone I, and the pressure given by C_{p_I} acts on it. The point remains in zone I during the time interval

$$0 < t \leq \frac{x-ky}{U+a\sqrt{1+k^2}}$$

At the upper time limit the point passes into zone II, and it is seen that Equation (52) reduces to Equation (37) for $t = \frac{x-ky}{U+a\sqrt{1+k^2}}$, so that the pressure is continuous. The point lies in zone II, acted on by the pressure given by $C_{p_{II}}$, during the time interval

$$\frac{x-ky}{U+a\sqrt{1+k^2}} < t \leq \frac{x-ky}{U-a\sqrt{1+k^2}}$$

after which it passes into zone III, where it remains. Equation (52) reduces to Equation (57) for $t = \frac{x-ky}{U-a\sqrt{1+k^2}}$ so that the pressure is again continuous.

Thus zones I, II, and III give respectively the initial, transient, and steady-state effects at the point.

c. Pressure in Zones IV, V, and VI. It is convenient to group zones IV, V, and VI together because the results for them are either already known or obtainable by superposition of known results.

Zone IV. It can be seen from Figure 7 that points in zone IV are influenced by disturbances from both leading edges, but not by disturbances from the neighbourhood of the vertex. Thus R_w for a point in zone IV is as shown in Figure 10a, and Equation (34) could be applied using this R_w directly. However, Figs. 10b, 10c, and 10d show that

$$R_w = R_b + R_c - R$$

and the integral in Equation (34) taken over R_b is seen to be φ_{II} as given by Equation (51), while the integral over R is of course φ_I as given by Equation (36). Moreover, the integral over R_c gives the counterpart of φ_{II} for the left wing and is accordingly given, from the symmetry of conditions about the wing center line, by Equation (51) with -k replacing k everywhere. Therefore the potential in zone IV is given immediately by

$$\varphi_{\underline{IV}}(x,y,0+,t) = \varphi_{\underline{II}}(x,y,0+,t;k) + \varphi_{\underline{II}}(x,y,0+,t;-k) - \varphi_{\underline{I}}(x,y,0+,t)$$

$$= \frac{W_0 at}{\pi}\left[\cos^{-1}\left\{\frac{Mat-(x-ky)}{\sqrt{1+k^2}\,at}\right\} - \cos^{-1}\left\{\frac{(x+ky)-Mat}{\sqrt{1+k^2}\,at}\right\}\right] \qquad (58)$$

$$+ \frac{W_0}{\pi\sqrt{\beta^2-k^2}}\left[(x-ky)\cos^{-1}\left\{\frac{M(x-ky)-(\beta^2-k^2)at}{\sqrt{1+k^2}\,(x-ky)}\right\} + (x+ky)\cos^{-1}\left\{\frac{M(x+ky)-(\beta^2-k^2)at}{\sqrt{1+k^2}\,(x+ky)}\right\}\right]$$

where

$$0 \le \cos^{-1}\{\ \} \le \pi$$

The pressure coefficient in zone IV is given in the same way by

$$C_{p_{\underline{IV}}}(x,y,0+,t) = -\frac{2\alpha_0}{\pi M}\left[\cos^{-1}\left\{\frac{Mat-(x-ky)}{\sqrt{1+k^2}\,at}\right\} - \cos^{-1}\left\{\frac{(x+ky)-Mat}{\sqrt{1+k^2}\,at}\right\}\right]$$

$$(59)$$

$$-\frac{2\alpha_0}{\pi\sqrt{\beta^2-k^2}}\left[\cos^{-1}\left\{\frac{M(x-ky)-(\beta^2-k^2)at}{\sqrt{1+k^2}\,(x-ky)}\right\} + \cos^{-1}\left\{\frac{M(x+ky)-(\beta^2-k^2)at}{\sqrt{1+k^2}\,(x+ky)}\right\}\right]$$

where

$$0 \le \cos^{-1}\{\ \} \le \pi$$

Thus the results for zone IV are obtained simply by superposition of previous results.

Zone V. It can be seen from Figure 7 that points in zone V are influenced by disturbances from both leading edges, and that R_w for a point does not change with time. R_w is shown in Figure 11, and application of Equation (34) is made without difficulty. Puckett (Ref. 3) has given the results, which are

$$\varphi_{\underline{V}}(x,y,0+,t) = \frac{W_0}{\pi\sqrt{\beta^2-k^2}}\left[(x-ky)\cos^{-1}\left\{\frac{kx-\beta^2 y}{\beta(x-ky)}\right\} + (x+ky)\cos^{-1}\left\{\frac{kx+\beta^2 y}{\beta(x+ky)}\right\}\right] \qquad (60)$$

where

$$0 \leq \cos^{-1}\{\ \} \leq \pi$$

and

$$C_{p_V}(x,y,0+,t) = -\frac{4\alpha_0}{\pi\sqrt{\beta^2-k^2}}\cos^{-1}\left\{\frac{k}{\beta}\sqrt{\frac{x^2-\beta^2y^2}{x^2-k^2y^2}}\right\} \tag{61}$$

where

$$0 \leq \cos^{-1}\{\ \} \leq \frac{\pi}{2}$$

The flow is here seen to be conical in space. The pressure, for example, is constant on conical rays through the vertex in zone V. Conditions in zone V are not time-dependent, and just as $C_{p_{III}}$ gives the steady-state pressure for points on the right wing outside the Mach cone from the vertex, so does C_{pV} give the steady-state pressure for points inside. Eventually zone V covers the whole right wing inside the Mach cone from the vertex.

Zone VI. Points in zone VI are found to be influenced by disturbances from both leading edges, and R_w for a point is shown in Figure 12a. Again, instead of applying Equation (34) directly to R_w, it is convenient to use the superposition of zones indicated by Figures 12b, 12c, and 12d. Thus

$$R_w = R_b + R_c - R_d$$

and the integrals from Equation (34) taken over R_b, R_c, and R_d separately give respectively φ_{II}, φ_V, and φ_{III}. Therefore

$$\varphi_{\underline{VI}}(x,y,0+,t) = \varphi_{\underline{II}}(x,y,0+,t) + \varphi_{\underline{V}}(x,y,0+,t) - \varphi_{\underline{III}}(x,y,0+,t)$$

$$= \frac{W_0 at}{\pi} \cos^{-1}\left\{\frac{Mat-(x-ky)}{\sqrt{1+k^2}\,at}\right\} + \frac{W_0(x+ky)}{\pi\sqrt{\beta^2-k^2}} \cos^{-1}\left\{\frac{kx+\beta^2 y}{\beta(x+ky)}\right\} \qquad (62)$$

$$+ \frac{W_0(x-ky)}{\pi\sqrt{\beta^2-k^2}}\left[\cos^{-1}\left\{\frac{kx-\beta^2 y}{\beta(x-ky)}\right\} - \cos^{-1}\left\{\frac{(\beta^2-k^2)at-M(x-ky)}{\sqrt{1+k^2}\,(x-ky)}\right\}\right]$$

where

$$0 \le \cos^{-1}\{\ \} \le \pi$$

The pressure coefficient in zone VI is given in the same way by

$$C_{p_{\underline{VI}}}(x,y,0+,t) = -\frac{2\alpha_0}{\pi M} \cos^{-1}\left\{\frac{Mat-(x-ky)}{\sqrt{1+k^2}\,at}\right\}$$

$$-\frac{2\alpha_0}{\pi\sqrt{\beta^2-k^2}}\left[2\cos^{-1}\left\{\frac{k}{\beta}\sqrt{\frac{x^2-\beta^2y^2}{x^2-k^2y^2}}\right\} - \cos^{-1}\left\{\frac{(\beta^2-k^2)at-M(x-ky)}{\sqrt{1+k^2}\,(x-ky)}\right\}\right] \qquad (63)$$

where

$$0 \le \cos^{-1}\{\ \} \le \pi$$

This completes the results for zones IV, V, and VI.

d. Pressure in Zone VII. It is clear from Figure 7 that R_w for points in zone VII will always have the vertex of the wing inside the circular region R_1 of Figure 6, as shown in Figure 13a. Equation (34) can be applied directly to R_w, but it is again more convenient to use a superposition of zones, as indicated by Figures 13a, 13b, and 13c. Thus

$$R_w = R_b - R_c$$

and the integral from Equation (34) taken over R_b is $\varphi_{\underline{II}}$, as given by Equation (51). The integral taken over R_c remains to be calculated.

Now intuition suggests that φ ought to be given by the same function throughout zone VII. Nevertheless, because of the several possible shapes R_c may take, six superficially different forms of φ for zone VII can be obtained. Variations of R_c giving rise to these six forms are shown in Figures 13d through 13i. It appears from the figures that the differences arise from the relative positions of points 1, 3, 4, and 5 on the circle bounding the original region R_1 of Figure 6. Point 3 is the intersection point of this circle with the left leading edge, and points 1, 4, and 5 have the same significance as in Figure 8. It will be shown later that a change in the relative positions of these points corresponds, as before, to a change in the branch of an inverse trigonometric function, and that these changes can be reconciled so that φ is actually given by one function throughout zone VII.

Integration over R_c will be carried out in detail only for the shape shown in Figure 13d. Thus

$$\varphi_{VII}(x,y,0;t) = \varphi_{II}(x,y,0;t) - \frac{W_0}{2\pi}\int_{\eta_3}^{\eta_1} d\eta \int_{x-Ut-\sqrt{a^2t^2-(y-\eta)^2}}^{-k\eta} \frac{d\xi}{\sqrt{(x-\xi)^2-\beta^2(y-\eta)^2}} - \frac{W_0}{2\pi}\int_{\eta_1}^{k\eta} d\eta \int_{0}^{-k\eta} \frac{d\xi}{\sqrt{(x-\xi)^2-\beta^2(y-\eta)^2}} \qquad (64)$$

where

$$\eta_3' = \frac{1}{1+k^2}\left[y \pm k(x-Ut) - \sqrt{(1+k^2)a^2t^2-(x \mp ky - Ut)^2} \right]$$

When the inner integrations are performed and the result is simplified slightly as in Equation (39), Equation (64) becomes

$$\varphi_{\underline{VII}}(x,y,0+,t) = \varphi_{\underline{II}}(x,y,0+,t) - \frac{W_0}{2\pi}\int_{\eta_3}^{\eta_1} d\eta \log\left\{\frac{(M+1)(at+\sqrt{a^2t^2-(y-\eta)^2})}{(x+k\eta)+\sqrt{(x+k\eta)^2-\beta^2(y-\eta)^2}}\right\}$$
$$-\frac{W_0}{2\pi}\int_{\eta_1}^{0} d\eta \log\left\{\frac{(x-k\eta)+\sqrt{(x-k\eta)^2-\beta^2(y-\eta)^2}}{(x+k\eta)+\sqrt{(x+k\eta)^2-\beta^2(y-\eta)^2}}\right\} \tag{65}$$

Next integration by parts is carried out for the two integrals in Equation (65), similar to that leading to Equation (40). Again the combination of logarithmic terms which results vanishes identically, and the remaining integrals are of the same type as those in Equation (40) and either cancel one another or lead to inverse trigonometric functions. Thus

$$\varphi_{\underline{VII}}(x,y,0+,t) = \varphi_{\underline{II}}(x,y,0+,t) - \frac{W_0 at}{2\pi}\left[\sin^{-1}\left\{\frac{y-\eta}{at}\right\}\right]_{\eta_1}^{\eta_3} - \frac{W_0}{2\pi\sqrt{\beta^2-k^2}}\left[(x-ky)\sin^{-1}\left\{\frac{kx-\beta^2 y}{\beta(x-ky)}\right\} - (x+ky)\sin^{-1}\left\{\frac{-kx-\beta^2 y}{\beta(x+ky)}\right\}\right] \tag{66}$$
$$-\frac{W_0}{2\pi\sqrt{\beta^2-k^2}}\left[(x+ky)\sin^{-1}\left\{\frac{-k(x+ky)-(\beta^2-k^2)(y-\eta_3)}{\beta(x+ky)}\right\} - (x-ky)\sin^{-1}\left\{\frac{k(x-ky)-(\beta^2-k^2)(y-\eta_1)}{\beta(x-ky)}\right\}\right]$$

where all inverse functions are principal values. Like Equation (41), Equation (66) can be simplified considerably.

From Figure 13j it can be seen that

$$\sin^{-1}\left\{\frac{y-\eta_3}{at}\right\} - \sin^{-1}\left\{\frac{y-\eta_1}{at}\right\} = \gamma_k \tag{67}$$

But from the results for zone II, the first term in $\varphi_{\underline{II}}$ in Equation (66), as given by Equation (51), is the angle Γ_k in Figure 13j multiplied by $\frac{W_0 at}{2\pi}$. Therefore all terms in Equation (66) multiplied by $\frac{W_0 at}{2\pi}$ can be combined in the form

$$\frac{W_0 at}{2\pi}\left[\Gamma_k - \gamma_k\right] = \frac{W_0 at}{2\pi}\Gamma \tag{68}$$

where Γ is shown in Figure 13j. It is desirable to express Γ simply in terms of the coordinates, and this can be done by observing that also

$$\Gamma = \Gamma_{-k} - \gamma_{-k} \tag{69}$$

where Γ_{-k} and γ_{-k} are shown in Figure 13j. Γ_{-k} is clearly the angle corresponding to Γ_k but appearing in the first term of the expression for φ_{II} on the left wing. Therefore

$$2\Gamma = \Gamma_k + \Gamma_{-k} - (\gamma_k + \gamma_{-k})$$

But in Figure 13j

$$\gamma_k = 2\{\text{angle } 183\} \quad , \quad \gamma_{-k} = 2\{\text{angle } 218\}$$

Therefore

$$\Gamma = \frac{1}{2}\{\Gamma_k + \Gamma_{-k}\} - 2\sigma \tag{70}$$

Thus Equation (68) can be written simply in the form

$$\frac{W_0 at}{2\pi}\Gamma = \frac{W_0 at}{2\pi}\left[\cos^{-1}\left\{\frac{Mat-(x-ky)}{\sqrt{1+k^2}\,at}\right\} + \cos^{-1}\left\{\frac{Mat-(x+ky)}{\sqrt{1+k^2}\,at}\right\} - 2\sigma\right] \tag{71}$$

where the inverse functions are principal values.

The first step in simplifying the remainder of Equation (66) is to eliminate the unwieldy forms

$$\sin^{-1}\left\{\frac{k(x-ky)-(\beta^2-k^2)(y-\eta_1)}{\beta(x-ky)}\right\} \quad \text{and} \quad \sin^{-1}\left\{\frac{-k(x+ky)-(\beta^2-k^2)(y-\eta_3)}{\beta(x+ky)}\right\}$$

Comparison of Figure 13j with Figure 8a shows that, with the

appropriate change of variables, both of these functions are equivalent, one for the right leading edge and the other for the left, to the function

$$\sin^{-1}\left\{\frac{kx'+(\beta^2-k^2)\eta_1'}{\beta x'}\right\}$$

discussed in the analysis for zone II. In particular, the analysis which led to Equation (45) goes through as before, and the two equations result:

$$\sin^{-1}\left\{\frac{k(x-ky)-(\beta^2-k^2)(y-\eta_1)}{\beta(x-ky)}\right\}=\sin^{-1}\left\{\frac{Mk}{\beta\sqrt{1+k^2}}\right\}-\cos^{-1}\left\{\frac{M(x-ky)-(\beta^2-k^2)a\tau}{\sqrt{1+k^2}(x-ky)}\right\} \quad (72)$$

and

$$\sin^{-1}\left\{\frac{-k(x+ky)-(\beta^2-k^2)(y-\eta_3)}{\beta(x+ky)}\right\}=\sin^{-1}\left\{\frac{-Mk}{\beta\sqrt{1+k^2}}\right\}-\cos^{-1}\left\{\frac{M(x+ky)-(\beta^2-k^2)a\tau}{\sqrt{1+k^2}(x+ky)}\right\} \quad (73)$$

where all inverse functions are principal values. To complete the simplification of Equation (66), Equations (72) and (73) are applied to it, the resulting terms are combined with the remaining term of $\varphi_{\underline{II}}$, and all remaining inverse sines are expressed as inverse cosines. The resulting expression may be written

$$\varphi_{\underline{VII}}(x,y,0;t)=\frac{W_0 a\tau}{2\pi}\left[\cos^{-1}\left\{\frac{Ma\tau-(x-ky)}{\sqrt{1+k^2}\,a\tau}\right\}+\cos^{-1}\left\{\frac{Ma\tau-(x+ky)}{\sqrt{1+k^2}\,a\tau}\right\}-2\sigma\right]$$

$$+\frac{W_0(x-ky)}{2\pi\sqrt{\beta^2-k^2}}\left[\cos^{-1}\left\{\frac{M(x-ky)-(\beta^2-k^2)a\tau}{\sqrt{1+k^2}(x-ky)}\right\}+\cos^{-1}\left\{\frac{kx-\beta^2y}{\beta(x-ky)}\right\}-\cos^{-1}\left\{\frac{Mk}{\beta\sqrt{1+k^2}}\right\}\right] \quad (74)$$

$$+\frac{W_0(x+ky)}{2\pi\sqrt{\beta^2-k^2}}\left[\cos^{-1}\left\{\frac{M(x+ky)-(\beta^2-k^2)a\tau}{\sqrt{1+k^2}(x+ky)}\right\}+\cos^{-1}\left\{\frac{kx+\beta^2y}{\beta(x+ky)}\right\}-\cos^{-1}\left\{\frac{Mk}{\beta\sqrt{1+k^2}}\right\}\right]$$

where all inverse functions are principal values.

Equation (74) gives φ_{VII} for R_w corresponding to Figure 13d. It was obtained by simplifying Equation (66). That the equations equivalent to Equation (66) obtained for the other variations of R_w all reduce to Equation (74) follows readily from the analysis for zone II. Thus, as before, whenever the order on the circle of point 4 in Figure 13 changes with respect to point 1 or point 3 the branch of one of the inverse functions multiplied by $\frac{W_0 at}{2\pi}$ changes, and the term multiplied by $-\frac{W_0 at}{2\pi}$ obtained after integration is superficially different from the corresponding term of Equation (66). In all cases, however, the term is still represented by the geometrical angle γ_k, and so Equation (71) still results and the inverse functions in it are still principal values. Similarly, whenever the order on the circle of point 5 in Figure 13 changes with respect to point 1 or point 3 the branch of one of the inverse functions on the left side of Equations (72) and (73) changes, and the terms multiplied by $\frac{W_0}{2\pi\sqrt{\beta^2-k^2}}$ obtained after integration appear different from the corresponding terms of Equation (66). Again, however, the differences are superficial and Equations (72) and (73) still hold. Moreover, despite the change in branch of the functions on the left side of these two equations, the functions on the right side remain principal values. Accordingly, all forms in which φ_{VII} is first obtained reduce to Equation (74), so that this equation

holds throughout zone VII, and all inverse functions in it are principal values.

The pressure coefficient in zone VII is obtained simply by first observing that Equation (74) can be written in the form

$$\varphi_{\underline{VII}}(x,y,0+,t) = \frac{1}{2}\left[\varphi_{\underline{II}}(x,y,0+,t;k) + \varphi_{\underline{II}}(x,y,0+,t;-k) + \varphi_{\underline{V}}(x,y,0+,t)\right]$$

$$-\frac{W_0}{\pi}\left[at\cos^{-1}\left\{\frac{1}{\sqrt{1+k^2}}\right\} + \frac{x}{\sqrt{\beta^2-k^2}}\cos^{-1}\left\{\frac{Mk}{\beta\sqrt{1+k^2}}\right\}\right]$$

When Equation (15) is applied to this form the result is known for the first bracketed term and easily calculated for the second. Thus the pressure coefficient in zone VII is given by

$$C_{p_{\underline{VII}}}(x,y,0+,t) = \frac{1}{2}\left[C_{p_{\underline{II}}}(x,y,0+,t;k) + C_{p_{\underline{II}}}(x,y,0+,t;-k) + C_{p_{\underline{V}}}(x,y,0+,t)\right]$$

$$+\frac{2\alpha_0}{\pi}\left[\frac{1}{M}\cos^{-1}\left\{\frac{1}{\sqrt{1+k^2}}\right\} + \frac{1}{\sqrt{\beta^2-k^2}}\cos^{-1}\left\{\frac{Mk}{\beta\sqrt{1+k^2}}\right\}\right]$$

or, by substitution from Equations (52) and (61),

$$C_{p_{\underline{VII}}}(x,y,0+,t) = -\frac{\alpha_0}{\pi M}\left[\cos^{-1}\left\{\frac{Mat-(x-ky)}{\sqrt{1+k^2}\,at}\right\} + \cos^{-1}\left\{\frac{Mat-(x+ky)}{\sqrt{1+k^2}\,at}\right\} - 2\cos^{-1}\left\{\frac{1}{\sqrt{1+k^2}}\right\}\right]$$

$$-\frac{\alpha_0}{\pi\sqrt{\beta^2-k^2}}\left[\cos^{-1}\left\{\frac{M(x-ky)-(\beta^2-k^2)at}{\sqrt{1+k^2}(x-ky)}\right\} + \cos^{-1}\left\{\frac{M(x+ky)-(\beta^2-k^2)at}{\sqrt{1+k^2}(x+ky)}\right\} + 2\cos^{-1}\left\{\frac{k}{\beta}\sqrt{\frac{x^2-\beta^2y^2}{x^2-k^2y^2}}\right\} - 2\cos^{-1}\left\{\frac{Mk}{\beta\sqrt{1+k^2}}\right\}\right] \tag{75}$$

where all inverse functions are principal values.

The pressure given by $C_{p_{VII}}$ may be regarded as the main transient pressure for a point on the right wing within the Mach cone from the vertex. Any such point lies originally in zone I,

acted upon by C_{p_I}. At some later time it passes into zone VII, where it lies for an interval acted upon by $C_{p_{VII}}$. Eventually it passes into zone V, where it remains acted upon by C_{p_V}. In addition, as can be seen from Figure 7, all points also pass through one or both of zones II and IV, and some points pass through zone VI. These zones may be regarded as intermediate transient zones for points within the Mach cone from the vertex.

With the pressure given for all the zones of Figure 7 (by Equations (37), (52), (57), (59), (61), (63), and (75)), the pressure field is known for the whole wing at any time. Correspondingly, the pressure is known for any point on the wing at all times. The pressure field is discussed further in the next section.

e. The Pressure Field on the Wing. The pressure should be continuous across all the internal boundaries of the seven zones. This condition was shown previously to be satisfied at the common boundaries of zones I and II, and zones II and III. In the same way it is easily shown to be satisfied on all other boundaries except that of zone VII, because the equations for C_p on both sides of these boundaries reduce by inspection to the same functions on the boundaries.

Now zone VII is bounded by zones IV, II, VI, and V in counterclockwise sequence around the boundary. To show that

$C_{p_{VII}}$ reduces to $C_{p_{IV}}$, $C_{p_{II}}$, $C_{p_{VI}}$, and C_{p_V} on the appropriate sections of the boundary, it is convenient to use the polar angle θ, shown in Figure 14a, as a boundary coordinate. Thus

$$x=(M+\cos\theta)at \qquad y=\sin\theta\cdot at \qquad 0\leq\theta\leq\pi$$

As given by Equation (75), $C_{p_{VII}}$ consists of a term multiplied by $-\frac{\alpha_o}{\pi M}$ and one multiplied by $-\frac{\alpha_o}{\pi\sqrt{\beta^2k^2}}$. It was shown that the first term is represented by the angle $\sqcap$ of Figure 13j. As the point of evaluation (x,y) moves out of zone VII across the various sections of the boundary into zones IV, II, and VI, this angle $\sqcap$ changes continuously into the angles indicated by the shaded areas of Figures 14b, 14c, and 14d respectively. Also, as the point moves into zone V, angle $\sqcap$ becomes zero, as can be seen from Figure 14e.

But it follows readily from previous analysis that the terms of the equations for $C_{p_{IV}}$, $C_{p_{II}}$, and $C_{p_{VI}}$ multiplied by $-\frac{\alpha_o}{\pi M}$ can be represented by the angles shown in Figures 14b, 14c, and 14d respectively, and the equation for C_{p_V} has no term multiplied by $-\frac{\alpha_o}{\pi M}$. Thus the part of the pressure coefficient multiplied by $-\frac{\alpha_o}{\pi M}$ is continuous across the whole boundary of zone VII. The remaining part must now be considered.

The terms of $C_{p_{VII}}$, $C_{p_{IV}}$, $C_{p_{II}}$, $C_{p_{VI}}$, and C_{p_V} multiplied by $-\frac{\alpha_o}{\pi\sqrt{\beta^2k^2}}$ will be denoted by $\mathcal{J}_{\underline{VII}}$, $\mathcal{J}_{\underline{IV}}$, $\mathcal{J}_{\underline{II}}$, $\mathcal{J}_{\underline{VI}}$, and $\mathcal{J}_{\underline{V}}$ respectively. $\mathcal{J}_{\underline{VII}}$ can be written in terms of θ for points on the boundary of zone VII:

$$\mathcal{J}_{VII} = \cos^{-1}\left\{\frac{M(\cos\theta - k\sin\theta) + 1 + k^2}{\sqrt{1+k^2}\,(M+\cos\theta - k\sin\theta)}\right\} + \cos^{-1}\left\{\frac{M(\cos\theta + k\sin\theta) + 1 + k^2}{\sqrt{1+k^2}\,(M+\cos\theta + k\sin\theta)}\right\}$$

$$+ 2\cos^{-1}\left\{\frac{k\,|1+M\cos\theta|}{\beta\sqrt{(M+\cos\theta)^2 - k^2\sin^2\theta}}\right\} - 2\cos^{-1}\left\{\frac{Mk}{\beta\sqrt{1+k^2}}\right\} \qquad (76)$$

$$= \cos^{-1}A + \cos^{-1}B + 2\cos^{-1}C - 2\cos^{-1}D$$

Also the first two inverse cosines can be combined to give

$$\cos^{-1}A + \cos^{-1}B = \cos^{-1}\left\{\frac{M^2(\cos^2\theta - k^2\sin^2\theta) + (1+k^2)^2 + 2(1+k^2)M\cos\theta - (\beta^2 - k^2)\left|k^2 - (1+k^2)\sin^2\theta\right|}{(1+k^2)\left[(M+\cos\theta)^2 - k^2\sin^2\theta\right]}\right\} \qquad (77)$$

$$= \cos^{-1}E$$

Consider first the section of boundary common to zones VII and IV. Here

$$0 \le \theta \le \theta_1 = \cos^{-1}\left\{\frac{1}{\sqrt{1+k^2}}\right\}$$

Therefore in Equations (76) and (77):

$$|1 + M\cos\theta| = 1 + M\cos\theta$$

and

$$\left|k^2 - (1+k^2)\sin^2\theta\right| = k^2 - (1+k^2)\sin^2\theta$$

Then the last two terms of $\mathcal{J}_{VII}$ can be combined as follows:

$$2\cos^{-1}C - 2\cos^{-1}D = 2\cos^{-1}\left\{\frac{Mk^2(1+M\cos\theta) + (\beta^2 - k^2)(M+\cos\theta)}{\beta^2\sqrt{1+k^2}\sqrt{(M+\cos\theta)^2 - k^2\sin^2\theta}}\right\}$$

$$= 2\cos^{-1}\left\{\frac{M + (1+k^2)\cos\theta}{\sqrt{1+k^2}\sqrt{(M+\cos\theta)^2 - k^2\sin^2\theta}}\right\} \qquad (78)$$

$$= \cos^{-1}\left\{\frac{\left[M + (1+k^2)\cos\theta\right]^2 - k^2(\beta^2 - k^2)}{(1+k^2)\left[(M+\cos\theta)^2 - k^2\sin^2\theta\right]}\right\}$$

$$= \cos^{-1}E = \cos^{-1}A + \cos^{-1}B$$

Therefore

$$\mathcal{J}_{VII} = 2\cos^{-1}A + 2\cos^{-1}B = \mathcal{J}_{IV} \qquad (79)$$

Next is the section of boundary common to zones VII and II. Here

$$\theta_1 = \cos^{-1}\left\{\frac{1}{\sqrt{1+k^2}}\right\} \leq \theta \leq \theta_2 = \cos^{-1}\left\{\frac{-1}{M}\right\}$$

Therefore in Equations (76) and (77):

$$|1+M\cos\theta| = 1+M\cos\theta$$

and

$$|k^2-(1+k^2)\sin^2\theta| = -k^2+(1+k^2)\sin^2\theta$$

Here combination of the last two terms of $\mathcal{J}_{\underline{VII}}$ leads to a different result. Thus

$$2\cos^{-1}C - 2\cos^{-1}D = \cos^{-1}\left\{\frac{[M+(1+k^2)\cos\theta]^2 - k^2(\beta^2-k^2)}{(1+k^2)[(M+\cos\theta)^2-k^2\sin^2\theta]}\right\} \tag{80}$$

$$= \cos^{-1}\left\{\frac{M^2(\cos^2\theta-k^2\sin^2\theta)+(1+k^2)^2+2(1+k^2)M\cos\theta+(\beta^2-k^2)|k^2-(1+k^2)\sin^2\theta|}{(1+k^2)[(M+\cos\theta)^2-k^2\sin^2\theta]}\right\}$$

$$= \cos^{-1}F = \cos^{-1}A - \cos^{-1}B$$

Therefore

$$\mathcal{J}_{\underline{VII}} = 2\cos^{-1}A = \mathcal{J}_{\underline{II}} \tag{81}$$

The section of boundary common to zones VII and VI is next. Here

$$\theta_2 = \cos^{-1}\left\{\frac{-1}{M}\right\} \leq \theta \leq \theta_3 = \cos^{-1}\left\{\frac{-1}{\sqrt{1+k^2}}\right\}$$

Therefore in Equations (76) and (77):

$$|1+M\cos\theta| = -1-M\cos\theta$$

and

$$|k^2-(1+k^2)\sin^2\theta| = -k^2+(1+k^2)\sin^2\theta$$

Then from Equation (80) it follows that

$$\cos^{-1}A - \cos^{-1}B = 2\cos^{-1}C - 2\cos^{-1}D = 2\pi - 2\cos^{-1}C - 2\cos^{-1}D$$

or

$$\cos^{-1}B = \cos^{-1}A + 2\cos^{-1}C - 2\pi + 2\cos^{-1}D \tag{82}$$

Therefore

$$\mathcal{J}_{\underline{VII}} = 2\cos^{-1}A + 4\cos^{-1}C - 2\pi = \mathcal{J}_{\underline{VI}} \tag{83}$$

Finally the section of boundary common to zones VII and V is to be considered. Here

$$\theta_3 = \cos^{-1}\left\{\frac{-1}{\sqrt{1+k^2}}\right\} \leq \theta \leq \pi$$

Therefore in Equations (76) and (77):

$$|1+M\cos\theta| = -1 - M\cos\theta$$

and

$$|k^2-(1+k^2)\sin^2\theta| = k^2-(1+k^2)\sin^2\theta$$

Then from Equation (78) it follows that

$$\cos^{-1}A + \cos^{-1}B = 2\pi - \cos^{-1}E = 2\pi - 2\cos^{-1}C + 2\cos^{-1}D = 2\cos^{-1}C + 2\cos^{-1}D \tag{84}$$

Therefore

$$\mathcal{J}_{\underline{VII}} = 4\cos^{-1}C = \mathcal{J}_{\underline{V}} \tag{85}$$

Thus the part of the pressure coefficient multiplied by $-\frac{\alpha_0}{\pi\sqrt{\beta^2-k^2}}$ is also continuous across the whole boundary of zone VII, so that

the pressure is indeed continuous across all internal zone boundaries.

The pressure at any point on the wing at any time can be obtained simply by a semi-graphical scheme. This scheme is shown in Figure 15 for a wing of unit chord with k = 1, flying at M = 2. The zones are drawn on the wing for time $t_o = \frac{1}{2U}$. The curve below the wing gives the spanwise pressure variation at the trailing edge at time t_o, and the curve above the wing gives the spanwise pressure variation at any section across zone V. The scheme makes use of the superposition properties of the pressure formulae, as given previously.

The pressure is constant in zone I and in zone III, and the appropriate values can be read off on scale II of the lower curve. Pressures in other zones are obtained most directly for time $t = t_o$. Thus for a point in zone II use is made of the fact that pressure is constant on lines parallel to the right leading edge, and for the point shown:

$$-\frac{\sqrt{\beta^2 k^2}}{2\alpha_o} C_{p_{II}} = i_1 \quad , \text{or} \quad C_{p_{II}} = -\sqrt{2}\,\alpha_o i_1 \tag{86}$$

The value i_1 is read off on scale II. For the point shown in zone IV, using the superposition properties, the pressure is given as follows:

$$-\frac{\sqrt{\beta^2 k^2}}{2\alpha_o} C_{p_{IV}} = i_2 + i_3 \quad , \text{or} \quad C_{p_{IV}} = -\sqrt{2}\,\alpha_o (i_2 + i_3) \tag{87}$$

The values i_2 and i_3 are read off on scale IV. In zone V the pressure is constant on conical rays, and for the point shown:

$$-\frac{\sqrt{\beta^2 k^2}}{2\alpha_0} C_{p_V} = i_4 \quad , or \quad C_{p_V} = -\sqrt{2}\,\alpha_0\, i_4 \tag{88}$$

For the point shown in zone VI the pressure is given as follows:

$$-\frac{\sqrt{\beta^2 k^2}}{2\alpha_0} C_{p_{VI}} = i_5 + i_6 \quad , or \quad C_{p_{VI}} = -\sqrt{2}\,\alpha_0 (i_5 + i_6) \tag{89}$$

The value i_5 is read off on scale VI. For the point shown in zone VII the pressure is given as follows:

$$-\frac{\sqrt{\beta^2 k^2}}{2\alpha_0} C_{p_{VII}} = \frac{1}{2}(i_4 + i_7 + i_8) \, , or \, C_{p_{VII}} = -\frac{\alpha_0}{\sqrt{2}}(i_4 + i_7 + i_8) \tag{90}$$

The values i_7 and i_8 are read off on scale VII.

To obtain the pressure at points on the wing for times $t \neq t_0$, it is necessary to use the fact that the pressure is conical in space-time. Thus consider the point P_0 of Figure 15. At time t_0 it lies in zone IV and is acted on by $C_{p_{IV}}$ as given by Equation (87). At some later time t_1 it will lie in zone VII. To find the pressure then acting upon it it is necessary to find the point which at time t_0 corresponds to point P_0 at time t_1. If this point is denoted by P_1, then P_0 and P_1 lie on the same conical ray through the vertex of the wing, and

$$x_1 = \left(\frac{t_0}{t_1}\right) x_0 \tag{91}$$

The pressure is then obtained directly for point P_1 at time t_o, and this gives the pressure at P_o at time t_1. For the example shown in Figure 15, P_o lies on the conical ray $\frac{y}{x} = .10$; and $x_o = .75$. Time t_1 is taken as $\frac{1}{U}$, so that Equation (91) gives $x_1 = .375$, and P_1 is located on the conical ray through P_o by means of the scale to the right of the wing. Thus the pressure coefficient at P_o at time t_1 is $C_{P_{VII}}$ as given by Equation (90).

Still later P_o lies in zone V, where it remains acted on by constant pressure given by Equation (88) for point P_2. Similarly, at an earlier time t_3, P_o lay in zone II, acted on by pressure given by Equation (86) for point P_3, while still earlier it lay in zone I acted on by the known initial pressure.

The complete pressure distribution is sketched in Figure 16 for the right wing of Figure 15 at time t_o. At a given time t the minimum pressure on the wing occurs at the point x = Ut, y=0, the center of zone VII. The value is independent of t, from the conical properties of the pressure, and is given by

$$C_{P_{min.}} = -\frac{2\alpha_o}{\pi}\left[\frac{1}{M}\cos^{-1}\left\{\frac{k}{\sqrt{1+k^2}}\right\} + \frac{1}{\sqrt{\beta^2-k^2}}\left(\cos^{-1}\left\{\frac{\sqrt{1+k^2}}{M}\right\} + \cos^{-1}\left\{\frac{k}{\beta}\right\} - \cos^{-1}\left\{\frac{Mk}{\beta\sqrt{1+k^2}}\right\}\right)\right] \qquad (92)$$

The maximum pressure is the constant pressure acting on zone III and given by Equation (57).

f. The Infinite Swept Wing. It was pointed out previously that conditions in zones I, II, and III are not influenced by the left leading

edge of the delta wing. It follows that C_{p_I}, $C_{p_{II}}$, and $C_{p_{III}}$ give the initial, transient, and steady-state pressures for the unit-step motion of an infinite swept wing with supersonic edges of sweep-back σ, as shown in Figure 17a. Conditions are constant on lines parallel to the leading edge, and it is sufficient to give the formulae for y = 0. Thus

$$C_{p_I}(x,0+,t) = -\frac{2\alpha_0}{M} \quad , \quad (M+\sqrt{1+k^2})at < x \leq c \tag{93}$$

$$C_{p_{II}}(x,0+,t) = -\frac{2\alpha_0}{\pi}\left[\frac{1}{M}\cos^{-1}\left\{\frac{Mat-x}{\sqrt{1+k^2}at}\right\} + \frac{1}{\sqrt{\beta^2-k^2}}\cos^{-1}\left\{\frac{Mx-(\beta^2-k^2)at}{\sqrt{1+k^2}\,x}\right\}\right] \tag{94}$$

$$(M-\sqrt{1+k^2})at \leq x \leq (M+\sqrt{1+k^2})at$$

$$C_{p_{III}}(x,0+,t) = -\frac{2\alpha_0}{\sqrt{\beta^2-k^2}} \quad , \quad 0 \leq x < (M-\sqrt{1+k^2})at \tag{95}$$

where all quantities are defined as before. The limiting form of the infinite swept wing as k becomes small is the two-dimensional wing, shown in Figure 17b. The pressure formulae are obtained by setting k = 0 in Equations (93), (94), and (95). Thus

$$C_{p_I}(x,0+,t) = -\frac{2\alpha_0}{M} \quad , \quad (M+1)at < x \leq c \tag{96}$$

$$C_{p_{II}}(x,0+,t) = -\frac{2\alpha_0}{\pi}\left[\frac{1}{M}\cos^{-1}\left\{\frac{Mat-x}{at}\right\} + \frac{1}{\beta}\cos^{-1}\left\{\frac{Mx-\beta^2at}{x}\right\}\right] \tag{97}$$

$$(M-1)at \leq x \leq (M+1)at$$

$$C_{p_{III}}(x,0+,t) = -\frac{2\alpha_0}{\beta} \quad , \quad 0 \leq x < (M-1)at \tag{98}$$

These results agree with those obtained before by Miles (Reference 7) and others.

The limiting form of the infinite swept wing as $k \to \beta$ is also of interest. This form is shown in Figure 17c, and the pressure formulae are obtained for it by letting $k \to \beta$ in Equations (93), (94), and (95). Equation (93) is of course unchanged, but in Equation (94) it is necessary to apply the rule of L'Hospital to the second term. The limit is found to be finite. From Equation (95) it is seen that the constant pressure acting over zone III becomes in the limit an infinite pressure along the leading edge. The pressure distribution is thus given by

$$C_{p_I}(x,0+,t) = -\frac{2\alpha_0}{M} \quad , \quad 2Ut < x \leq c \tag{99}$$

$$C_{p_{II}}(x,0+,t) = -\frac{2\alpha_0}{M\pi}\left[\cos^{-1}\left\{1-\frac{x}{Ut}\right\} + \sqrt{2\frac{Ut}{x}-1}\right] \quad , \quad 0 \leq x \leq 2Ut \tag{100}$$

Equation (100) reduces to Equation (99) for x = 2Ut, so the pressure is still continuous across the boundary between zones I and II. For x = 0, Equation (100) gives infinite pressure, which agrees with the limiting value obtained from Equation (95). Moreover, the singularity in Equation (100) at x = 0 is seen to be of the square-root type, characteristic of the subsonic leading edges of a lifting wing

in linearized theory.

Since $k = \beta$ is the limiting value of k for which the leading edge of the infinite swept wing is supersonic (the edge might in fact be called "sonic" for $k = \beta$), it seems reasonable to suppose that the pressure distribution for the unit-step motion of an infinite swept wing with $k > \beta$ will not be greatly different from that given by Equations (99) and (100), and that these equations will be approached as limits as $k \to \beta$ from above. A similar argument could be given for the limiting form of the wide delta wing as $k \to \beta$, although this will not be attempted here. The pressure distribution for the unit-step motion of the infinite swept wing is plotted in Figure 18 for $k = 0$, $k = 1$, and $k = \beta$, at the same time t and for $M = 2$.

It was shown in the analysis for the delta wing that the terms in the pressure formulae multiplied by $-\frac{\alpha_0}{\pi M}$ could be represented by geometrical angles occurring naturally in the regions of integration on the wing. It will now be shown that for the two-dimensional wing both terms in Equation (97) are capable of geometric interpretation, and that the analysis can be extended to the infinite swept wing.

Figure 19a shows the domain of dependence of a typical point P for the unit-step motion of the two-dimensional wing. The Mach cone containing the sphere is bisected by the plane of the wing,

and only the upper half is shown. The domain is also cut off at the vertical plane through the leading edge, the yz plane.

First, by inspection of Figure 19a it is seen that

$$\cos^{-1}\left\{\frac{Mat-X}{at}\right\} = \frac{\Gamma}{2}$$

where

$$0 \leq \Gamma \leq 2\pi$$

Next, in the second term of Equation (97),

$$\frac{Mx-\beta^2 at}{x} = \frac{\frac{Mx}{\beta}-\beta at}{\frac{x}{\beta}}$$

and

$$\frac{x}{\beta} = \frac{[OP]}{\beta} = [OP_1]$$

Also

$$[OP_2] = [OP_3] = \sqrt{a^2t^2-(x-Mat)^2}$$

Therefore

$$[P_1P_2]^2 = [OP_1]^2-[OP_2]^2 = \left(\frac{x}{\beta}\right)^2 - a^2t^2+(x-Mat)^2$$

Or

$$[P_1P_2] = \frac{Mx}{\beta}-\beta at$$

Therefore

$$\cos^{-1}\left\{\frac{Mx-\beta^2 at}{x}\right\} = \cos^{-1}\left\{\frac{[P_1P_2]}{[OP_1]}\right\} = \frac{\Lambda}{2}$$

where

$$0 \leq \Lambda \leq 2\pi$$

For $x < \frac{\beta^2 at}{M}$, $\Lambda > \pi$ and points P_2 and P_4 lie on the lower half of the sphere, not shown in Figure 19a.

Thus Equation (97) can be written in the simple form,

$$C_{P_{\underline{II}}}(x,0+,t) = -\frac{\alpha_0}{\pi}\left[\frac{\Gamma}{M} + \frac{\Lambda}{\beta}\right] \tag{101}$$

where

$$0 \leq \Gamma \leq 2\pi \quad , \quad 0 \leq \Lambda \leq 2\pi$$

For small enough values of t, the sphere is not cut by the yz plane, so that $\Lambda = 0$ and $\Gamma = 2\pi$. Thus Equation (101) reduces to Equation (96). As t increases, Λ increases and Γ decreases until the sphere lies completely ahead of the yz plane. Then $\Lambda = 2\pi$ and $\Gamma = 0$, so that Equation (101) reduces to Equation (98).

To extend this analysis to the infinite swept wing, it is convenient to introduce what may be called normal quantities, as follows:

$$M_n = \frac{M}{\sqrt{1+k^2}} \quad , \quad \beta_n = \sqrt{M_n^2 - 1} = \frac{\sqrt{\beta^2 - k^2}}{\sqrt{1+k^2}} \quad , \quad a_n = a\sqrt{1+k^2} \quad , \quad \alpha_{0_n} = \frac{\alpha_0}{\sqrt{1+k^2}} \tag{102}$$

M_n, the normal Mach number, is the component of the Mach number (here considered as a vector in the free-stream direction) normal to the wing leading edge. The other quantities are defined to conform with M_n and preserve the free-stream velocity U. Thus

$$U = M_n a_n = Ma$$

If normal quantities are substituted in Equation (94) by use of Equation (102) the result is

$$C_{p_{II}}(x,0+,t) = -\frac{2\alpha_{0_n}}{\pi}\left[\frac{1}{M_n}\cos^{-1}\left\{\frac{M_n a_n t - x}{a_n t}\right\} + \frac{1}{\beta_n}\cos^{-1}\left\{\frac{M_n x - \beta_n^2 a_n t}{x}\right\}\right] \tag{103}$$

But Equation (103) gives the transient pressure coefficient for a two-dimensional wing flying at Mach number M_n in air with speed of sound a_n, and undergoing a unit-step motion resulting in an effective angle of attack α_{0_n}. This fictitious wing is shown superimposed on the real wing in Figure 19b. The geometrical interpretation of the terms of Equation (103) is obtained as before, but the results apply to the real wing. Thus the transient pressure coefficient for the unit-step motion of an infinite swept wing can be written

$$C_{p_{II}}(x,0+,t) = -\frac{\alpha_{0_n}}{\pi}\left[\frac{\Gamma}{M_n} + \frac{\Lambda}{\beta_n}\right] \tag{104}$$

where Λ and Γ are shown in Figure 19b. Eliminating the normal quantities from Equation (104) puts it in the form

$$C_{p_{II}}(x,0+,t) = -\frac{\alpha_0}{\pi}\left[\frac{\Gamma}{M} + \frac{\Lambda}{\sqrt{\beta^2 - k^2}}\right] \tag{105}$$

where

$$0 \leq \Gamma \leq 2\pi, \quad 0 \leq \Lambda \leq 2\pi$$

It will be recalled that, as previously defined, Γ for the infinite swept wing was the angle subtended at the center of the circle by the chord representing the leading edge. A little geometry is sufficient to show that Γ as defined in Figure 19b is the same angle

given by the previous definition. Again Equation (105) reduces to Equations (93) and (95) at the limits, as it should. It is doubtful that any worthwhile simplification would be obtained by extending these ideas to the delta wing.

IV. LIFT AND PITCHING MOMENT OF THE WIDE DELTA WING

a. Theoretical Background. It is of course possible to obtain the lift and pitching-moment coefficients at any time for the unit-step motion of the delta wing by integrating the pressures found in PART III over the wing. This procedure is not, however, followed in this paper. Instead, the lift of a spanwise element of the wing is found directly by means of a method of descent and a manipulation of the fundamental wing formula. The lift and moment coefficients are then obtained simply by suitably integrating this function over the wing chord. The method is convenient and informative, the latter because it illustrates the nature of solutions for lifting wings with entirely supersonic edges.

The velocity potential φ, as considered in the $(\bar{x},\bar{y},\bar{z},\bar{t})$ system, satisfied Equation (10) and the boundary condition that the upwash is known in the plane of the wing, at least ahead of the trailing edge. Consider the function ϕ obtained by integrating the spanwise coordinate $\bar{y}$ out of φ. Thus

$$\phi(\bar{x},\bar{z},\bar{t}) = \int_{-\infty}^{\infty} \varphi(\bar{x},\bar{y},\bar{z},\bar{t})\,d\bar{y} \tag{106}$$

Froehlich (Reference 4) has shown that ϕ satisfies the differential equation

$$\frac{\partial^2\phi}{\partial\bar{x}^2} + \frac{\partial^2\phi}{\partial\bar{z}^2} - \frac{1}{a^2}\frac{\partial^2\phi}{\partial\bar{t}^2} = 0 \tag{107}$$

and the boundary condition

$$\frac{\partial \phi}{\partial \bar{z}}(\bar{x}, 0^+, \bar{t}) = \int_{-\infty}^{\infty} \frac{\partial \varphi}{\partial \bar{z}}(\bar{x}, \bar{y}, 0^+, \bar{t})\, d\bar{y} \tag{108}$$

If the wing leading edges are supersonic, and the trailing edge is straight and parallel to the $\bar{y}$-axis, then the integral in Equation (108) can be evaluated, so that $\frac{\partial \phi}{\partial \bar{z}}$ is known in the plane of the wing ahead of the trailing edge.

It was shown previously that the velocity potential satisfying Equation (10) and giving specified upwash in the plane of the wing ahead of the trailing edge is given by the fundamental wing formula, Equation (28). If the flow field has no dependence on $\bar{y}$, Equation (10) reduces to the form of Equation (107). It follows that the solution to Equations (107) and (108) is given by the fundamental wing formula. Thus

$$\phi(\bar{x}, \bar{z}, \bar{t}) = -\frac{a}{2\pi} \int_0^{\bar{t} - \frac{\bar{z}}{a}} \int_0^{2\pi} \frac{\partial \phi}{\partial \bar{z}}(\bar{\xi}, 0^+, \bar{\tau})\, d\bar{\theta}\, d\bar{\tau} \tag{109}$$

where

$$\bar{\xi} = \bar{x} + \sqrt{a^2(\bar{t} - \bar{\tau})^2 - \bar{z}^2}\, \cos\bar{\theta} \tag{109a}$$

The variables are the same as those in Equation (28).

The next step is to determine $\frac{\partial \phi}{\partial \bar{t}}$ in the plane of the wing. Because the pressure is zero in the plane of the wing off the wing, $\frac{\partial \phi}{\partial \bar{t}}$ is seen to represent the lift of a spanwise element of the wing,

except for a multiplicative constant. Now Equation (109) cannot be differentiated formally with respect to $\bar{t}$ because the integrand and its derivatives are in general discontinuous across the edges of the wing, which may lie inside the region of integration. Instead the limiting procedure defining $\frac{\partial \phi}{\partial \bar{t}}$ is applied to the integral in Equation (109), with $\bar{z} = 0+$. Thus

$$\phi(\bar{x},0+,\bar{t}+d\bar{t})-\phi(\bar{x},0+,\bar{t}) = -\frac{a}{2\pi}\left[\int_0^{\bar{t}+d\bar{t}}\int_0^{2\pi}\frac{\partial \phi}{\partial \bar{z}}\left(\bar{\xi}\{\bar{t}+d\bar{t}\},0+,\bar{\tau}\right)d\bar{\theta}\,d\bar{\tau} - \int_0^{\bar{t}}\int_0^{2\pi}\frac{\partial \phi}{\partial \bar{z}}\left(\bar{\xi}\{\bar{t}\},0+,\bar{\tau}\right)d\bar{\theta}\,d\bar{\tau}\right] \tag{110}$$

The first inner integral in Equation (110) is over a circle of center $\bar{x}$ and radius $a(\bar{t}+d\bar{t}-\bar{\tau})$ in the plane $\bar{z} = 0+$. It should be kept in mind that this is still the $\bar{x}\bar{y}$ plane, although the equations are independent of $\bar{y}$. The second inner integral is over a circle also of center $\bar{x}$ but with radius $a(\bar{t}-\bar{\tau})$. If the integral

$$-\frac{a}{2\pi}\int_0^{\bar{t}}\int_0^{2\pi}\frac{\partial \phi}{\partial \bar{z}}\left(\bar{\xi}\{\bar{t}+d\bar{t}\},0+,\bar{\tau}\right)d\bar{\theta}\,d\bar{\tau}$$

is added to and subtracted from the right side of Equation (110), it can be written in the form

$$\phi(\bar{x},0+,\bar{t}+d\bar{t})-\phi(\bar{x},0+,\bar{t}) = -\frac{a}{2\pi}\int_{\bar{t}}^{\bar{t}+d\bar{t}}\int_0^{2\pi}\frac{\partial \phi}{\partial \bar{z}}\left(\bar{\xi}\{\bar{t}+d\bar{t}\},0+,\bar{\tau}\right)d\bar{\theta}\,d\bar{\tau} - \frac{a}{2\pi}\int_0^{\bar{t}}\left[\int_0^{2\pi}\frac{\partial \phi}{\partial \bar{z}}\left(\bar{\xi}\{\bar{t}+d\bar{t}\},0+,\bar{\tau}\right)d\bar{\theta} - \int_0^{2\pi}\frac{\partial \phi}{\partial \bar{z}}\left(\bar{\xi}\{\bar{t}\},0+,\bar{\tau}\right)d\bar{\theta}\right]d\bar{\tau} \tag{111}$$

If both sides of Equation (111) are now divided by $d\bar{t}$, which is then made to approach zero, the left side of the equation approaches $\frac{\partial \phi}{\partial \bar{t}}$

and both terms on the right side approach finite limits. The result may be written

$$\frac{\partial \phi}{\partial \bar{t}}(\bar{x}, 0^+, \bar{t}) = \frac{\partial \phi_1}{\partial \bar{t}}(\bar{x}, 0^+, \bar{t}) + \frac{\partial \phi_2}{\partial \bar{t}}(\bar{x}, 0^+, \bar{t}) \tag{112}$$

By inspection of the integral in Equation (111) giving $\frac{\partial \phi_1}{\partial \bar{t}}$, it is evaluated readily. Thus

$$\frac{\partial \phi_1}{\partial \bar{t}}(\bar{x}, 0^+, \bar{t}) = -\frac{a}{2\pi}\int_0^{2\pi} \frac{\partial \phi}{\partial \bar{z}}(\bar{x}, 0^+, \bar{t})\, d\bar{\theta} = -a\frac{\partial \phi}{\partial \bar{z}}(\bar{x}, 0^+, \bar{t}) \tag{113}$$

$\frac{\partial \phi}{\partial \bar{t}}$ gives the value of the inner integral for ϕ at the upper limit of the outer integral. It therefore corresponds to one of the terms obtained by formal differentiation of the integral for ϕ. $\frac{\partial \phi_2}{\partial \bar{t}}$ represents the differentiation with respect to $\bar{t}$ of the inner integral for ϕ. It is this term which cannot in general be evaluated by formal differentiation, owing to the discontinuities involved. In the next section, Equation (112) will be evaluated for the unit-step motion of the delta wing.

b. Application. For the unit-step motion of the delta wing, the upwash function $\frac{\partial \phi}{\partial \bar{z}}$ is obtained by substitution of Equation (33), which is the same in both coordinate systems, into Equation (108). $\frac{\partial \varphi}{\partial \bar{z}}$ is zero in the range of integration except on the wing, so the result is

$$\frac{\partial \phi}{\partial \bar{z}}(\bar{x}, 0^+, \bar{t}) = -2W_0\, 1(\bar{t}) \int_0^{\frac{\bar{x}+U\bar{t}}{k}} d\bar{y} = -\frac{2W_0}{k}\, 1(\bar{t})(\bar{x}+U\bar{t}), \quad 0 \le \bar{x}+U\bar{t} \le c \tag{114}$$

$$= 0, \quad \bar{x}+U\bar{t} < 0$$

Equation (114) may be regarded as specifying the upwash function for a two-dimensional wing of zero thickness and chord c. This fictitious wing has a parabolic profile given by

$$h_u(x) = h_l(x) = -\frac{W_o}{kU} x^2 \tag{115}$$

If it is considered to start from rest at $\bar{t} = 0$ in the $(\bar{x},\bar{y},\bar{z},\bar{t})$ system with supersonic velocity U in the negative $\bar{x}$-direction, the resulting flow field is governed by Equations (107) and (114). The pressure on this wing, given by $\frac{\partial \phi}{\partial \bar{t}}$, represents the lift of a spanwise element of the delta wing at the same chord point, except for a multiplicative constant.

$\frac{\partial \phi}{\partial \bar{t}}$ is found directly from Equations (113) and (114):

$$\frac{\partial \phi}{\partial \bar{t}}(\bar{x},0+,\bar{t}) = \frac{2W_o a}{k} 1(\bar{t})(\bar{x}+U\bar{t}) \quad , \quad 0 \le \bar{x}+U\bar{t} \le c$$
$$= 0 \quad , \quad \bar{x}+U\bar{t} < 0 \tag{116}$$

To determine $\frac{\partial \phi_2}{\partial \bar{t}}$, it is necessary to examine further the second term on the right side of Equation (111). The integrand $\frac{\partial \phi}{\partial \bar{z}}$ is obtained by substituting $\bar{\xi}, \bar{\tau}$ for $\bar{x},\bar{t}$ in Equation (114), where $\bar{\xi}$ is given in terms of $\bar{x}$, $\bar{t}$, $\bar{\tau}$, and $\bar{\theta}$ by Equation (109a). Thus

$$\frac{\partial \phi}{\partial \bar{z}}\left(\bar{\xi}\{\bar{t}\},0+,\bar{\tau}\right) = -\frac{2W_o}{k} 1(\bar{\tau})\left\{\bar{x}+a(\bar{t}-\bar{\tau})\cos\bar{\theta}+U\bar{\tau}\right\} \quad , \quad 0 \le \{\} \le c \tag{117}$$
$$= 0 \quad , \quad \{\} < 0$$

Accordingly, the second term of Equation (111) may be rewritten:

$$\phi_2(\bar{x},0+,\bar{t}+d\bar{t}) - \phi_2(\bar{x},0+,\bar{t}) = \frac{2W_0 a}{k\bar{\Pi}} \int_0^{\bar{t}} \left[\int_0^{\bar{\theta}_2(\bar{t}+d\bar{t})} \left\{ \bar{x} + a(\bar{t}+d\bar{t}-\bar{\tau})\cos\bar{\theta} + U\bar{\tau} \right\} d\bar{\theta} \right.$$
$$\left. - \int_0^{\bar{\theta}_2(\bar{t})} \left\{ \bar{x} + a(\bar{t}-\bar{\tau})\cos\bar{\theta} + U\bar{\tau} \right\} d\bar{\theta} \right] d\bar{\tau} \qquad (118)$$

where

$$\bar{x} + a(\bar{t}-\bar{\tau})\cos\bar{\theta} + U\bar{\tau} \geq 0 \quad \text{for} \quad 0 \leq \bar{\theta} \leq \bar{\theta}_2(\bar{t})$$

The conditions represented by Equation (118) are illustrated in Figure 20. Figure 20a shows the time history of the motion of the fictitious two-dimensional wing, with the domains of dependence of a typical point $\bar{x}$ on the wing at times $\bar{t}$ and $\bar{t} + d\bar{t}$. Figure 20b shows the situation in the plane $\bar{z} = 0+$ at a typical time $\bar{\tau}$ for which the wing leading edge falls inside the domain of dependence of $\bar{x}$ at times $\bar{t}$ and $\bar{t} + d\bar{t}$. That is, disturbances produced by the wing at time $\bar{\tau}$ influence point $\bar{x}$ at times $\bar{t}$ and $\bar{t} + d\bar{t}$ as specified by the two inner integrals of Equation (118). It is also clear from Figure 20a that the outer integration should have the limits $\bar{\tau}_1$ and $\bar{\tau}_2$ instead of 0 and $\bar{t}$, because the wing leading edge lies inside the domain of dependence of $\bar{x}$ only during the interval $(\bar{\tau}_2 - \bar{\tau}_1)$, as shown in Figure 20a.

After the inner integrations have been performed, Equation (118) can be written in the form

$$\phi_2(\bar{x},0+,\bar{t}+d\bar{t}) - \phi_2(\bar{x},0+,\bar{t}) = \frac{2W_0 a}{k\bar{\Pi}} \int_{\bar{\tau}_1}^{\bar{\tau}_2} \left[(\bar{x}+U\bar{\tau}) \left\{ \bar{\theta}_2(\bar{t}+d\bar{t}) - \bar{\theta}_2(\bar{t}) \right\} \right.$$
$$\left. + a \left\{ (\bar{t}+d\bar{t}-\bar{\tau})\sin\bar{\theta}_2(\bar{t}+d\bar{t}) - (\bar{t}-\bar{\tau})\sin\bar{\theta}_2(\bar{t}) \right\} \right] d\bar{\tau} \qquad (119)$$

If now both sides of Equation (119) are divided by $d\bar{t}$, in the limit as $d\bar{t} \to 0$ Equation (119) becomes:

$$\frac{\partial \phi_2}{\partial \bar{t}}(\bar{x}, 0+, \bar{t}) = \frac{2W_0 a}{k\pi} \int_{\bar{\tau}_1}^{\bar{\tau}_2} \left[(\bar{x} + U\bar{\tau}) \frac{\partial \bar{\theta}_2}{\partial \bar{t}} + a \frac{\partial}{\partial \bar{t}} \{ (\bar{t} - \bar{\tau}) \sin \bar{\theta}_2 \} \right] d\bar{\tau}$$

$$= \frac{2W_0 a}{k\pi} \int_{\bar{\tau}_1}^{\bar{\tau}_2} \left[\{ \bar{x} + a(\bar{t} - \bar{\tau}) \cos \bar{\theta}_2 + U\bar{\tau} \} \frac{\partial \bar{\theta}_2}{\partial \bar{t}} + a \sin \bar{\theta}_2 \right] d\bar{\tau} \qquad (120)$$

$$= \frac{2W_0 a}{k\pi} \int_{\bar{\tau}_1}^{\bar{\tau}_2} \sqrt{a^2(\bar{t} - \bar{\tau})^2 - (\bar{x} + U\bar{\tau})^2} \; \frac{d\bar{\tau}}{\bar{t} - \bar{\tau}}$$

since the coefficient of $\frac{\partial \bar{\theta}_2}{\partial \bar{t}}$ vanishes identically, as may be seen from Figure 20b. Equation (120) is integrated easily, the result being

$$\frac{\partial \phi_2}{\partial \bar{t}}(\bar{x}, 0+, \bar{t}) = -\frac{2W_0 a}{k\pi} \left[\sqrt{a^2(\bar{t} - \bar{\tau})^2 - (\bar{x} + U\bar{\tau})^2} - \frac{M}{\beta} (\bar{x} + U\bar{t}) \sin^{-1} \left\{ \frac{M(\bar{x} + U\bar{t}) - \beta^2 a(\bar{t} - \bar{\tau})}{\bar{x} + U\bar{t}} \right\} \right]_{\bar{\tau}_1}^{\bar{\tau}_2}$$

$$+ \frac{2W_0 a}{k\pi} \left[(\bar{x} + U\bar{t}) \sin^{-1} \left\{ \frac{U(\bar{t} - \bar{\tau}) - (\bar{x} + U\bar{t})}{a(\bar{t} - \bar{\tau})} \right\} \right]_{\bar{\tau}_1}^{\bar{\tau}_2} \qquad (121)$$

where all inverse functions are principal values.

In applying the limits $\bar{\tau}_1$ and $\bar{\tau}_2$, three different cases arise, depending on the position of the point of evaluation in the time history of the motion. The three possibilities are shown in Figure 21. In zone A, $\bar{\tau}_1 = \bar{\tau}_2 = 0$, so that

$$\frac{\partial \phi_{A_2}}{\partial \bar{t}}(\bar{x}, 0+, \bar{t}) = 0 \qquad (122)$$

Therefore, from Equations (112) and (116),

$$\frac{\partial \phi_A}{\partial \bar{t}}(\bar{x}, 0+, \bar{t}) = \frac{2W_0 a}{k} (\bar{x} + U\bar{t}) \quad ; \quad \bar{t} \geq 0, \; a\bar{t} \leq \bar{x} \leq c - U\bar{t} \qquad (123)$$

In zone B, $\bar{\tau}_1 = 0$ and $\bar{\tau}_2 = \frac{a\bar{t}-\bar{x}}{U+a}$, so that

$$\frac{\partial \phi_{B_2}}{\partial \bar{t}}(\bar{x},0+,\bar{t}) = \frac{2W_0 a}{k\bar{\Pi}}\left[\sqrt{a^2\bar{t}^2-\bar{x}^2} - (\bar{x}+U\bar{t})\left\{\bar{\Pi} - \frac{M}{\beta}\cos^{-1}\left\{\frac{M\bar{x}+a\bar{t}}{\bar{x}+U\bar{t}}\right\} - \cos^{-1}\left\{\frac{-\bar{x}}{a\bar{t}}\right\}\right\}\right] \tag{124}$$

Therefore, from Equations (112) and (116),

$$\frac{\partial \phi_B}{\partial \bar{t}}(\bar{x},0+,\bar{t}) = \frac{2W_0 a}{k\bar{\Pi}}\left[\sqrt{a^2\bar{t}^2-\bar{x}^2} + (\bar{x}+U\bar{t})\left(\frac{M}{\beta}\cos^{-1}\left\{\frac{M\bar{x}+a\bar{t}}{\bar{x}+U\bar{t}}\right\} + \cos^{-1}\left\{\frac{-\bar{x}}{a\bar{t}}\right\}\right)\right] \tag{125}$$

where

$$\bar{t} \geq 0 \quad , \quad -a\bar{t} \leq \bar{x} \leq a\bar{t}$$

In zone C, $\bar{\tau}_1 = -\frac{\bar{x}+a\bar{t}}{U-a}$ and $\bar{\tau}_2 = -\frac{\bar{x}-a\bar{t}}{U+a}$, so that

$$\frac{\partial \phi_{C_2}}{\partial \bar{t}}(\bar{x},0+,\bar{t}) = \frac{2W_0 a}{k\bar{\Pi}}(\bar{x}+U\bar{t})\left(\frac{M}{\beta}-1\right)\bar{\Pi} \tag{126}$$

Therefore, from Equations (112) and (116),

$$\frac{\partial \phi_C}{\partial \bar{t}}(\bar{x},0+,\bar{t}) = \frac{2W_0 U}{k\beta}(\bar{x}+U\bar{t}) \; ; \; \bar{t} \geq 0 \; , -U\bar{t} \leq \bar{x} \leq -a\bar{t} \tag{127}$$

The pressure at any point on the fictitious two-dimensional wing at any time is given by one of the three equations (123), (125), or (127). In combination they give the chordwise pressure distribution. It is clear from Figure 21 that at $\bar{t} = 0$ Equation (123) holds over the entire chord, and that eventually Equation (127) holds over the entire chord. At intermediate times each of the three holds over part of the chord. By inspection of Equation (125) it is seen that it reduces to Equation (123) on the zone boundary $\bar{x} = a\bar{t}$, and to Equation (127) on the zone boundary $\bar{x} = -a\bar{t}$, so that the pressure is continuous across

the zone boundaries in the time history.

Since these equations for $\frac{\partial \phi}{\partial \bar{t}}$ also represent the lift of spanwise elements of the delta wing resulting from its unit-step motion, they can now be used in obtaining the lift and pitching-moment coefficients.

c. Lift. Because the pressure on the underside of the wing is the negative of that on the top side at every point, the lift is given as twice the integral of the pressure over the top surface. Thus

$$L = -2 \iint_{wing} (p - p_\infty) \, d\bar{y} \, d\bar{x} \tag{128}$$

On substitution for $(p - p_\infty)$ using the linearized pressure relation and Equation (9), Equation (128) becomes

$$L = 2 d_\infty \int_{-U\bar{t}}^{c-U\bar{t}} \left\{ \int_{-\infty}^{\infty} \frac{\partial \varphi}{\partial \bar{t}} (\bar{x}, \bar{y}, 0+, \bar{t}) \, d\bar{y} \right\} d\bar{x} = 2 d_\infty \int_{-U\bar{t}}^{c-U\bar{t}} \frac{\partial \phi}{\partial \bar{t}} (\bar{x}, 0+, \bar{t}) \, d\bar{x} \tag{129}$$

The limits of the inner integral in Equation (129) are properly written as infinite because $\frac{\partial \varphi}{\partial \bar{t}}$ is zero in the plane $\bar{z} = 0$ off the wing. The area of the wing is $\frac{c^2}{k}$, so that in terms of the lift coefficient,

$$L = \frac{1}{2} C_L d_\infty U^2 \frac{c^2}{k} \tag{130}$$

It is also convenient to express $\frac{\partial \phi}{\partial \bar{t}}$ in the form

$$\frac{\partial \phi}{\partial \bar{t}} (\bar{x}, 0+, \bar{t}) = \frac{2 w_0 a}{k} F(\bar{x}, \bar{t}) \tag{131}$$

where $F(\bar{x},\bar{t})$ is independent of k, as may be seen from Equations (123), (125), and (127). Therefore, on relating Equations (129) and (130), C_L is given by:

$$C_L(\bar{t}) = \frac{8\alpha_0}{MC^2}\int_{-U\bar{t}}^{c-U\bar{t}} F(\bar{x},\bar{t})\,d\bar{x} \quad , \bar{t} \geq 0 \tag{132}$$

This equation shows that the lift coefficient for the unit-step motion of a wide delta wing is independent of the sweepback. All wide deltas of the same chord undergoing the same unit-step motion produce the same lift coefficient, although the total lifts will of course vary. This phenomenon, previously mentioned by Froehlich (Reference 4), will be considered further later.

The initial lift coefficient, at $\bar{t} = 0+$, is obtained first. $F(\bar{x},\bar{t})$ is obtained from Equation (123), and the result is:

$$C_{L_0} = C_L(0+) = \frac{8\alpha_0}{MC^2}\int_0^c \bar{x}\,d\bar{x} = \frac{4\alpha_0}{M} \tag{133}$$

The transient lift coefficient is considered next. It can be seen from Figure 21 that the chordwise integration involves zones A, B, and C in the time history for the interval

$$0 \leq \bar{t} \leq \bar{t}_1 = \frac{c}{U+a}$$

and zones B and C only during the interval

$$\bar{t}_1 = \frac{c}{U+a} \leq \bar{t} \leq \bar{t}_2 = \frac{c}{U-a}$$

The coefficient for the first case will be called the initial transient lift coefficient. The functions $F(\bar{x},\bar{t})$ for the three zones are obtained from Equations (123), (125), and (127). Thus

$$C_{L_1}(\bar{t}) = \frac{8\alpha_0}{Mc^2}\left[\frac{M}{\beta}\int_{-U\bar{t}}^{-a\bar{t}}(\bar{x}+U\bar{t})\,d\bar{x} + \frac{1}{\pi}\int_{-a\bar{t}}^{a\bar{t}}\left\{\sqrt{a^2\bar{t}^2-\bar{x}^2}+(\bar{x}+U\bar{t})\left(\frac{M}{\beta}\cos^{-1}\left\{\frac{M\bar{x}+a\bar{t}}{\bar{x}+U\bar{t}}\right\}+\cos^{-1}\left\{\frac{-\bar{x}}{a\bar{t}}\right\}\right)\right\}d\bar{x}\right]$$

$$+\frac{8\alpha_0}{Mc^2}\left[\int_{a\bar{t}}^{c-U\bar{t}}(\bar{x}+U\bar{t})\,d\bar{x}\right] \qquad (134)$$

The integrals in Equation (134) can either be evaluated directly or by a single integration by parts. The result is

$$C_{L_1}(\bar{t}) = \frac{4\alpha_0}{M}\left\{1+\frac{1}{2}\left(\frac{a\bar{t}}{c}\right)^2\right\} \quad , \quad 0 \le \bar{t} \le \frac{c}{U+a} \qquad (135)$$

The coefficient for the second case will be called the final transient lift coefficient. Here

$$C_{L_2}(\bar{t}) = \frac{8\alpha_0}{Mc^2}\left[\frac{M}{\beta}\int_{-U\bar{t}}^{-a\bar{t}}(\bar{x}+U\bar{t})\,d\bar{x} + \frac{1}{\pi}\int_{-a\bar{t}}^{c-U\bar{t}}\left\{\sqrt{a^2\bar{t}^2-\bar{x}^2}+(\bar{x}+U\bar{t})\left(\frac{M}{\beta}\cos^{-1}\left\{\frac{M\bar{x}+a\bar{t}}{\bar{x}+U\bar{t}}\right\}+\cos^{-1}\left\{\frac{-\bar{x}}{a\bar{t}}\right\}\right)\right\}d\bar{x}\right] \qquad (136)$$

Again the integrals are evaluated simply, and the result is

$$C_{L_2}(\bar{t}) = \frac{2\alpha_0}{M\pi}\left[\left\{3-M\left(\frac{a\bar{t}}{c}\right)\right\}\sqrt{2M\left(\frac{a\bar{t}}{c}\right)-\beta^2\left(\frac{a\bar{t}}{c}\right)^2-1}+2\frac{M}{\beta}\cos^{-1}\left\{M-\beta^2\left(\frac{a\bar{t}}{c}\right)\right\}+\left\{2+\left(\frac{a\bar{t}}{c}\right)^2\right\}\cos^{-1}\left\{M-\left(\frac{c}{a\bar{t}}\right)\right\}\right] \qquad (137)$$

where all inverse functions are principal values, and

$$\frac{c}{U+a} \le \bar{t} \le \frac{c}{U-a}$$

Finally the steady state is reached, and for this

$$C_{L_3}(\bar{t}) = \frac{8\alpha_0}{Mc^2}\int_{-U\bar{t}}^{c-U\bar{t}}\frac{M}{\beta}(\bar{x}+U\bar{t})\,d\bar{x} = \frac{4\alpha_0}{\beta} \quad , \quad \bar{t} \ge \frac{c}{U-a} \qquad (138)$$

These lift coefficients are conveniently written in terms of the dimensionless time variable $(\frac{a\bar{t}}{c})$, which may be denoted by T. Thus, on collecting Equations (135), (137), and (138), the complete lift variation with time for the unit-step motion of the wide delta can be written:

Initial Transient: $0 \leq T \leq \frac{1}{M+1}$ $\qquad \frac{C_{L_1}}{C_{L_0}} = 1 + \frac{1}{2}T^2$ (139)

Final Transient: $\frac{1}{M+1} \leq T \leq \frac{1}{M-1}$

$$\frac{C_{L_2}}{C_{L_0}} = \frac{1}{2\pi}\left[(3-MT)\sqrt{2MT-\beta^2T^2-1} + 2\frac{M}{\beta}\cos^{-1}\left\{M-\beta^2T\right\} + (2+T^2)\cos^{-1}\left\{M-\frac{1}{T}\right\}\right] \quad (140)$$

Steady State: $T \geq \frac{1}{M-1}$ $\qquad \frac{C_{L_3}}{C_{L_0}} = \frac{M}{\beta}$ (141)

Inspection of Equation (140) shows that it reduces to Equation (139) for $T = \frac{1}{M+1}$ and to Equation (141) for $T = \frac{1}{M-1}$, so that the lift varies continuously with time as it should. $\frac{C_L}{C_{L_0}}$ is plotted versus T for three Mach numbers in Figure 22.

The above results show that the steady-state lift is always greater than the transient lift, the difference decreasing with increasing Mach number. It appears from Figure 22, and is proved easily by differentiation, that not only the ordinate but also the slope of the lift curve varies continuously with time.

d. Pitching Moment. The pitching moment about the vertex, $_o\mathcal{M}$, can be expressed as an integral of $\frac{\partial \phi}{\partial \bar{t}}$ in a way similar to that used

for the lift. Thus

$$
\begin{aligned}
{}_o\mathcal{M} &= 2\iint_{\text{wing}} (p-p_\infty)(\bar{X}+U\bar{t})\,d\bar{y}\,d\bar{X} = -2d_\infty \int_{-U\bar{t}}^{c-U\bar{t}} \left\{ \int_{-\infty}^{\infty} \frac{\partial \varphi}{\partial \bar{t}}(\bar{X},\bar{y},0+,\bar{t})\,d\bar{y} \right\} (\bar{X}+U\bar{t})\,d\bar{X} \\
&= -2d_\infty \int_{-U\bar{t}}^{c-U\bar{t}} (\bar{X}+U\bar{t}) \frac{\partial \phi}{\partial \bar{t}}(\bar{X},0+,\bar{t})\,d\bar{X}
\end{aligned}
\tag{142}
$$

where a stalling moment is considered positive. In terms of a coefficient based on the chord c and the area $\frac{c^2}{k}$, the moment is written:

$$
{}_o\mathcal{M} = \tfrac{1}{2}\,{}_oC_{\mathcal{M}}\, d_\infty U^2 \frac{c^3}{k} \tag{143}
$$

Therefore, on relating Equations (142) and (143) using Equation (131), ${}_oC_{\mathcal{M}}$ is given by

$$
{}_oC_{\mathcal{M}}(\bar{t}) = -\frac{8\alpha_o}{Mc^3} \int_{-U\bar{t}}^{c-U\bar{t}} (\bar{X}+U\bar{t}) F(\bar{X},\bar{t})\,d\bar{X}\,, \quad \bar{t} \geq 0 \tag{144}
$$

This equation shows that the pitching-moment coefficient also for the unit-step motion of a wide delta is independent of the sweepback.

The initial moment coefficient is obtained first. For this,

$$
{}_oC_{\mathcal{M}_o} = {}_oC_{\mathcal{M}}(0+) = -\frac{8\alpha_o}{Mc^3} \int_0^c \bar{X}^2\,d\bar{X} = -\frac{8\alpha_o}{3M} \tag{145}
$$

Again the transient effect is divided into initial and final stages, and the initial transient moment coefficient is given by

$$
\begin{aligned}
{}_oC_{\mathcal{M}_i}(\bar{t}) = -\frac{8\alpha_o}{Mc^3} \Bigg[\frac{M}{\beta} \int_{-U\bar{t}}^{-q\bar{t}} (\bar{X}+U\bar{t})^2\,d\bar{X} + \frac{1}{\pi} \int_{-d\bar{t}}^{q\bar{t}} \Big\{ (\bar{X}+U\bar{t}) \sqrt{d^2\bar{t}^2-\bar{X}^2} + (\bar{X}+U\bar{t})^2 \Big(\frac{M}{\beta} \cos^{-1}\Big\{ \frac{M\bar{X}+d\bar{t}}{\bar{X}+U\bar{t}} \Big\} + \cos^{-1}\Big\{ \frac{-\bar{X}}{d\bar{t}} \Big\} \Big) \Big\}\,d\bar{X} \Bigg] \\
-\frac{8\alpha_o}{Mc^3} \int_{d\bar{t}}^{c-U\bar{t}} (\bar{X}+U\bar{t})^2\,d\bar{X}
\end{aligned}
\tag{146}
$$

The integrals in Equation (146) can be evaluated directly or by integration by parts without difficulty. The result is

$$ {}_{o}C_{m_1}(\bar{T}) = -\frac{8\alpha_0}{3M}\left\{1 + \frac{M}{2}\left(\frac{a\bar{T}}{c}\right)^3\right\}, \quad 0 \le \bar{T} \le \frac{c}{U+a} \tag{147} $$

The final transient moment coefficient is given by

$$ {}_{o}C_{m_2}(\bar{T}) = -\frac{8\alpha_0}{Mc^3}\left[\frac{M}{\beta}\int_{-U\bar{T}}^{-a\bar{T}}(\bar{X}+U\bar{T})^2 d\bar{X} + \frac{1}{\pi}\int_{-a\bar{T}}^{c-U\bar{T}}\left\{(\bar{X}+U\bar{T})\sqrt{a^2\bar{T}^2-\bar{X}^2} + (\bar{X}+U\bar{T})^2\left(\frac{M}{\beta}\cos^{-1}\left\{\frac{M\bar{X}+a\bar{T}}{\bar{X}+U\bar{T}}\right\} + \cos^{-1}\left\{\frac{-\bar{X}}{a\bar{T}}\right\}\right)\right\} d\bar{X}\right] \tag{148} $$

The integrals here are the same as those in Equation (146), but with different limits. The result here is

$$ {}_{o}C_{m_2}(\bar{T}) = -\frac{4\alpha_0}{9M\pi}\left[\left\{8 - M\left(\frac{a\bar{T}}{c}\right) - (2+M^2)\left(\frac{a\bar{T}}{c}\right)^2\right\}\sqrt{2M\left(\frac{a\bar{T}}{c}\right) - \beta^2\left(\frac{a\bar{T}}{c}\right)^2 - 1} + 6\frac{M}{\beta}\cos^{-1}\left\{M - \beta^2\left(\frac{a\bar{T}}{c}\right)\right\}\right] \tag{149} $$

$$ -\frac{4\alpha_0}{9M\pi}\left\{6 + 3M\left(\frac{a\bar{T}}{c}\right)^3\right\}\cos^{-1}\left\{M - \left(\frac{c}{a\bar{T}}\right)\right\}, \quad \frac{c}{U+a} \le \bar{T} \le \frac{c}{U-a} $$

The steady-state coefficient is given by

$$ {}_{o}C_{m_3}(\bar{T}) = -\frac{8\alpha_0}{Mc^3}\int_{-U\bar{T}}^{c-U\bar{T}}\frac{M}{\beta}(\bar{X}+U\bar{T})^2 d\bar{X} = -\frac{8\alpha_0}{3\beta}, \quad \bar{T} \ge \frac{c}{U-a} \tag{150} $$

The complete pitching-moment variation with time for the unit-step motion of the wide delta wing is thus given by Equations (147), (149), and (150). These may be written in terms of T, giving finally the following pitching-moment variation:

Initial Transient: $0 \le T \le \frac{1}{M+1}$ $\qquad \frac{{}_{o}C_{m_1}}{{}_{o}C_{m_0}} = 1 + \frac{M}{2}T^3$ (151)

Final Transient: $\frac{1}{M+1} \le T \le \frac{1}{M-1}$

$$\frac{{}_oC_{m_2}}{{}_oC_{m_0}} = \frac{1}{6\pi}\left[\left\{8 - MT - (2+M^2)T^2\right\}\sqrt{2MT - \beta^2T^2 - 1} + 6\frac{M}{\beta}\cos^{-1}\left\{M - \beta^2 T\right\} + (6+3MT^3)\cos^{-1}\left\{M - \frac{1}{T}\right\}\right] \quad (152)$$

Steady State: $T \geq \frac{1}{M-1}$ $$\frac{{}_oC_{m_3}}{{}_oC_{m_0}} = \frac{M}{\beta} \quad (153)$$

Both Equation (152) and its derivative with respect to T reduce to the initial transient values for $T = \frac{1}{M+1}$ and to the steady-state values for $T = \frac{1}{M-1}$, so the pitching-moment variation is continuous in both ordinate and slope for all positive times. $\frac{{}_oC_m}{{}_oC_{m_0}}$ is plotted versus T for three Mach numbers in Figure 23.

The above results show that for the unit-step motion of a wide delta the steady-state pitching moment about the vertex is always greater than the transient pitching moment, the difference decreasing with increasing Mach number.

It is useful to determine the variation of the center of pressure on the wing with time. It falls, of course, on the wing centerline, and if ℓ denotes its x-coordinate, ℓ is given by

$$\frac{\ell(T)}{c} = -\frac{{}_oC_m(T)}{C_L(T)} = \frac{2}{3}\frac{\left(\frac{{}_oC_m(T)}{{}_oC_{m_0}}\right)}{\left(\frac{C_L(T)}{C_{L_0}}\right)} \quad (154)$$

This function is plotted for three Mach numbers in Figure 24 by taking ratios of corresponding values from Equations (139) and (151), (140) and (152), and (141) and (153). It is seen that initially the c.p. lies at the two-thirds chord point; i.e., the centroid of the wing area. This is of course proper, since the pressure is initially constant over the entire wing. Next the c.p. moves forward, because

of the influence of the higher steady-state pressures spreading over the fore-part of the wing. As the steady-state pressure continues to spread towards the trailing edge, the forward travel of the c.p. stops and changes to rearward travel. Finally the steady-state position is reached, and this again turns out to be the two-thirds chord point, although the pressure is not in this case constant over the wing. However, the average pressure on each spanwise element of the wing is the same, as can be seen by forming

$$\left(\frac{\partial \varphi}{\partial \bar{t}}\right)_{ave.} = \frac{1}{2\bar{y}_R} \frac{\partial \phi}{\partial \bar{t}}$$

where $\bar{y}_R$ is the $\bar{y}$-coordinate of the right leading edge. For the steady state, $\frac{\partial \phi}{\partial \bar{t}}$ is given by Equation (127) so that

$$\left(\frac{\partial \varphi}{\partial \bar{t}}\right)_{ave.} = \frac{1}{2\bar{y}_R} \frac{2W_0 U}{k\beta}(\bar{x} + U\bar{t}) = \frac{W_0 U}{\beta} \qquad (155)$$

This explains why the c.p. again lies at the centroid of the wing area. It can also be seen from Figure 24 that the maximum forward travel of the c.p. decreases with increasing Mach number. If the center of gravity of the wing is near the two-thirds chord point, this c.p. travel will be important in determining the stability of the transient effects of the unit-step motion.

e. Comparison with Two-Dimensional Wing. It was observed previously that the lift and pitching-moment coefficients for the unit-step motion of a wide delta wing are independent of the sweepback. One is tempted to conclude that the equations obtained for these coefficients therefore apply also to the unit-step motion of a flat two-dimensional wing, particularly since the correct local pressure coefficient for such a wing is obtained by setting $k = 0$ in the corresponding equation for the delta wing, as shown by Equations (96), (97), and (98). Such a conclusion would, nevertheless, be incorrect.

The sweepback enters into the determination of the local pressure coefficient only as the inclination to the free-stream direction of part of the boundary of the zone of integration. Accordingly, setting $k = 0$ gives the zone of integration for a two-dimensional wing and so reduces the results of the integration to the two-dimensional values. However, in determining the total coefficients effects integrated across the span are important, and the fact that the planform is triangular enters in, even though the size of the vertex angle does not. Thus the limiting value $k = 0$ is to be regarded as defining a flat delta wing of finite chord and infinite span, and not a flat two-dimensional wing. In fact, it was seen previously that in determining the total coefficients, the delta wing could be replaced by a two-dimensional wing of the same chord but of parabolic profile, the changed profile accounting for the spanwise effects

of the triangular planform.

Consider a flat two-dimensional wing of chord c which undergoes the same unit-step motion as the wide delta previously considered. The lift and pitching-moment coefficients are obtained simply as integrals of the pressure coefficient:

$$C_L = -\frac{2}{c}\int_0^c C_p\,dx \quad , \quad {}_oC_m = \frac{2}{c^2}\int_0^c x C_p\,dx \tag{156}$$

In Equation (156) the pitching moment is measured about the leading edge. The zones in the time history of the motion are the same as those of Figure 21 and C_p is given in zone A by Equation (96), in zone B by Equation (97), and in zone C by Equation (98). Initial, initial transient, final transient, and steady-state coefficients are defined as before, and are therefore given as follows:

$$C_{L_o} = -\frac{2}{c}\int_0^c\left(-\frac{2\alpha_o}{M}\right)dx = \frac{4\alpha_o}{M} \quad , \quad {}_oC_{m_o} = \frac{2}{c^2}\int_0^c\left(-\frac{2\alpha_o}{M}\right)x\,dx = -\frac{2\alpha_o}{M} \tag{157}$$

$$C_{L_1} = -\frac{2}{c}\left[\int_0^{(M-1)a_1}\left(-\frac{2\alpha_o}{\beta}\right)dx - \frac{2\alpha_o}{\pi}\int_{(M-1)a_1}^{(M+1)a_1}\left(\frac{1}{M}\cos^{-1}\left\{\frac{Ma_1-x}{a_1}\right\}+\frac{1}{\beta}\cos^{-1}\left\{\frac{Mx-\beta^2a_1}{x}\right\}\right)dx + \int_{(M+1)a_1}^{c}\left(-\frac{2\alpha_o}{M}\right)dx\right]$$

$$ {}_oC_{m_1} = \frac{2}{c^2}\left[\int_0^{(M-1)a_1}\left(-\frac{2\alpha_o}{\beta}\right)x\,dx - \frac{2\alpha_o}{\pi}\int_{(M-1)a_1}^{(M+1)a_1}\left(\frac{1}{M}\cos^{-1}\left\{\frac{Ma_1-x}{a_1}\right\}+\frac{1}{\beta}\cos^{-1}\left\{\frac{Mx-\beta^2a_1}{x}\right\}\right)x\,dx + \int_{(M+1)a_1}^{c}\left(-\frac{2\alpha_o}{M}\right)x\,dx\right] \tag{158}$$

$$C_{L_2} = -\frac{2}{c}\left[\int_0^{(M-1)a_1}\left(-\frac{2\alpha_o}{\beta}\right)dx - \frac{2\alpha_o}{\pi}\int_{(M-1)a_1}^{c}\left(\frac{1}{M}\cos^{-1}\left\{\frac{Ma_1-x}{a_1}\right\}+\frac{1}{\beta}\cos^{-1}\left\{\frac{Mx-\beta^2a_1}{x}\right\}\right)dx\right]$$

$$ {}_oC_{m_2} = \frac{2}{c^2}\left[\int_0^{(M-1)a_1}\left(-\frac{2\alpha_o}{\beta}\right)x\,dx - \frac{2\alpha_o}{\pi}\int_{(M-1)a_1}^{c}\left(\frac{1}{M}\cos^{-1}\left\{\frac{Ma_1-x}{a_1}\right\}+\frac{1}{\beta}\cos^{-1}\left\{\frac{Mx-\beta^2a_1}{x}\right\}\right)x\,dx\right] \tag{159}$$

$$C_{L_3} = -\frac{2}{c}\int_0^c \left(-\frac{2\alpha_0}{\beta}\right) dx \quad , \quad {}_oC_{m_3} = \frac{2}{c^2}\int_0^c \left(-\frac{2\alpha_0}{\beta}\right) x\,dx \tag{160}$$

These integrals are all evaluated without difficulty either directly or by integration by parts. When the results are expressed in terms of T, the following lift and pitching-moment variations are obtained for the unit-step motion of the flat two-dimensional wing.

Initial Transient: $0 \le T \le \frac{1}{M+1}$ $\qquad \frac{C_{L_1}}{C_{L_0}} = 1 \quad , \quad \frac{{}_oC_{m_1}}{{}_oC_{m_0}} = 1 - \frac{1}{2}T^2$ (161)

Final Transient: $\frac{1}{M+1} \le T \le \frac{1}{M-1}$

$$\frac{C_{L_2}}{C_{L_0}} = \frac{1}{\pi}\left[\sqrt{2MT - \beta^2T^2 - 1} + \frac{M}{\beta}\cos^{-1}\left\{M - \beta^2 T\right\} + \cos^{-1}\left\{M - \frac{1}{T}\right\}\right]$$

$$\frac{{}_oC_{m_2}}{{}_oC_{m_0}} = \frac{1}{2\pi}\left[(1+MT)\sqrt{2MT - \beta^2T^2 - 1} + 2\frac{M}{\beta}\cos^{-1}\left\{M - \beta^2 T\right\} + (2 - T^2)\cos^{-1}\left\{M - \frac{1}{T}\right\}\right] \tag{162}$$

Steady State: $T \ge \frac{1}{M-1}$ $\qquad \frac{C_{L_3}}{C_{L_0}} = \frac{M}{\beta} \quad , \quad \frac{{}_oC_{m_3}}{{}_oC_{m_0}} = \frac{M}{\beta}$ (163)

It is easily verified that Equations (162) reduce to Equations (161) for $T = \frac{1}{M+1}$ and to Equations (163) for $T = \frac{1}{M-1}$, and differentiation of these equations shows the same to be true of the derivatives. Thus the lift and pitching-moment variations are continuous both in ordinate and slope throughout the range of T. The results agree with those obtained previously by Miles (Reference 7) and others.

These results are compared with those for the wide delta in Figures 25 and 26 for $M = \sqrt{2}$. It is seen that both the lift and

the pitching moment, normalized to unit initial values, have larger values for the wide delta wing than for the two-dimensional wing throughout the transient range. This is explained by the observation that at any time during the transient state the delta wing has a larger proportion of its surface acted upon by the higher steady-state pressure than has the two-dimensional wing. The initial lift coefficients are the same for both wings, and in fact for all such wings, because disturbances from the leading edges have not had time to propagate, and the results are independent of planform at $t = 0+$. The steady-state lift coefficients are also seen to be the same for both wings. This is explained by the fact, indicated by Equation (155), that the average pressure over the delta wing in the steady state is exactly the two-dimensional pressure. In accordance with this, the normalized pitching-moment coefficients are also the same in the steady state for both wings.

V. FINAL COMMENTS

It appears to be advantageous to derive the fundamental formula of linearized wing theory using the concept of spherical pulses, because this approach avoids the awkward limiting procedures needed in other approaches. The background of the method lies in acoustics rather than aerodynamics, and its use in wing theory was brought to the attention of the author in a course of lectures by Dr. P. A. Lagerstrom.

Through its chief tool, the fundamental wing formula, small-disturbance wing theory leads to simple results for the unit-step motion of the wide delta wing. Not only the lift and moment, but also the complete pressure field on the wing resulting from the motion are obtained in closed form in terms of elementary functions. The simplicity of these results suggests their suitability for Duhamel integration to obtain the response to more general time-dependent motions, without pitching, of the wide delta wing.

The pressure caused by the unit-step motion at any point on the wing at any time can be determined quickly by a semi-graphical scheme. The pressure fields for the unit-step motion of the infinite swept wing with supersonic edges and its limiting form, the two-dimensional wing, are obtained as by-products of the solution for the wide delta wing. For these, the terms of the

transient pressure coefficient have simple geometric interpretations. The pressure distribution for the unit-step motion of the other limiting form of the infinite swept wing, in which the edges may be called sonic, exhibits the square-root leading-edge singularity characteristic of flow for lifting wings with subsonic edges. It is therefore felt that this limiting form may give some information about the unit-step motion of the infinite swept wing with subsonic edges.

Calculation of the force and moment coefficients of a thin wing with supersonic leading edges and straight trailing edge is simplified by the use of a method of descent, which also makes clear the nature of the dependence of these coefficients on planform. For non-uniform motions of the wing, it appears that this dependence is only on the general shape, such as the triangle, and not on variations within the family of such shapes.

A recent paper by Strang (1950) (Reference 14) has come to the author's attention, in which the unit-step motion of a wide delta wing is treated by an extension of the methods used by Strang in a previous paper (Reference 12). The results obtained for the pressure field on the wing are in agreement with those obtained by the author. However, the results for the lift and moment, although correct, are obtained by a method which masks the nature of their dependence on the wing planform.

Thus Strang is led to observe (Reference 14, p. 73) that the dependence of $\Psi_{2\alpha}$, his lift-growth function, on sweepback is not marked, the effect of Mach number being more important. Actually $\Psi_{2\alpha}$ is exactly $\frac{\beta}{M}$ times the function $\frac{C_L}{C_{L_0}}$ of the present paper, and accordingly is entirely independent of sweepback for the wide delta wing.

The same problem is solved by Miles in another recent paper (Reference 15), in which he obtains the lift and moment coefficients by a method of descent and an application of the Fourier transform to his previous solution (Reference 16) for the harmonic motion of a wide delta wing. Miles' results agree with those of the author and correctly show no dependence on sweepback. He does not determine the pressure field on the wing.

The duration of the transient effects of the unit-step motion is given by $\frac{c}{(M-1)a}$, so that it is extremely short for any normal chord length and any Mach number to which the linearized theory applies. Moreover, the transient lift is always less than the steady-state lift and the center of pressure travel is small. The unit-step motion of the wide delta wing is not, therefore, of much practical interest or importance. The interest lies in the simplicity of the solution for the pressure field, forces, and moments produced by the motion, and the importance lies in the possible application of the solution to Duhamel integration.

REFERENCES

1. Ackeret, J.: Luftkräfte auf Flügel, die mit grösserer als Schallgeschwindigkeit bewegt werden, Z.F.M., (1925), Vol. 16, pp. 72-74.

2. Possio, C.: L'azione aerodinamica sul profilo oscillante alle velocita ultrasonore, Acta. Pontif. Acad. Sci., (1937), Vol.1, No. 11, pp. 93-105.

3. Puckett, A. E.: Supersonic Wave Drag of Thin Airfoils, J.Ae.Sc., (1946), Vol. 13, No. 9, pp. 475-484.

4. Froehlich, J. E.: Non-stationary Motion of Purely Supersonic Wings, Doctor's Thesis, C.I.T., (1950).

5. Stewart, H. J.: The Lift of a Delta Wing at Supersonic Speeds, Q.A.M., (1946), Vol. IV, No. 3, pp. 246-254.

6. Hipsh, H. M.: Harmonic Oscillations of a Narrow Delta Wing in Supersonic Flow, Doctor's Thesis, C.I.T. (1951).

7. Miles, J. W.: Transient Loading of Airfoils at Supersonic Speeds, J.Ae.Sc., (1948), Vol. 15, pp. 592-598.

8. Biot, M. A.: Loads on a Supersonic Wing Striking a Sharp-Edged Gust, J.Ae. Sc., (1949), Vol. 16, pp. 296-300.

9. Chang, C. C.: The Transient Reaction of an Airfoil Due to Change in Angle of Attack at Supersonic Speed, J.Ae.Sc., (1948), Vol. 15, pp. 635-655.

10. Heaslet, M. A., and Lomax, H.: Two-dimensional Unsteady Lift Problems in Supersonic Flight, N.A.C.A. T.N. No. 1621, (1948).

11. Schwarz, L.: Plane Non-stationary Theory of the Wing at Supersonic Speed, U.S.A.A.F. Translation, F-TS-934-RE, (1947).

12. Strang, W. J.: A physical theory of supersonic aerofoils in unsteady flow, Proc. Royal Soc., (1948), Series A, Vol. 195, pp. 245-264.

13. Rayleigh, Lord: The Theory of Sound, Dover, (1945), Vol. II, p. 107.

14. Strang, W. J.: Transient lift of three-dimensional purely supersonic wings, Proc. Royal Soc., (1950), Series A, Vol. 202, pp. 54-80.

15. Miles, J. W.: Transient Loading of Wide Delta Airfoils at Supersonic Speeds, U.S.N.O.T.S., Inyokern, California, TM RRB-37, (1950).

16. Miles, J. W.: On Harmonic Motion of Wide Delta Airfoils at Supersonic Speeds, U.S.N.O.T.S., Inyokern, California, TM RRB-36, (1950).

TABLE OF NOTATION

Note: Barred space coordinates are stationary. Unbarred coordinates move with the main motion of the wing, and for the delta wing have their origin in the plane of the wing at the vertex. Primed coordinates have their origin at an arbitrary point of the leading edge in the plane of the wing.

Roman numeral subscripts refer to zones of pressure field on wing.

Capital letter subscripts refer to zones of chordwise time history on wing.

Numerical subscripts as applied to force and moment coefficients refer to time intervals.

SYMBOLS	MEANING
x, y, z ξ, η, ζ	Fixed and running cartesian space coordinates
t, τ	Fixed and running time coordinate
r	Spherical polar radius
ρ, θ	Cylindrical polar coordinates in plane of wing
p	Fluid static pressure
d	Fluid density
$( )_\infty$	Values far from the wing
$\vec{q} = \nabla\varphi$	Fluid perturbation velocity vector
φ	Fluid perturbation velocity potential
$s = \frac{d}{d_\infty} - 1$	Fluid condensation
K	Fluid ratio of specific heats
a_ℓ, a	Fluid local and free-stream velocity of sound
$\vec{Q}$	Wing velocity vector
U	Wing main velocity component

u, v, w	Wing perturbation velocity components
$\vec{i}, \vec{j}, \vec{k}$	Unit cartesian vectors
$\vec{n}$	Unit normal vector
ε	Small angle
α	Local instantaneous angle of attack
$\alpha_0 = \frac{W_0}{U}$	Wing angle of attack due to unit-step motion
$-W_0$	Wing perturbation velocity component due to unit-step motion
$M = \frac{U}{a}$	Mach number
β	$\sqrt{M^2-1}$
h_u, h_ℓ	z-coordinates of corresponding points on top and bottom surfaces of wing
c	Wing chord
σ	Wing sweepback angle
k	$\tan\sigma$
φ_1	Velocity potential for spherical pulse
S	Pulse strength
δ	Dirac delta function
1	Unit-step function
G	Constant of proportionality
dA	Element of area in plane of wing
P	Point in space; particular points denoted by numerical subscripts
b	Arbitrary value of $\bar{x}$
R	Region of integration for fundamental wing formula; particular regions denoted by subscripts

γ, Γ	Angles in region of integration in plane of wing; also used with subscripts $\pm k$
Λ	Angle in domain of dependence of point on wing
$\phi = \int_{-\infty}^{\infty} \varphi \, d\bar{y}$	Velocity potential for fictitious two-dimensional wing
$F = \frac{k}{2w_0 a} \frac{\partial \phi}{\partial \bar{T}}$	Function independent of sweepback
$T = \frac{a\bar{t}}{c}$	Dimensionless time variable
$C_p = \frac{p - p_\infty}{\frac{1}{2} d_\infty U^2}$	Pressure coefficient
L	Wing lift
$C_L = \frac{L}{\frac{1}{2} d_\infty U^2 (\text{area})}$	Wing lift coefficient based on area of delta wing and unit span of two-dimensional wing
${}_o\mathcal{M}$	Wing pitching moment about vertex of delta wing and leading edge of two-dimensional wing
${}_oC_{\mathcal{M}} = \frac{{}_o\mathcal{M}}{\frac{1}{2} d_\infty U^2 (\text{area}) c}$	Wing pitching moment coefficient based on chord
ℓ	x-coordinate of center of pressure of wing
$\bar{\theta}_2$	Limiting value of $\bar{\theta}$ in integration for spanwise lift
$\bar{\tau}_1, \bar{\tau}_2$	Limiting values of $\bar{\tau}$ in integration for spanwise lift
$(\ )_n$	"Normal" quantities
$[P_i P_j]$	Directed distance from P_i to P_j
$f, G, g, \mathcal{J}$ $A, B, C, D, \mathcal{F}$	Various function symbols; some used with subscripts

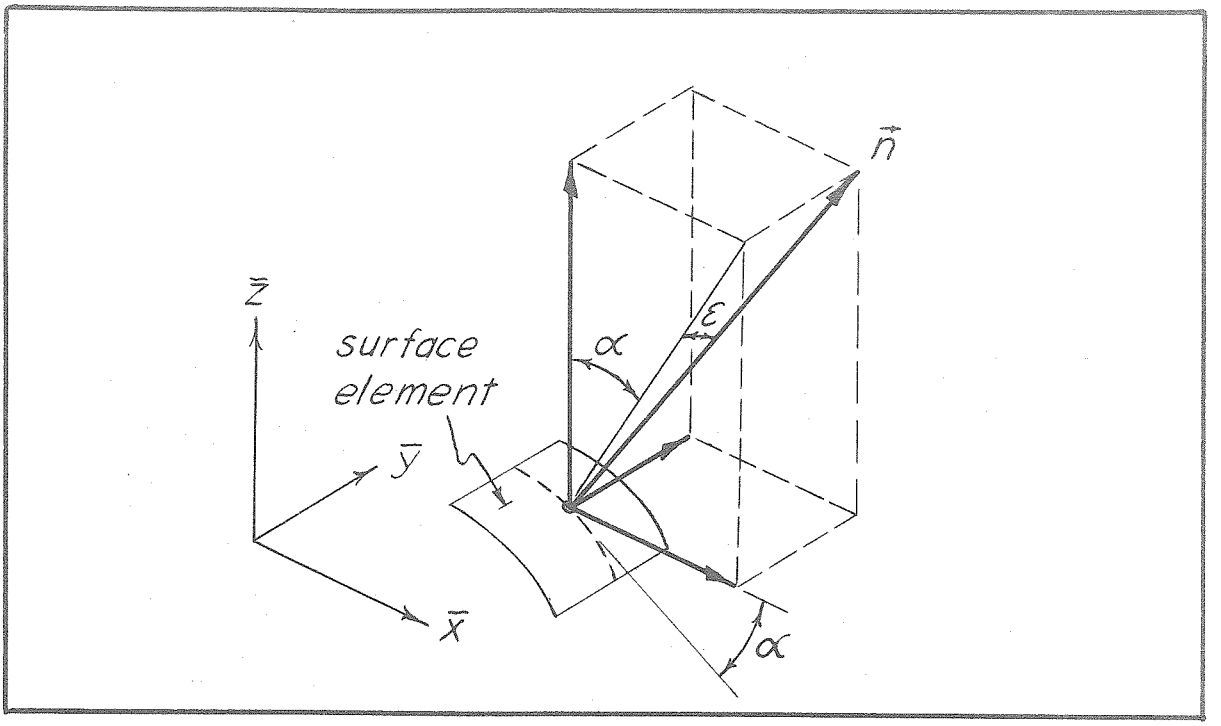

Figure 1. Decomposition of Unit Normal Vector

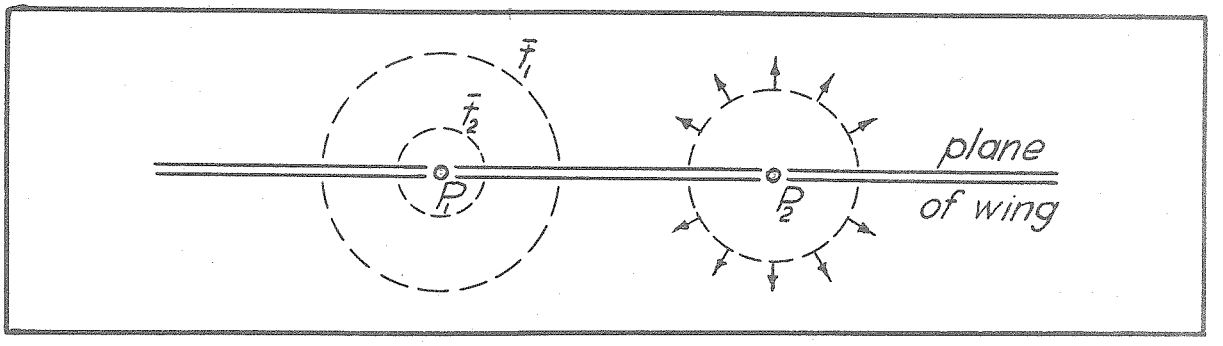

Figure 2. Properties of the Spherical Pulse

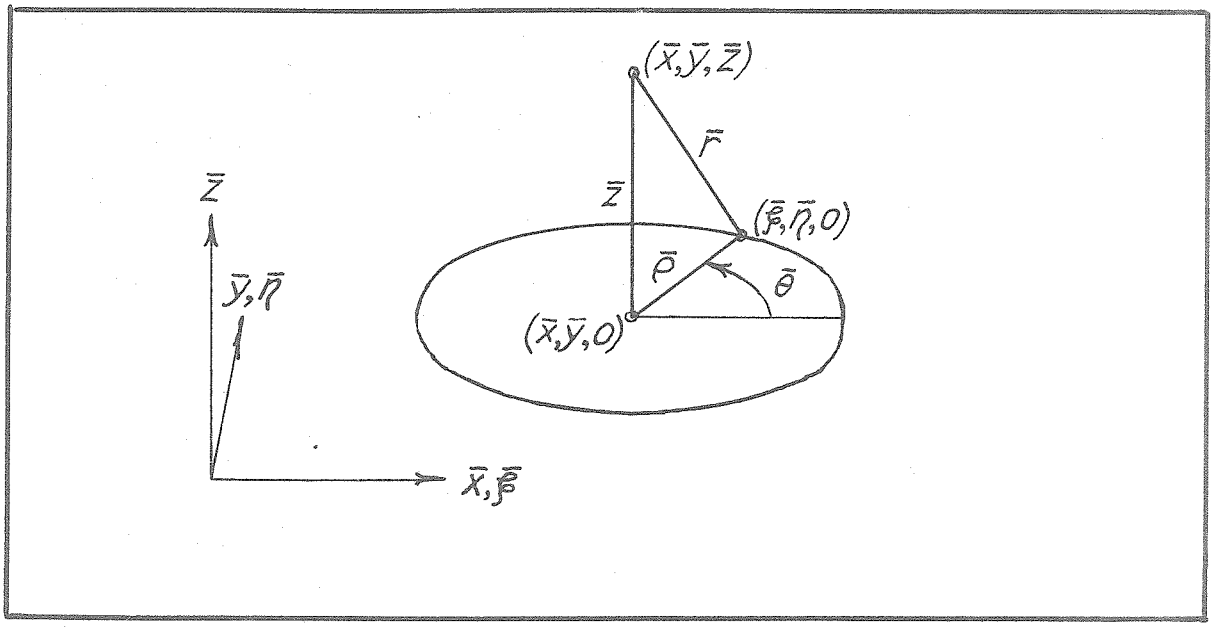

Figure 3. Coordinate Relations

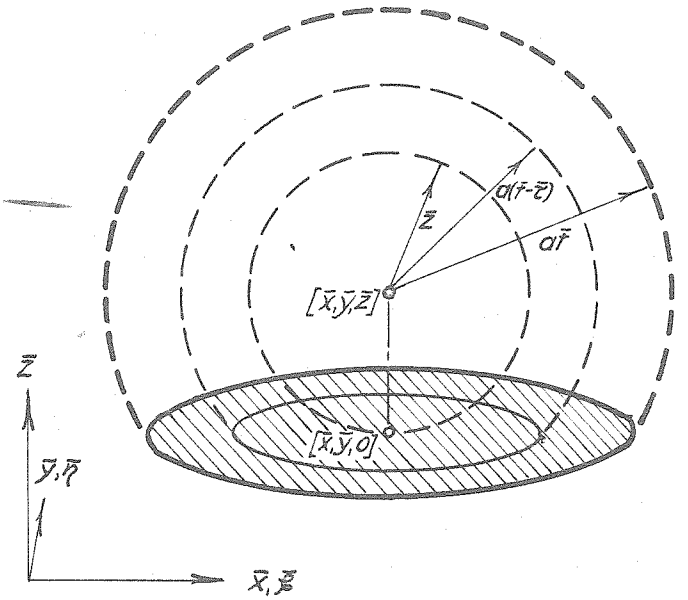

(a)

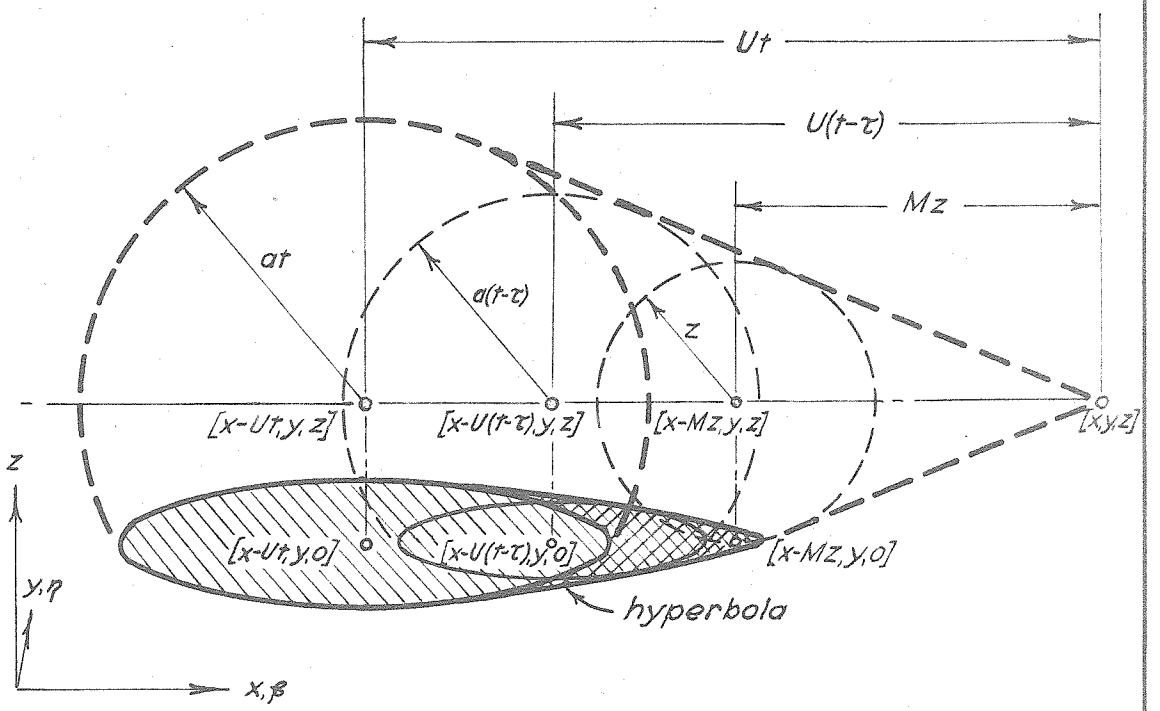

(b)

Figure 4. Domains of Dependence

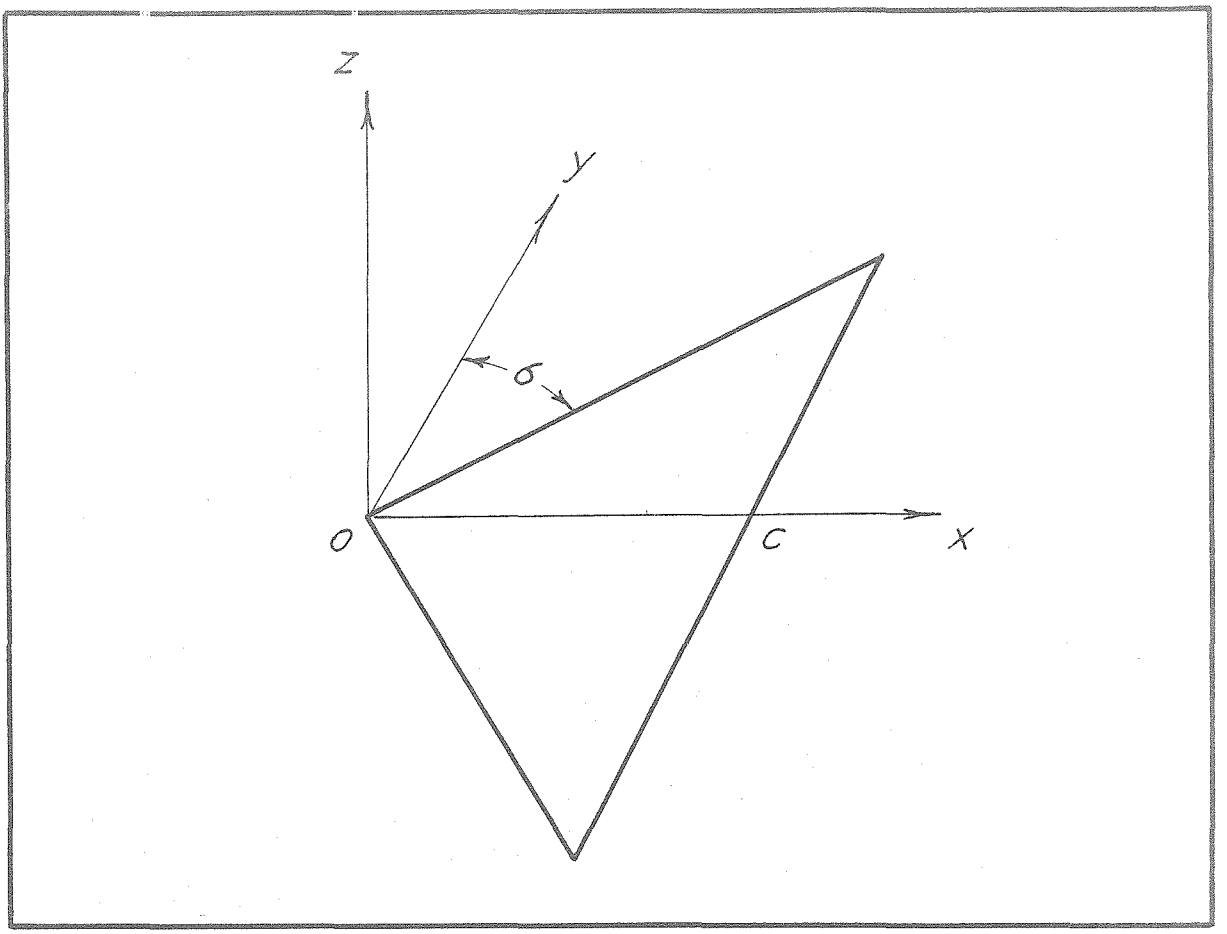

Figure 5. Delta Wing

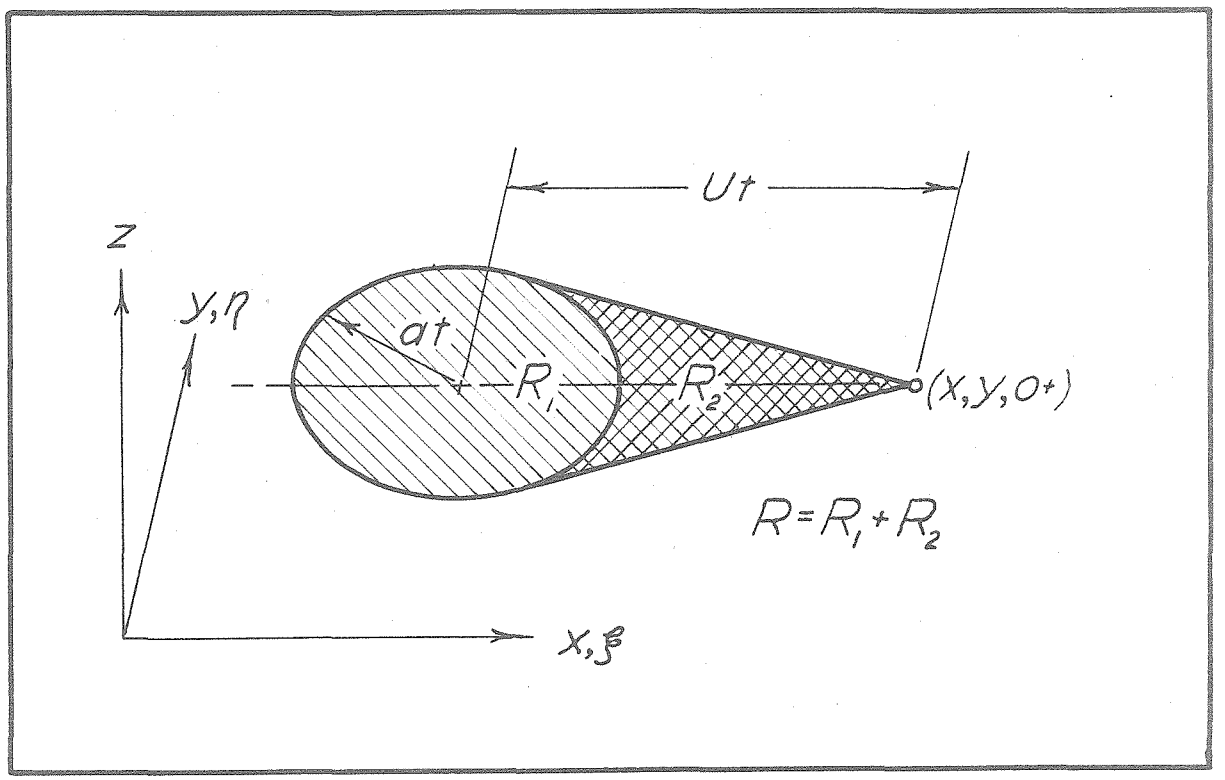

Figure 6. Basic Region of Integration

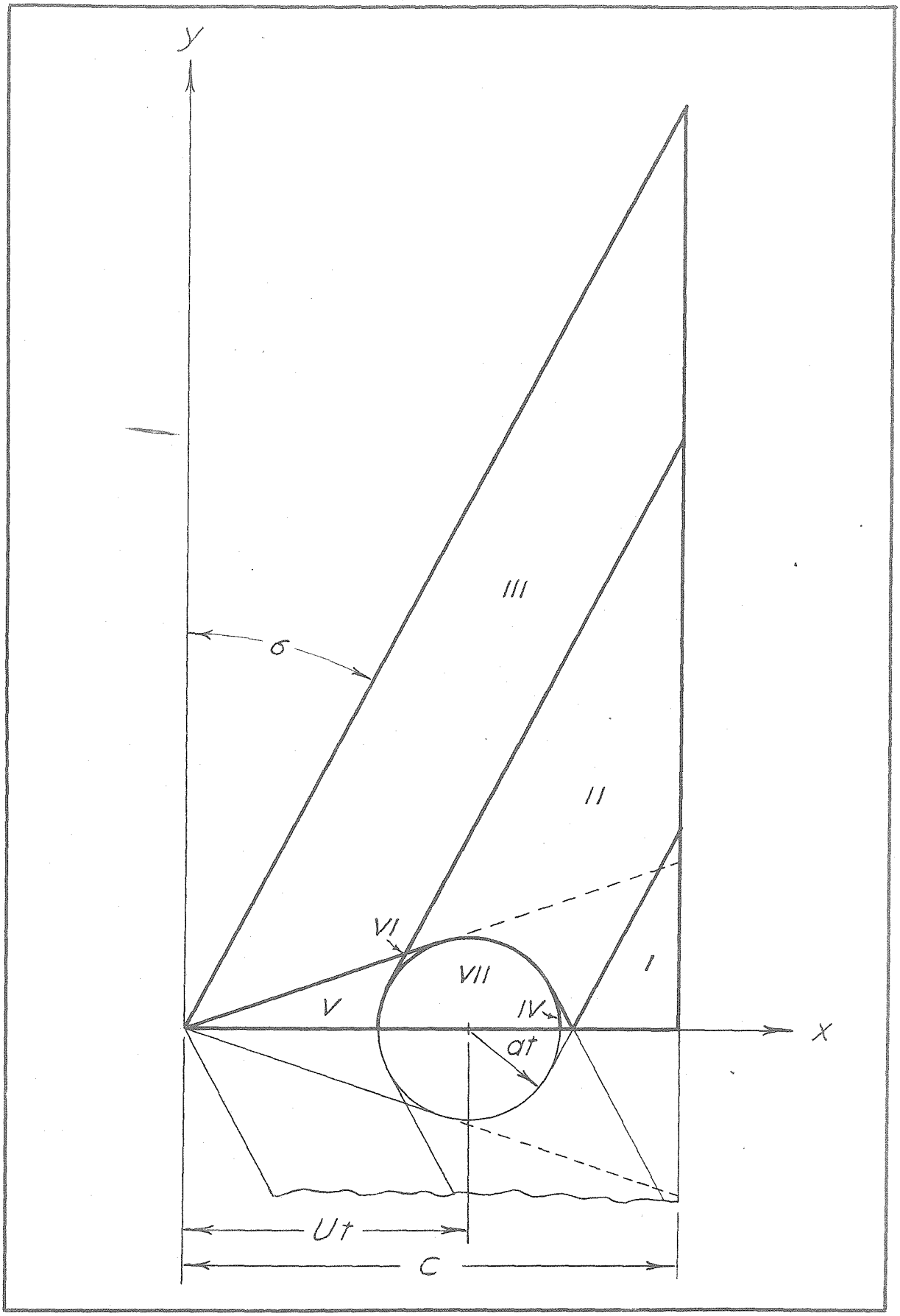

Figure 7. Zones on the Wing

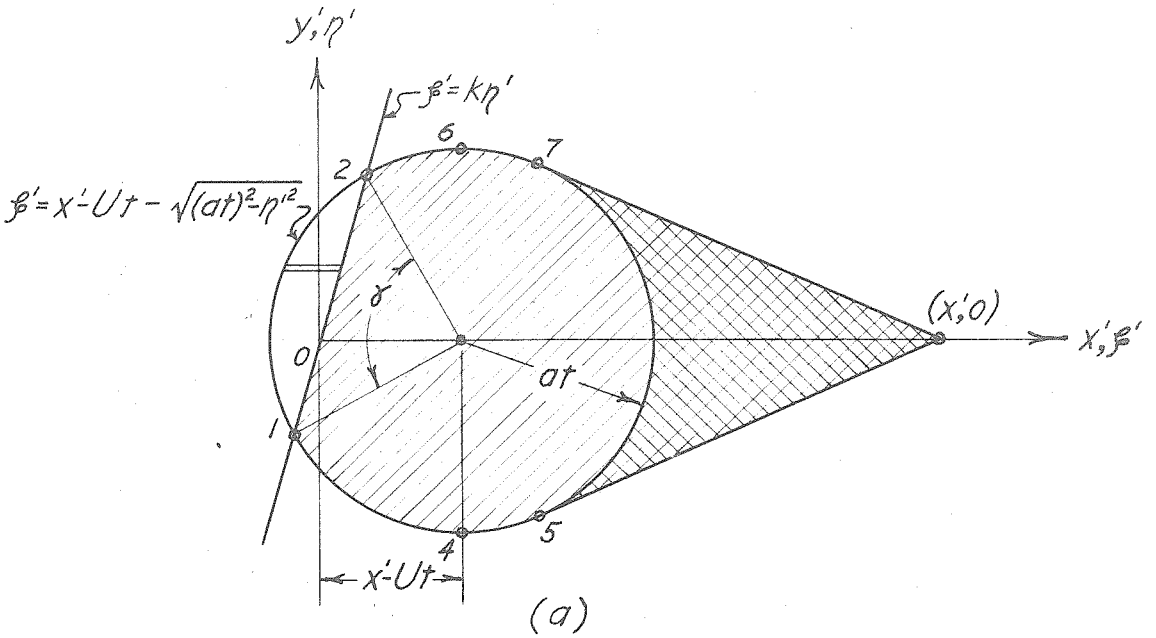

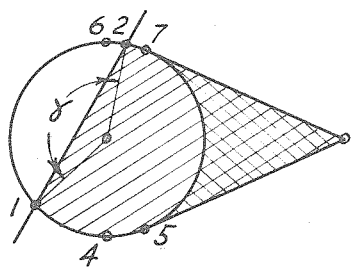

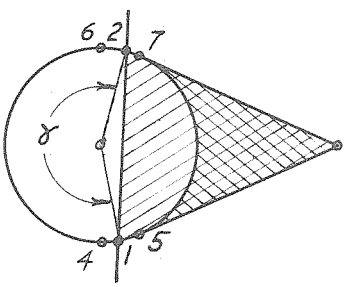

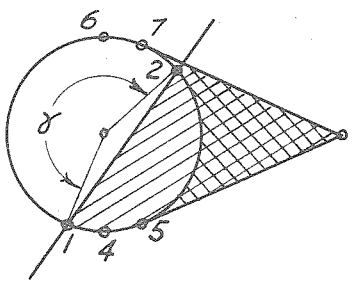

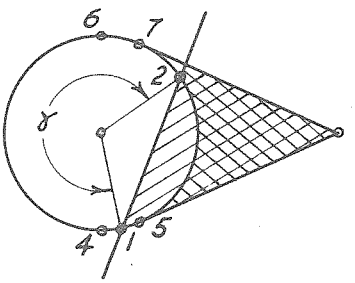

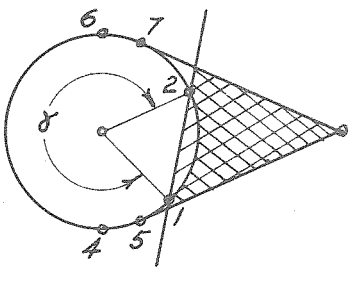

Figure 8. Regions of Integration for Zone II

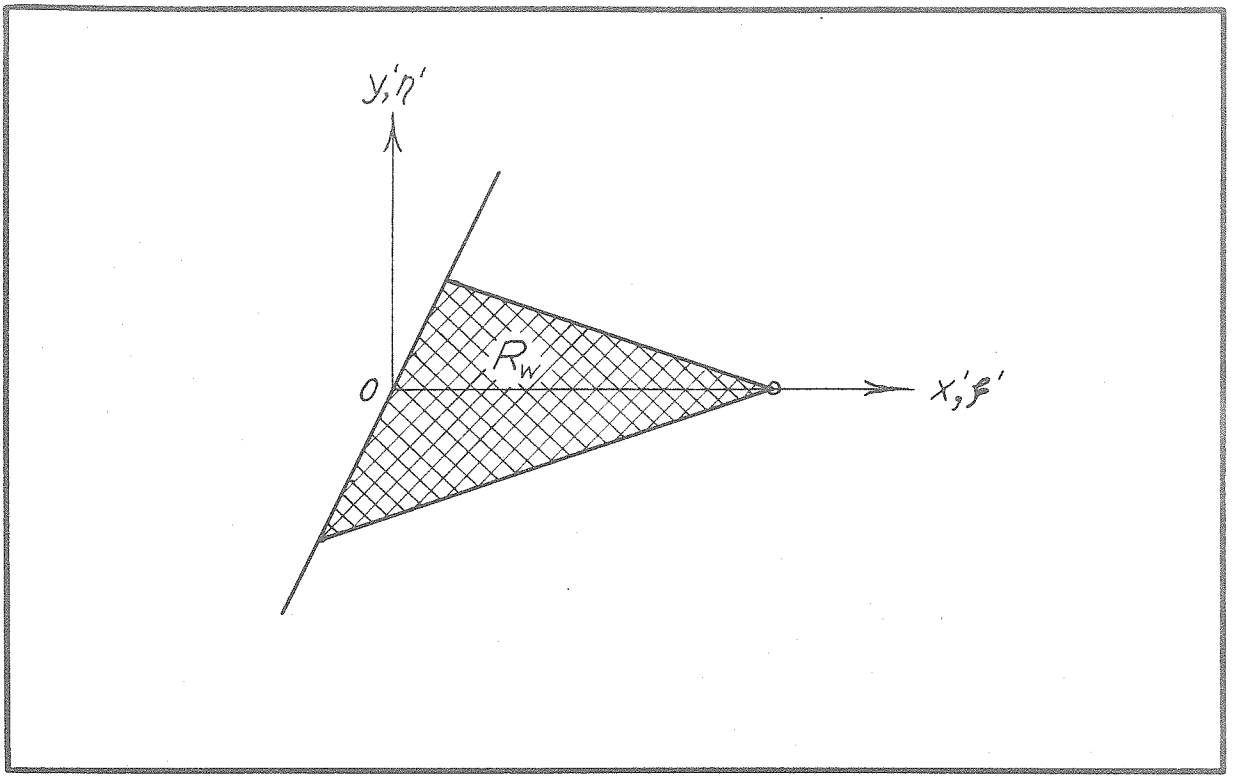

Figure 9. Region of Integration for Zone III

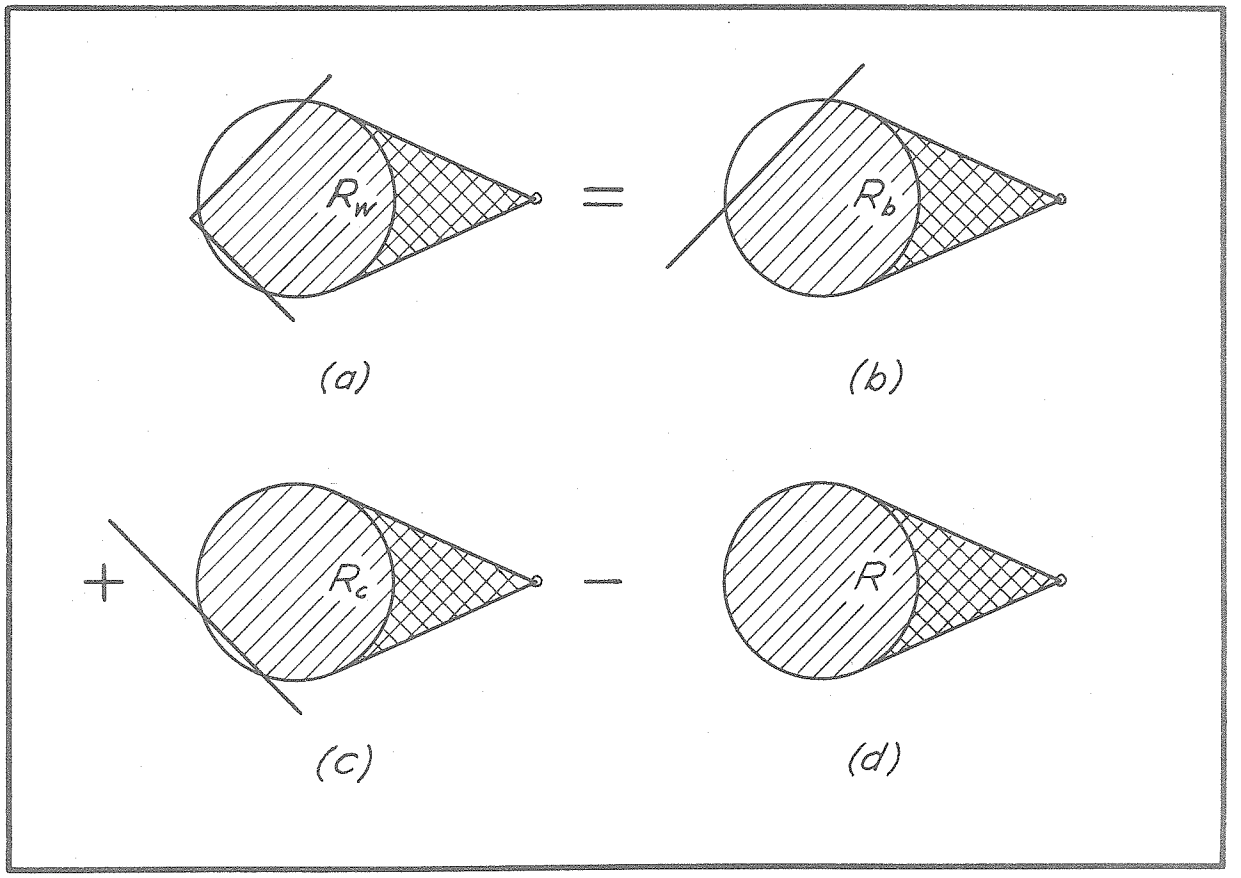

Figure 10. Superposition of Regions for Zone IV

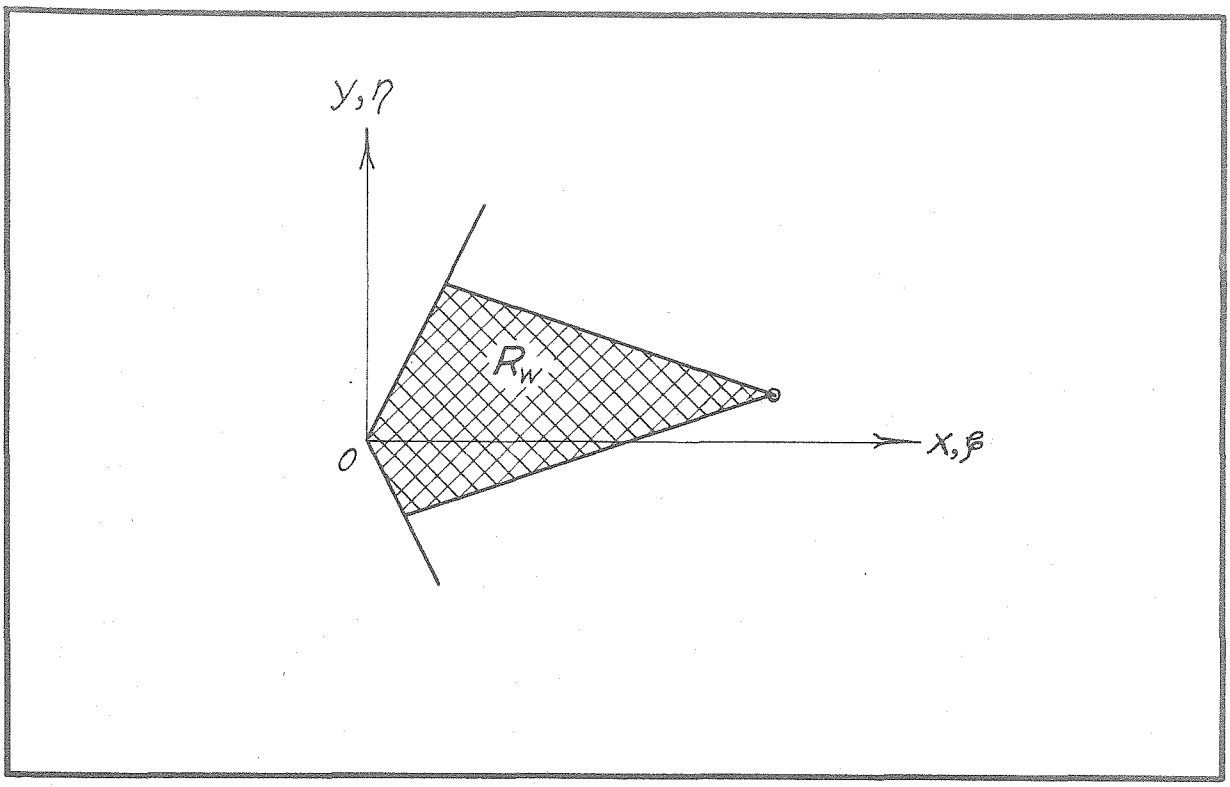

Figure 11. Region of Integration for Zone V

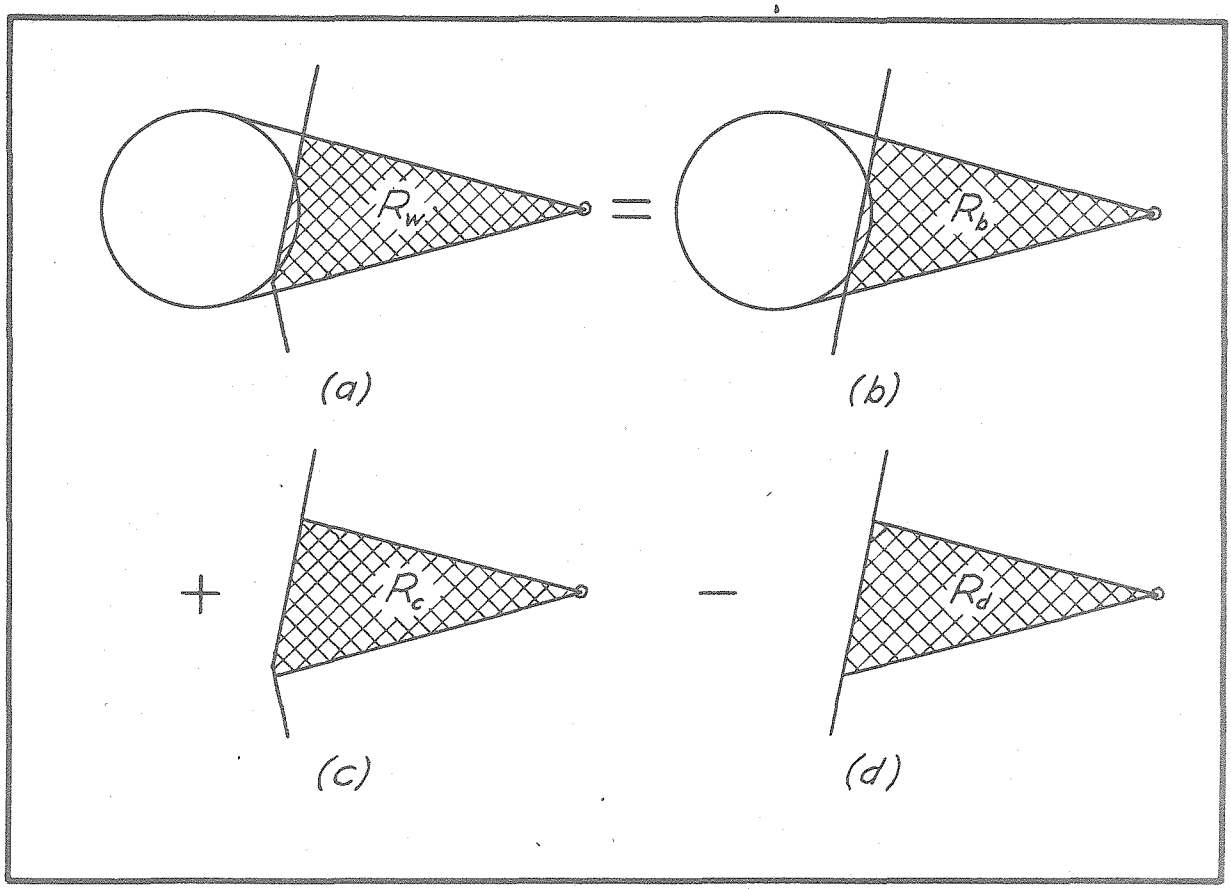

Figure 12. Superposition of Regions for Zone VI

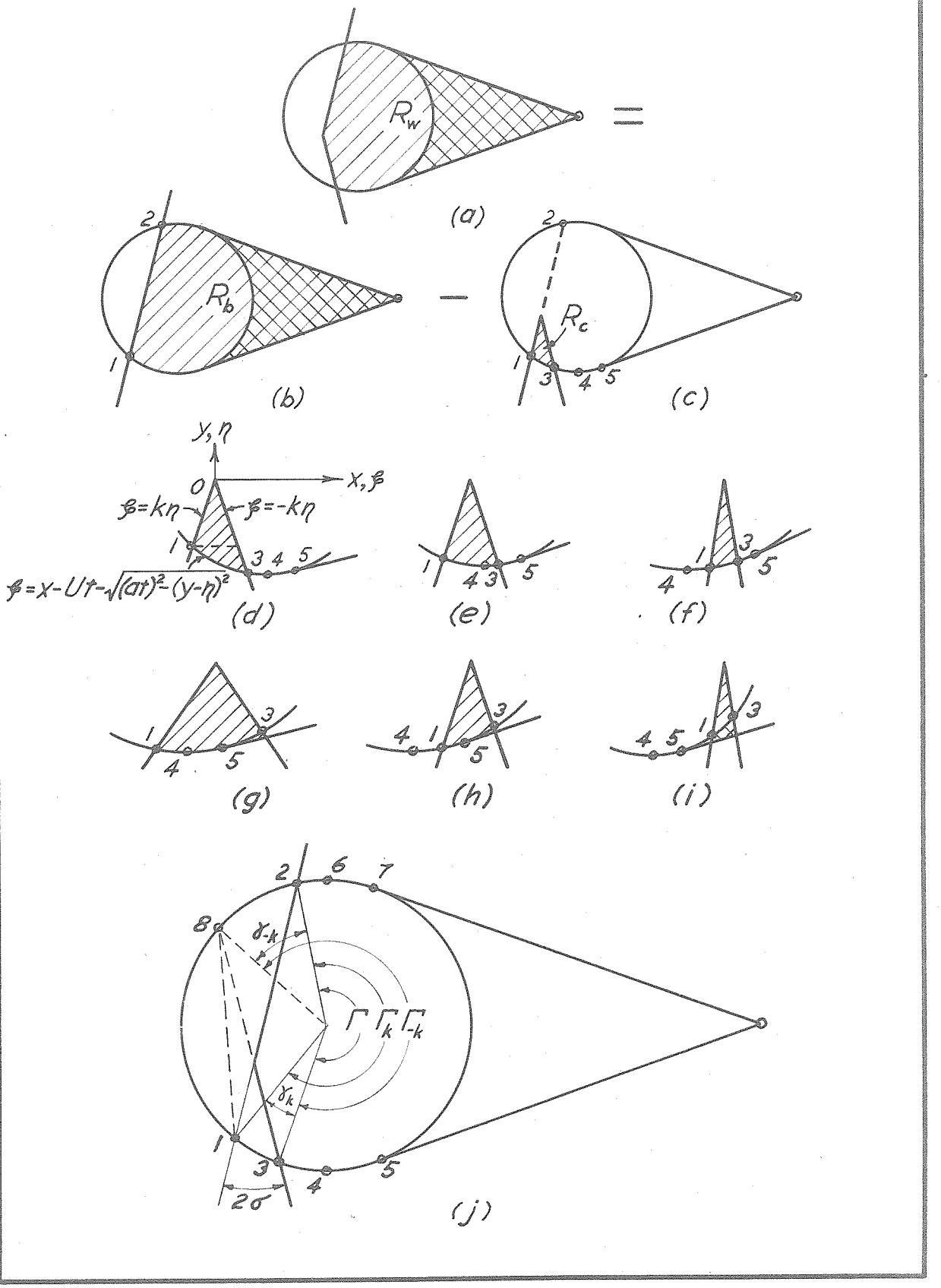

Figure 13. Regions of Integration for Zone VII

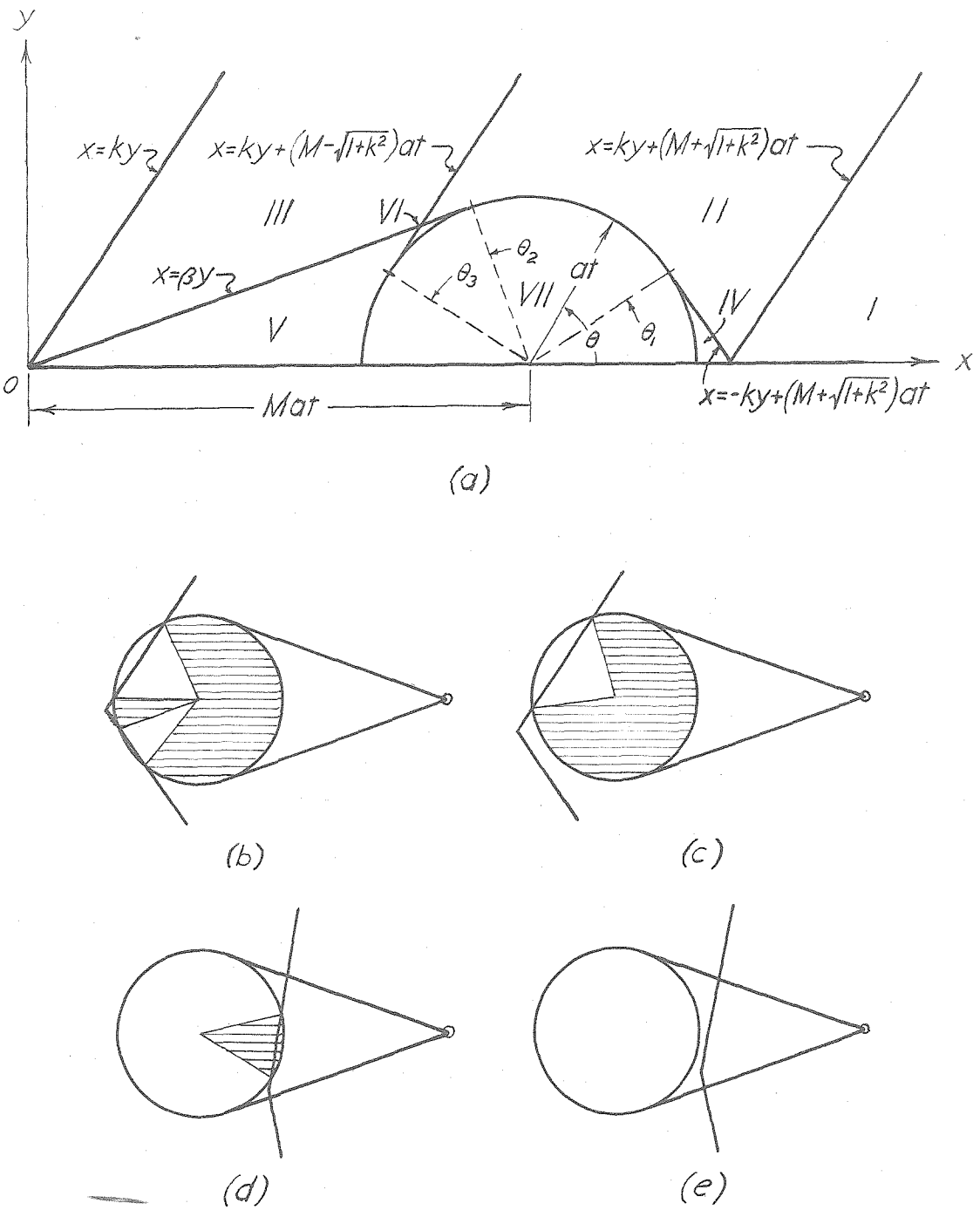

Figure 14. Zone Boundaries. Continuity of Pressure.

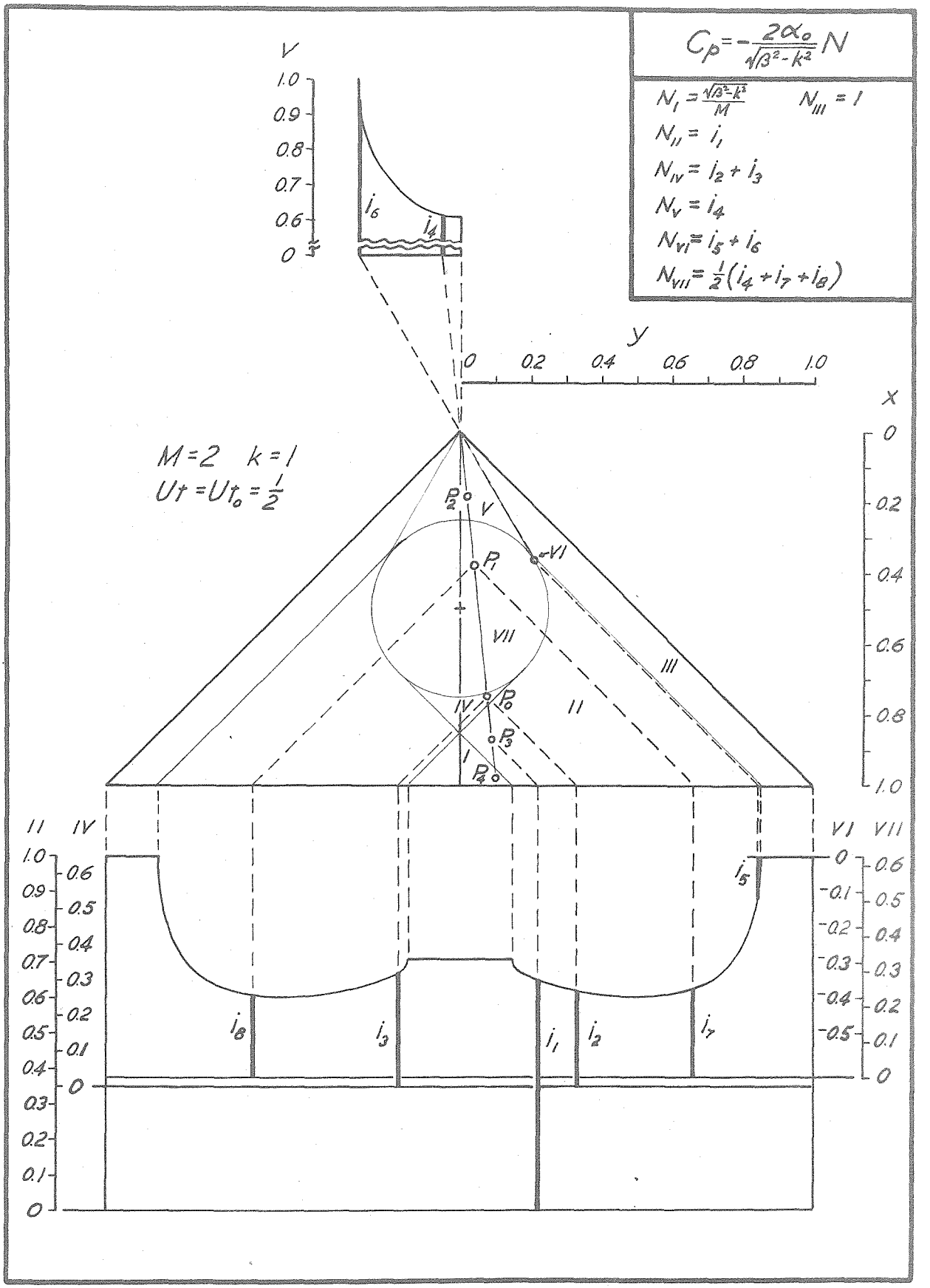

Figure 15. Scheme for Determination of Pressure

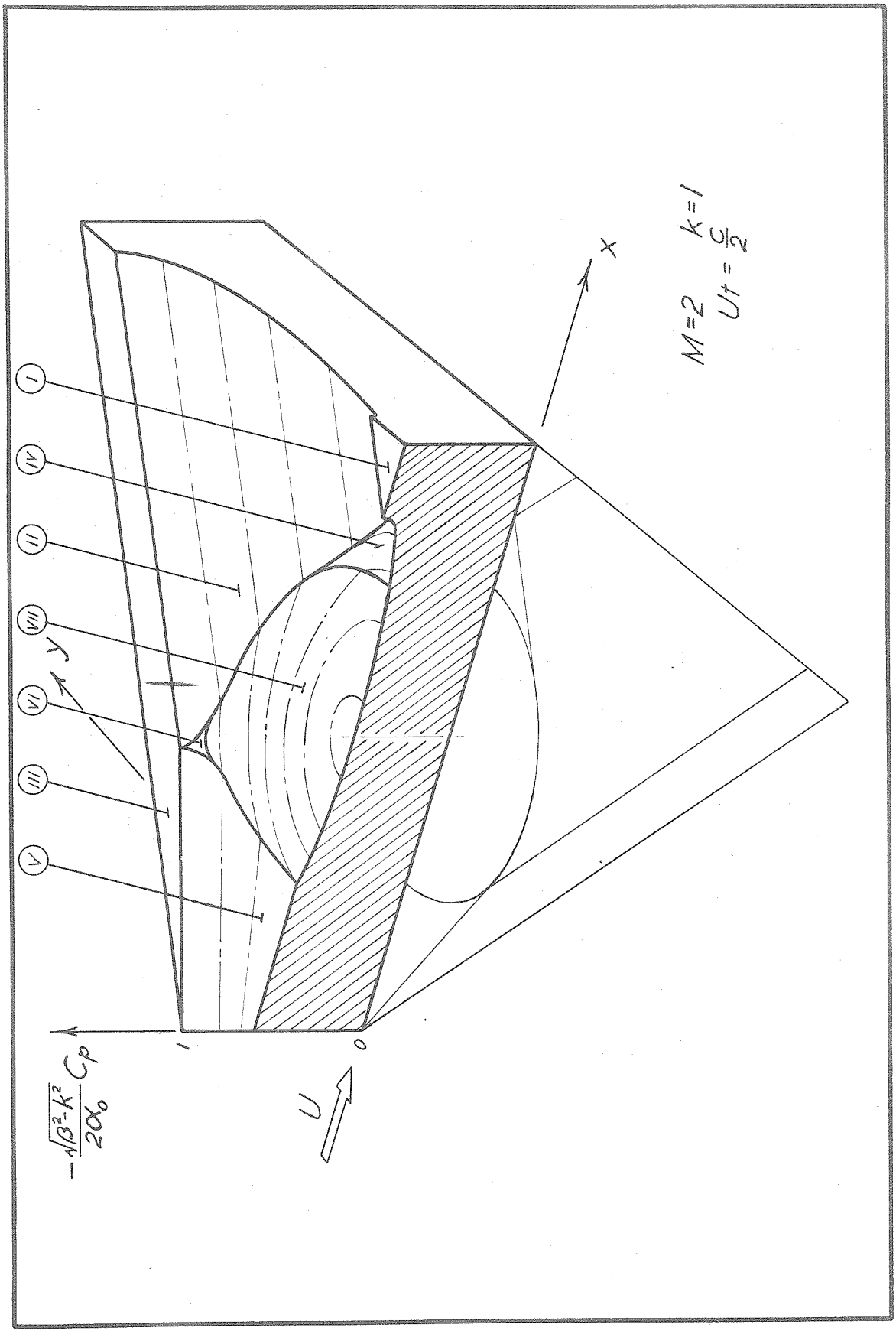

Figure 16. Pressure Field on the Right Wing

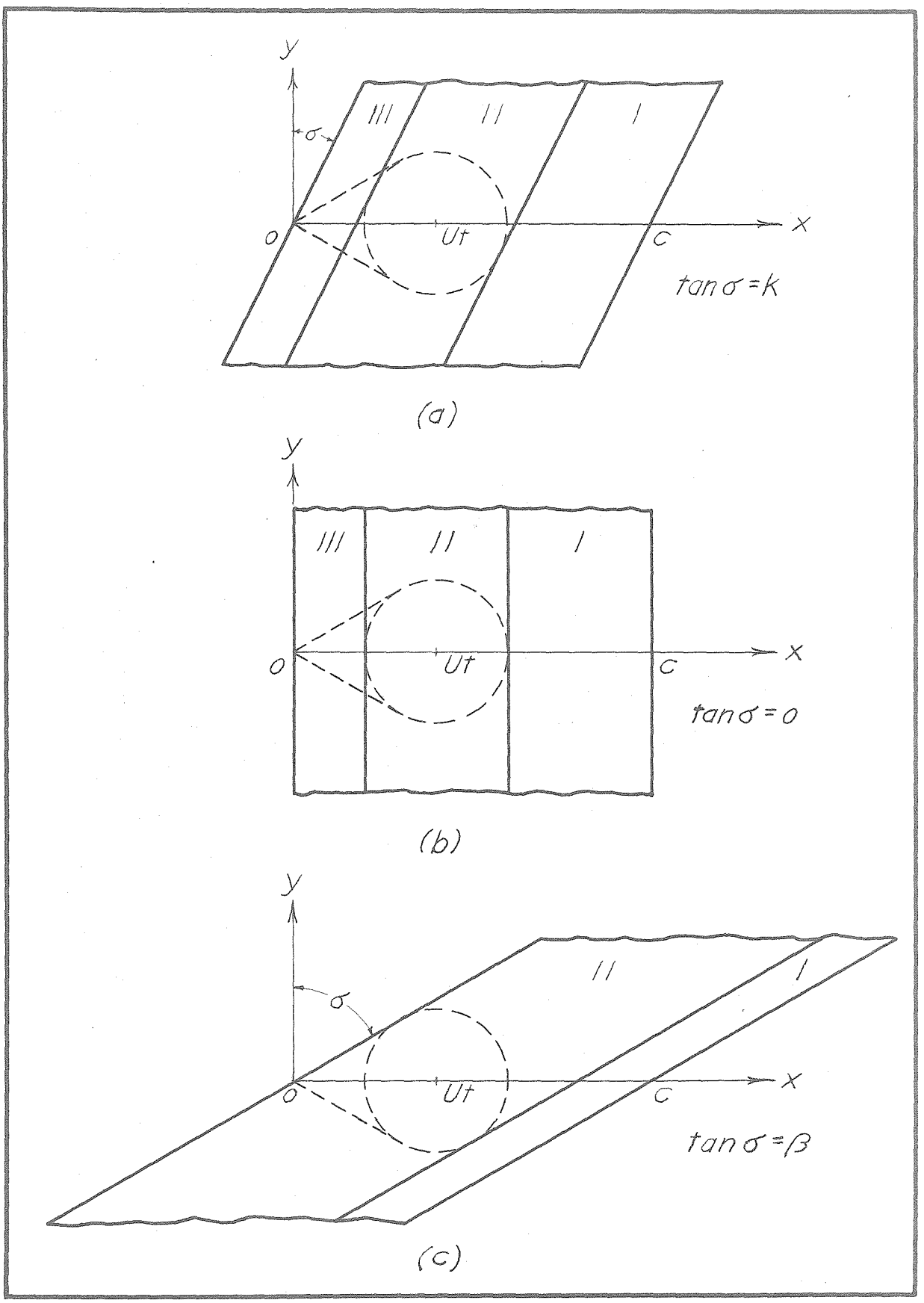

Figure 17. Infinite Swept Wings

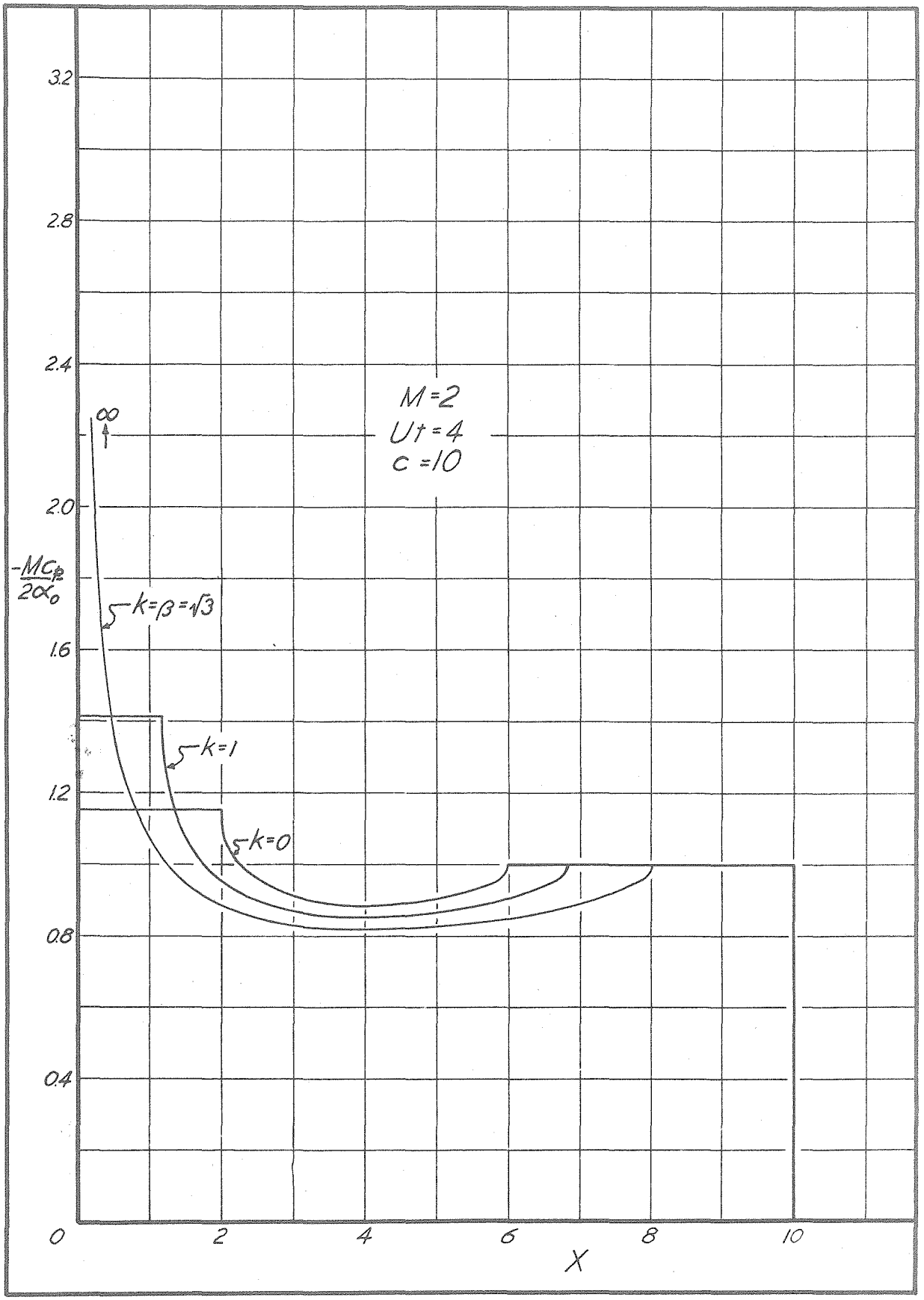

Figure 18. Pressure on Infinite Swept Wings

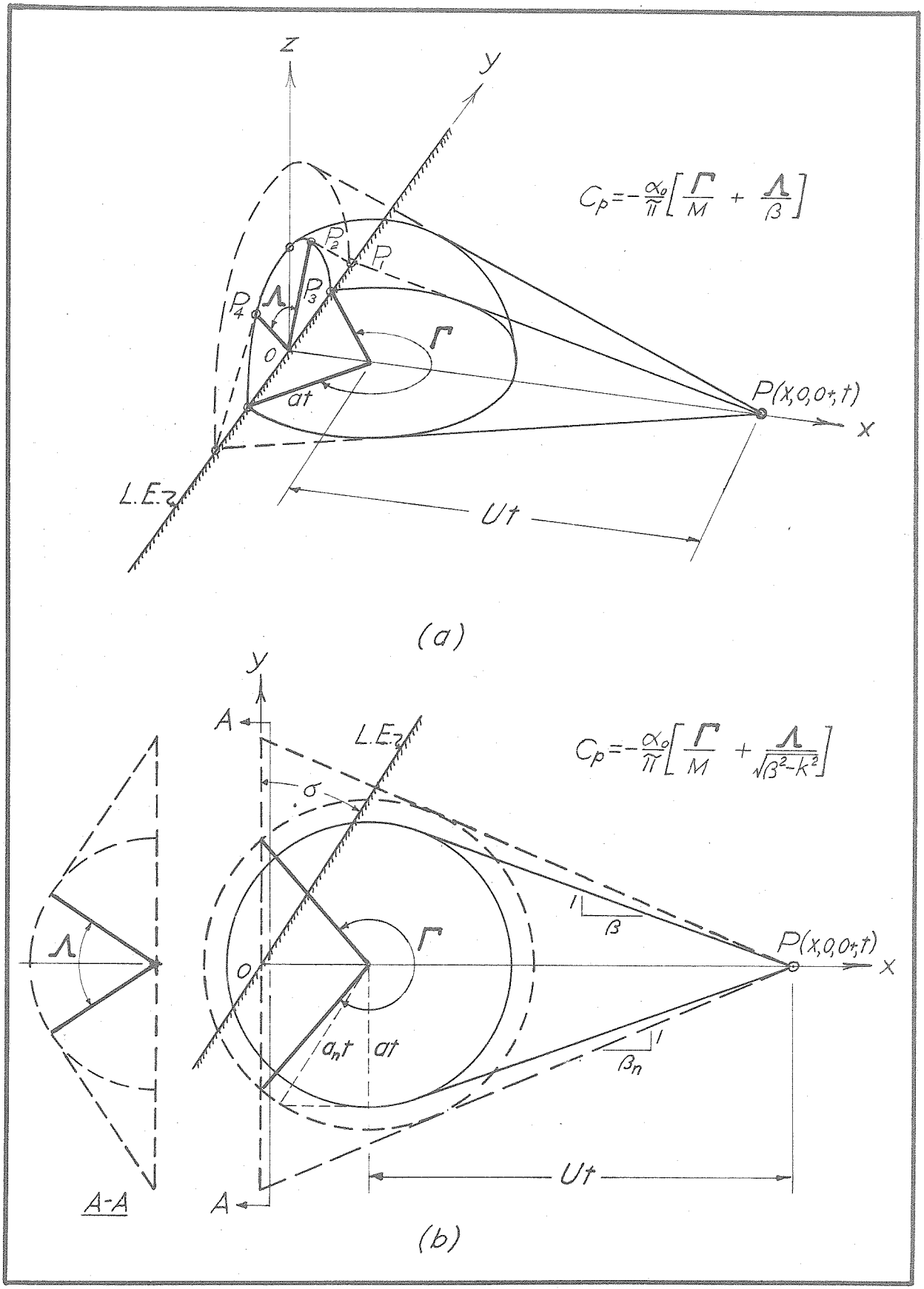

Figure 19. Geometric Meaning of Pressure Terms

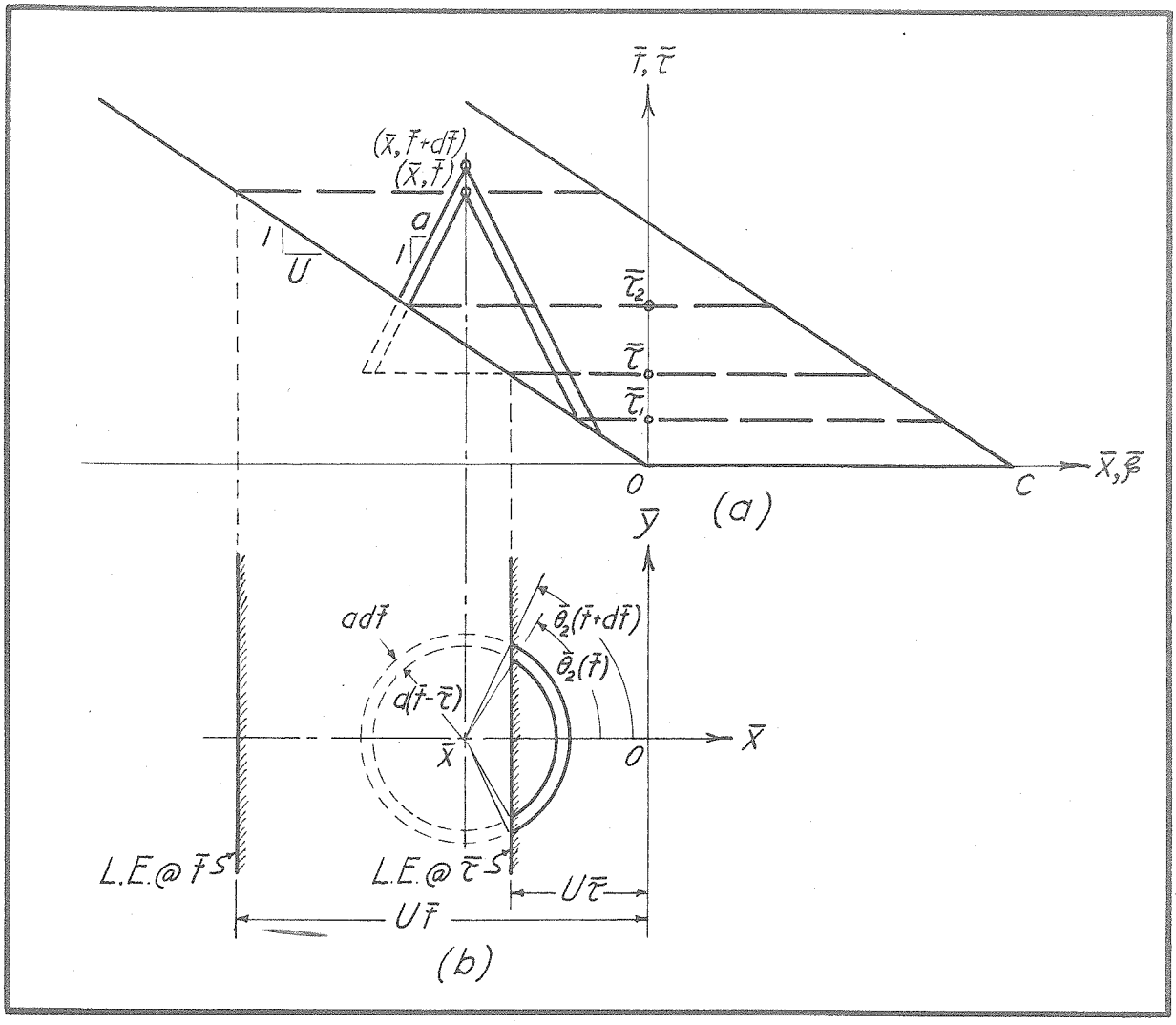

Figure 20. Region of Integration in Time History

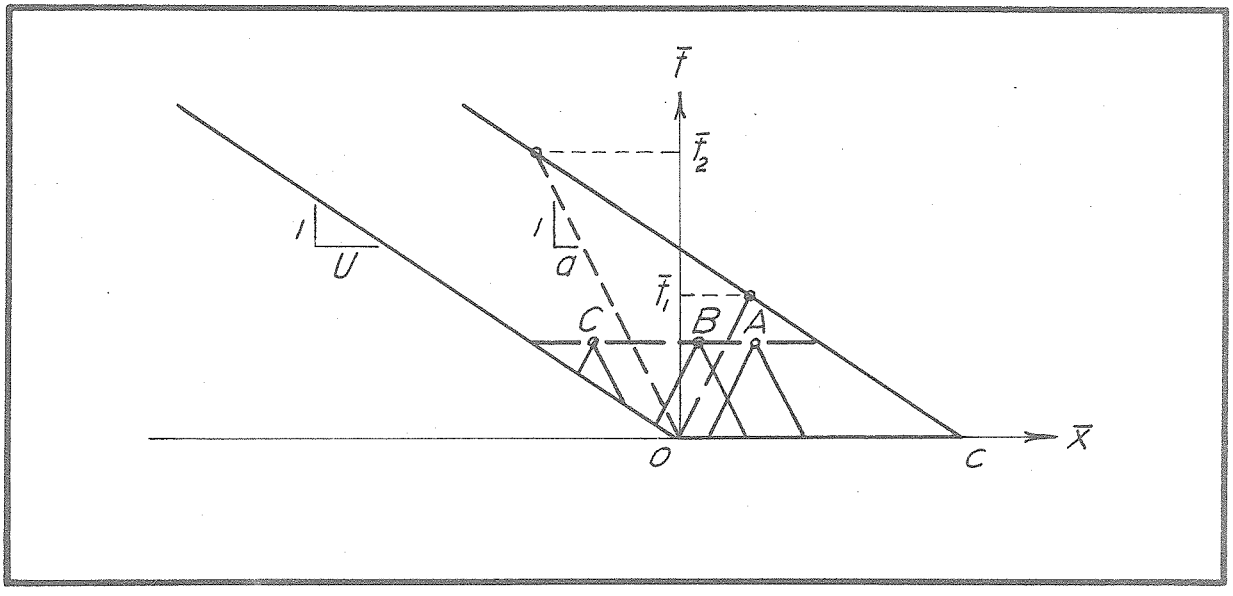

Figure 21. Zones in Time History

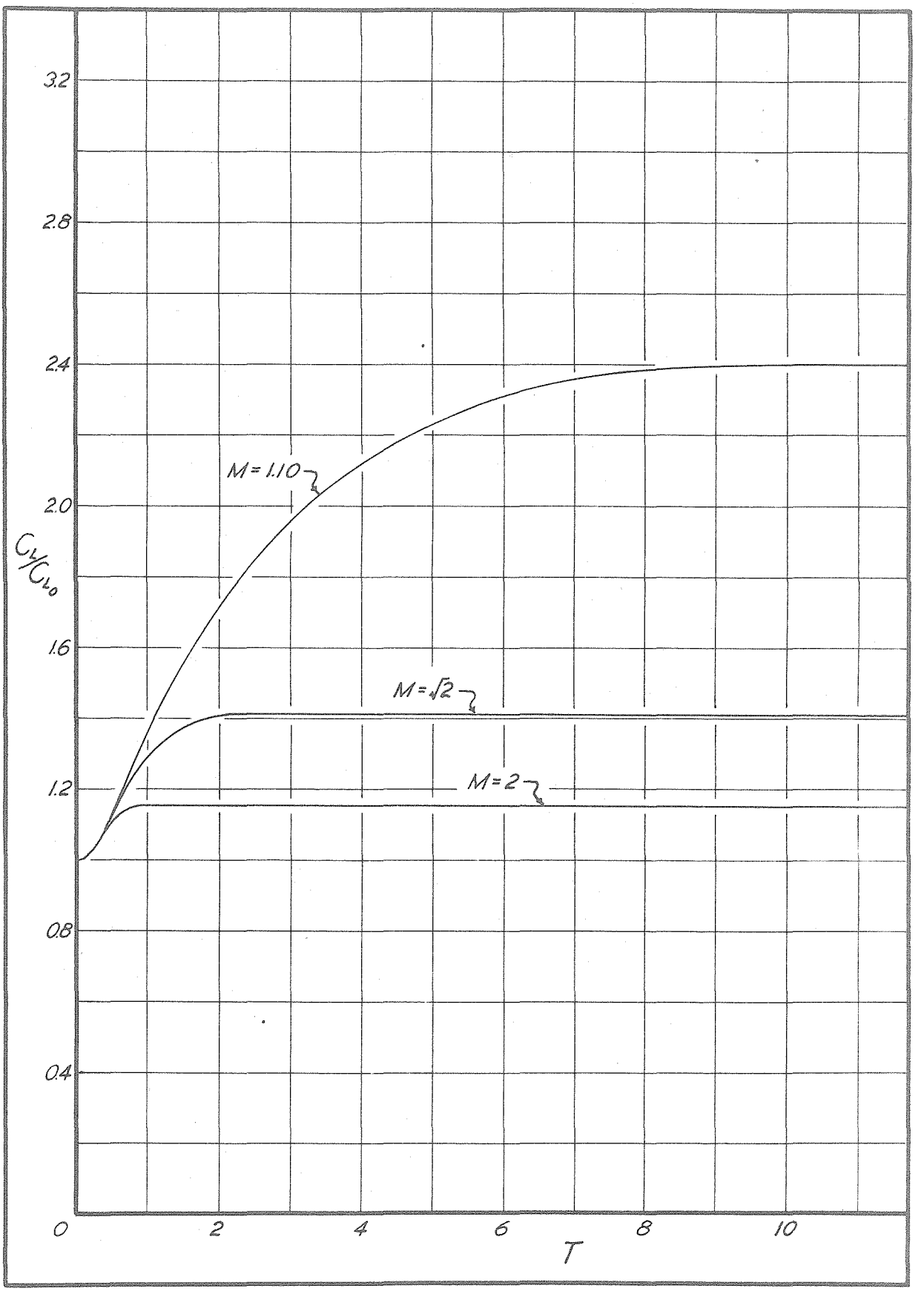

Figure 22. Lift

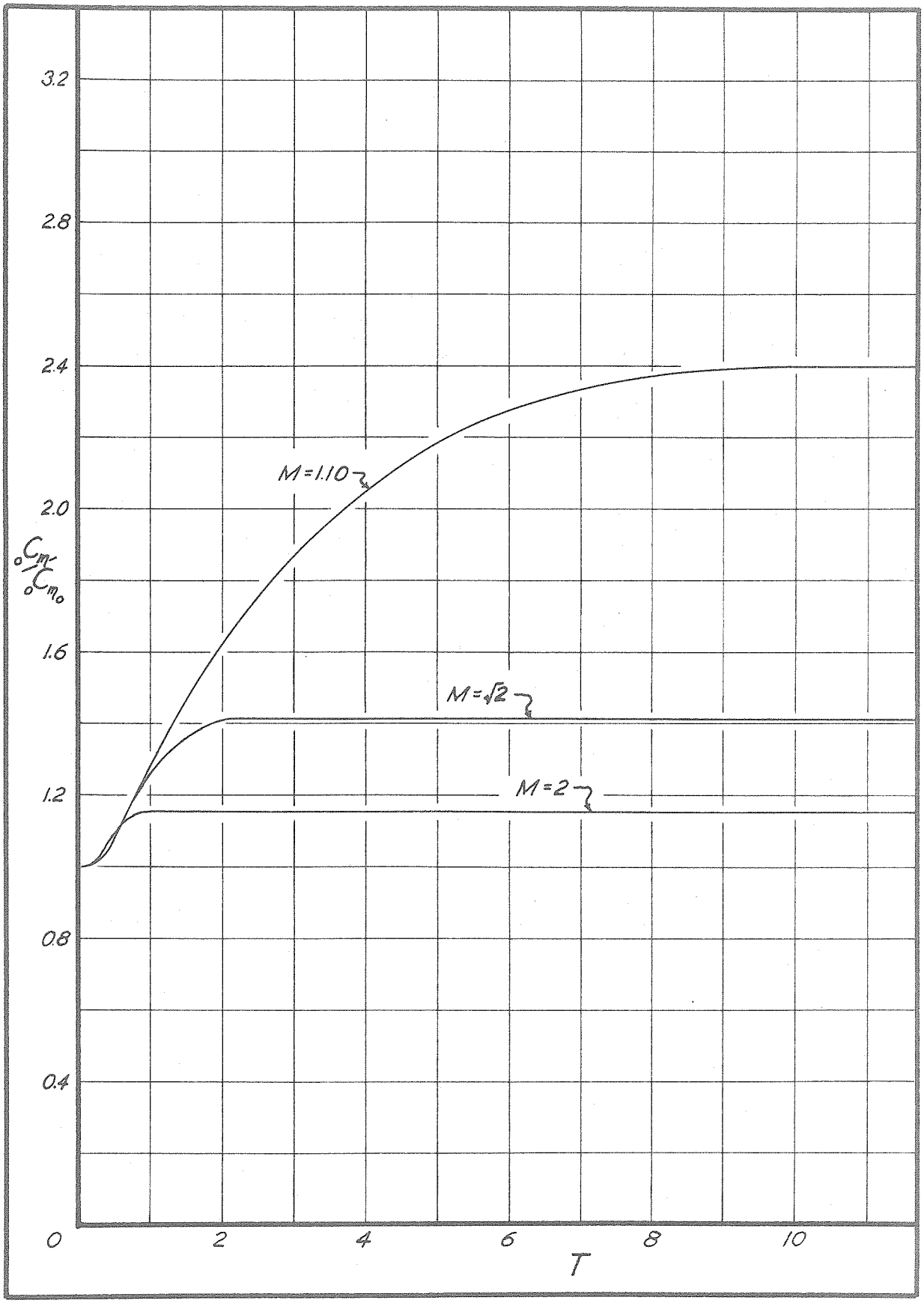

Figure 23. Pitching Moment about Vertex

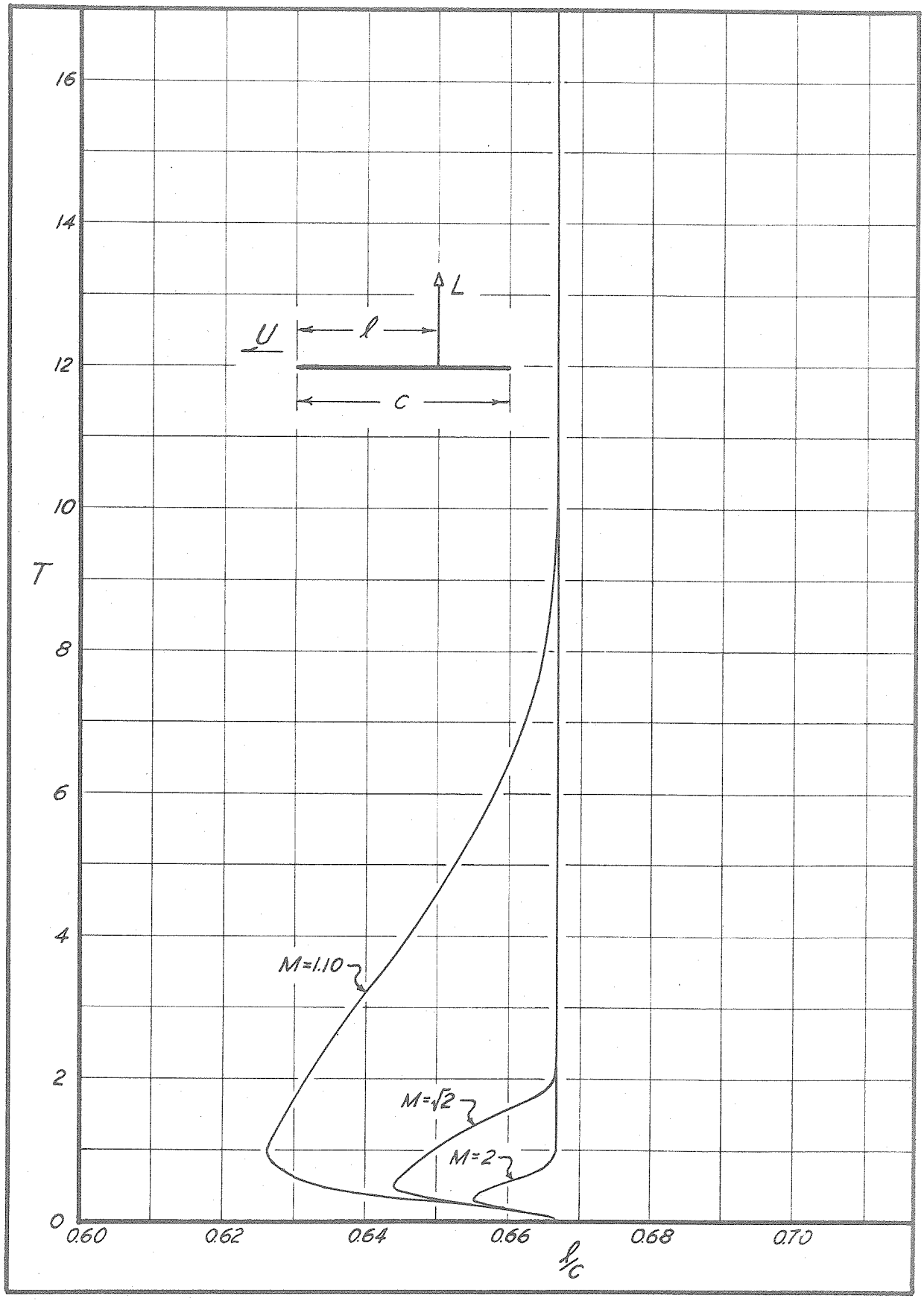

Figure 24. Center of Pressure Travel

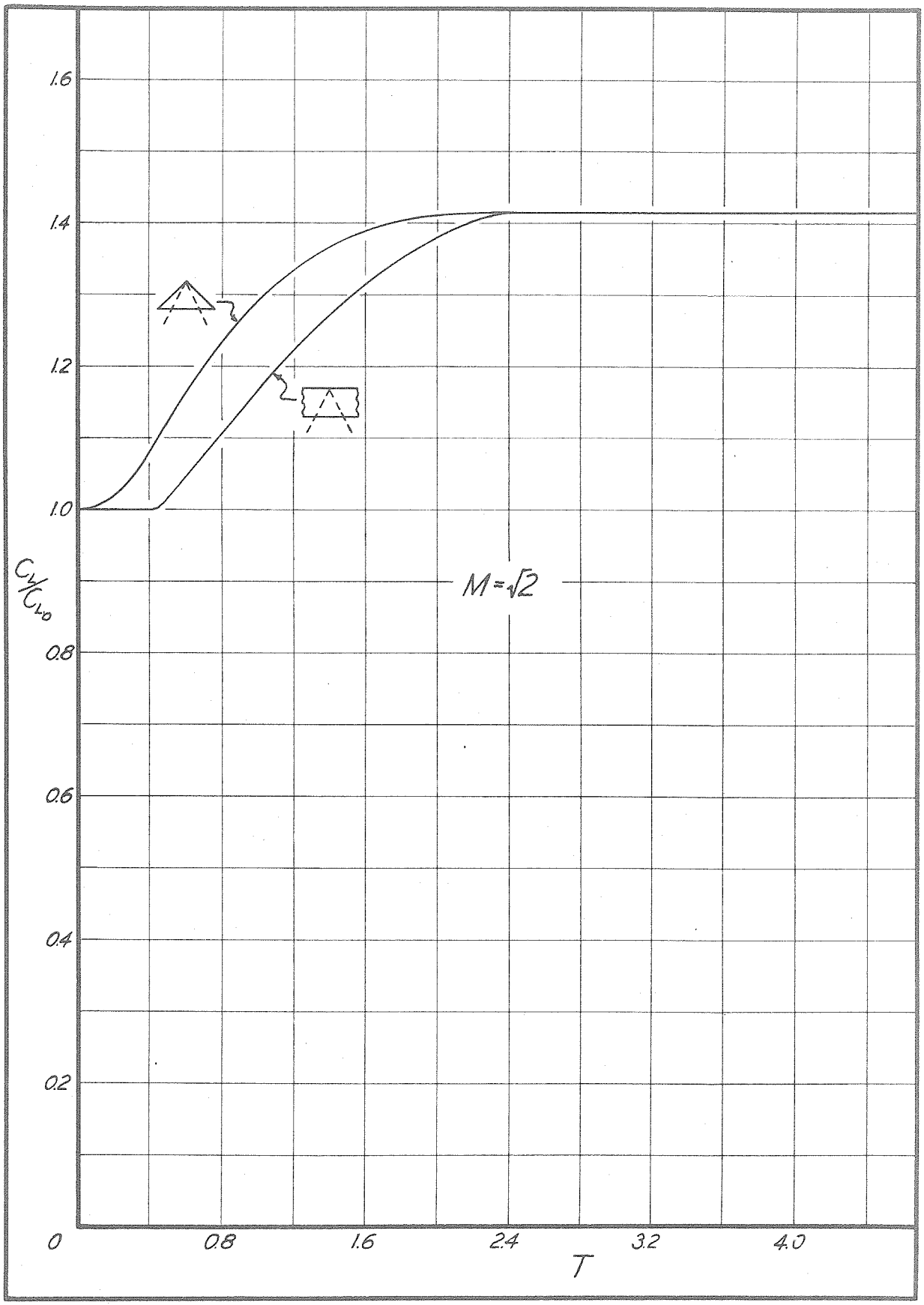

Figure 25. Comparison with Two-dimensional Wing. Lift.

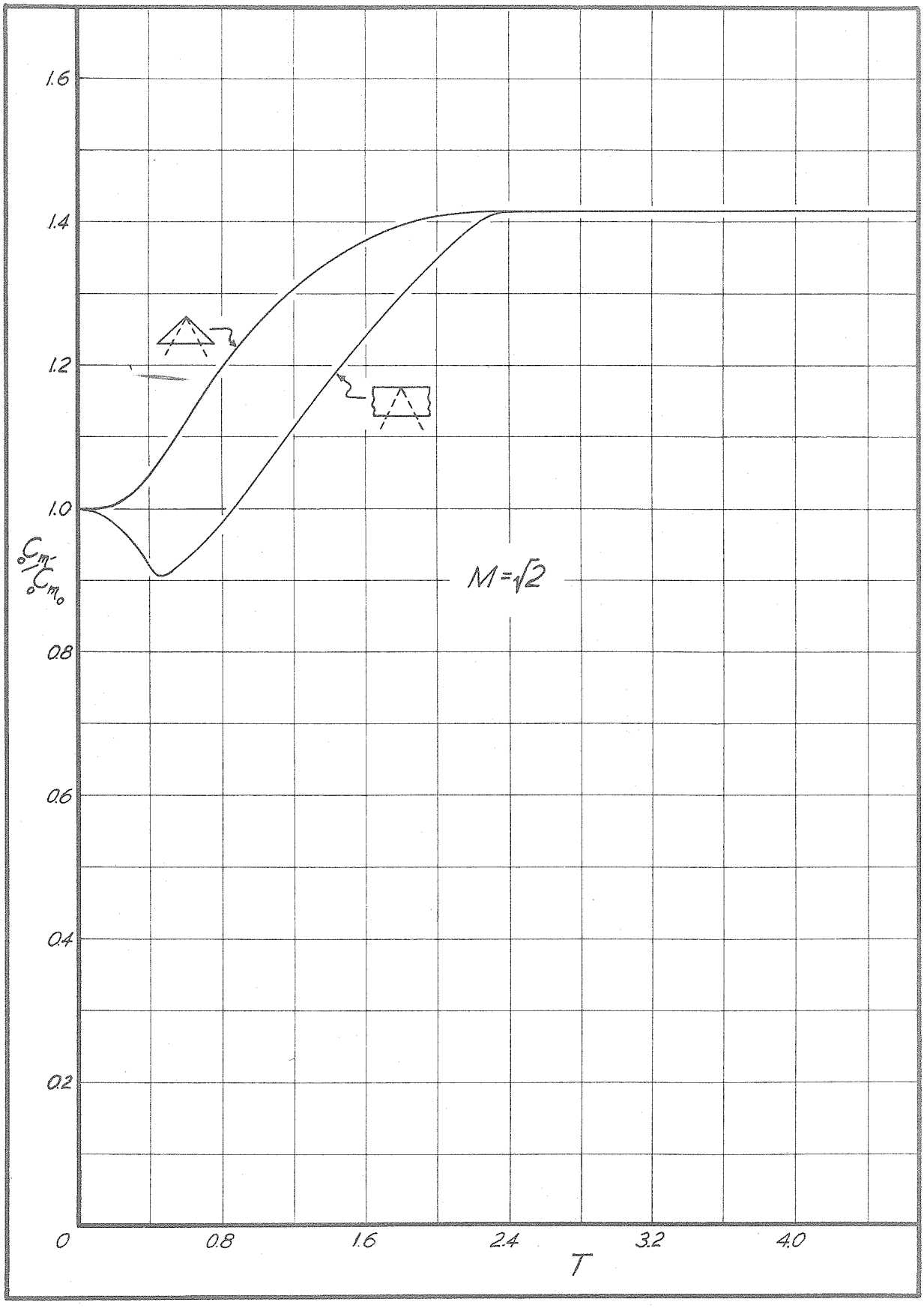

Figure 26. Comparison with Two-dimensional Wing. Moment.